الجمهورية الجزائرية الديمقراطية الشعبية
Democratic and Popular Algerian Republic
وزارة التعليم العالي و البحث العلمي
MinistryINISTRY of Higher Education and Scientific Research

Mohamed Boudiaf MSILA University
College of Technology
Department : Electrical Enginineering

جامعة محمد بوضياف - المسيلة
كلية التكنولوجيا
قسم : الهندسة الكهربائية

Thesis submitted in partial fulfillment of the requirements for the Master's degree

Option : Green Hydrogen a energy carrier

Présentés par :

BENNAADJA Oussama & NADJI Aymen

Theme :

Analysis of solar resources in the wilaya of Msila For the production of green hydrogen

Before the jury composed of:

Dr. Abdelghafour HERIZI	**President**	**University of Msila**
Dr. Ilhem BENSEHIL	**Examiner**	**University of Msila**
Dr. Abderrahim ZEMMIT	**Supervisor**	**University of Msila**
Dr. Abdelouadoud LOUKRIZ	**Co-supervisor**	**University of USTHB**

Academic year : 2024/2025


بسم الله الرحمن الرحيم

Dedication

I dedicate this work to Allah Almighty, my Creator, my source of strengt wisdom, and understanding, who guided me throughout this journey. To ou great teacher and messenger, Prophet Muhammad (peace be upon him), w taught us the purpose of life. To my dear father, may Allah have mercy o him — I deeply wished he could witness this moment, but praise be to Allah in all circumstances. To my beloved mother, may Allah protect her, whose love and support carried me through every step. To my brothers and sisters, and to our dear friends who always encouraged us. To my brother in-law Issam Boukhnissa , who is like a true brother to me — I am deep grateful for his open heart and generous support throughout the completion this thesis. To our respected professors, Dr. Abderrahim Zemmit and Pr. Abdelouadoud Loukriz — thank you for your teaching and guidance, we truly appreciate your efforts. To everyone who supported us near or fa — this work is dedicated to all our loved ones.

Oussama

Table of contents

Table of contents

Table of contents

List of Figures :

Chapitre I : The Art of Green Hydrogen Production

Chapitre II : Modeling of PV system - Electrolyzer

Chapitre III : Analysis of solar resources and characterization of climate data

Chapitre IV : Technical and economic study of green hydrogen production. Case study in Msila

List of Tables :

Chapitre I : The Art of Green Hydrogen Production

Chapitre II : Modeling of PV system - Electrolyzer

Chapitre IV : Technical and economic study of green hydrogen production. Case study in Msila

List of Abbreviations

HS : Hydrogen storage

GH : Green Hydrogen

FF : Fossil Fuel

LOHCs: Liquid Organic Hydrogen Carriers

CSP : Concentrated Solar Power

PV : ²Photovoltaic

MPPT: Maximum Power Point Tracking

P&O: Perturb and Observe

ANN: Artificial Neural Network

FC: Fuel Cell

AE: Alkaline Electrolysis

PEM: Proton Exchange Membrane

SOE: Solid Oxide Electrolysis

HRES: Hybrid Renewable Energy System

NPC: Net Present Cost

COE: Cost of Energy

DHI: Diffuse Horizontal Irradiation

GHI: Global Horizontal Irradiation

DNI: Direct Normal Irradiation

KT: Clearness Index

SA: Stand-Alone

NREL: National Renewable Energy Laboratory

IRENA: International Renewable Energy Agency

H_2 Tank: Hydrogen Tank

UC: Ultracapacitor

PVSYST: PVsyst Software

HOMER: Hybrid Optimization of Multiple Energy Resources

LCOE: Levelized Cost of Energy

ROI: Return on Investment

SOEC : Solid Oxide Electrolyzer Cell

DE : Differential Evolution

RE: Renewable Energy

List of Abbreviations

RES: Renewable Energy Source

ES: Energy Source

H_2: Hydrogen

P&O: Perturb and Observe

HRES: Hybrid Renewable Energy System

HOMER: Hybrid Optimization of Multiple Energy Resources

COE: Cost of Energy

LCOE: Levelized Cost of Energy

LCC: Life Cycle Cost

SC: System Capacity

CS: Capacity Shortage

NPC: Net Present Cost

TNPC: Total Net Present Cost

DC: Direct Current

AC: Alternating Current

NASA: National Aeronautics and Space Administration

O&M : Operation and Maintenance

List of Abbreviations

General Introduction

Since the beginning of the industrial era in the mid-nineteenth century, global energy consumption has increased rapidly to meet growing demands in industry, transportation, and daily life. Conventional ES such as coal, oil, and natural gas have long played a crucial role in this development. However, the excessive use of FF has led to the depletion of these resources, rising energy costs, and serious environmental consequences, including global warming and increased greenhouse gas emissions, particularly carbon dioxide (CO_2). [1]

In response, many nations have turned to renewable energy sources — clean, sustainable, and widely available in nature. Among these, solar energy stands out as the most abundant and accessible, derived from the nuclear fusion of H_2 atoms in the sun. It remains a fundamental ES , indirectly contributing to the formation of fossil, wind, and tidal energies[2]. The availability of solar energy, however, varies between regions; while Northern Europe receives limited sunlight, North Africa and Australia benefit from some of the highest solar irradiance levels worldwide.[3]

Algeria holds a prominent position in global energy markets as a major producer and exporter of natural gas. Yet, with 93% of its energy mix still dependent on fossil fuels in 2010 [4], the country faces the urgent need to diversify its energy portfolio. Recognizing its immense solar potential, the Algerian government has launched a national RE and Energy Efficiency Program to harness solar, wind, hydro, and biomass resources.]Notably, Algeria boasts some of the world's highest solar irradiance rates, with up to 3,500 hours of sunshine annually in its southern desert regions. [5]

In this context, H2 — often referred to as the fuel of the future — offers a clean, efficient, and environmentally friendly energy carrier when produced via water electrolysis powered by RE . This approach is particularly relevant for Algeria given its exceptional solar potential. With one of the largest solar fields globally, the country is ideally positioned to emerge as a regional leader in GH production. [6]

This dissertation aims to assess the potential of solar energy in the Wilaya of M'Sila for the production of green hydrogen, combining resource analysis with system modeling and performance simulations, contributing to Algeria's energy transition and sustainable development goals.

Chapter I

The Art of Green Hydrogen Production

I.1 Introduction

The increase in energy requirements and the possibility of a lack of energy resources in the future encourage research and the production of new energy sources. The sources of RE such as wind energy and solar energy provide a promising solution to deal with these problems.

Even though there are abundant amounts of these energies, there are many technological limitations to recover and store these energies in the form of electricity. RE intermittency creates operational difficulties, particularly their integration into an electrical grid. Besides, there are other electrochemical storage systems on offer, whether in the battery or H_2 sector. H_2 is a new carrier in our future electricity storage in the energy by its electrochemical conversion in a FC. But production, storage and distribution are three major issues concerned with the industrial growth of Hydrogen energy. Despite the fact that most of today's methods of hydrogen production are based on FF, in recent years many technologies have been developed to convert solar radiation directly to H_2 . To this extent, the method of coupling a solar panel with an electrolyzer is the most utilized technology at present for the production of H_2. This process has the potential to attain the efficiency of 13% with regard to conversion of solar radiation to H_2 [7].

I.2. Oerview of Global Hydrogen Devlopment :

I.2.1 History of Hydrogen :

Hydrogen has played a significant role in scientific discovery and industrial advancement. The historical milestones in H_2 development are as follows [8]:

- **1766 :** Henry Cavendish isolated hydrogen as an element and demonstrated that it could be utilized to create water.
- **1783 :** Jacques Charles flew the first hydrogen balloon.
- **1788 :** Antoine Lavoisier named H_2 using the Greek words for "water-forming."
- **1800 :** Nicholson and Carlisle invented electrolysis, splitting water into H_2 and O using electricity.
- **1839 :** Christian Friedrich Schönbein discovered the FC effect.
- **1845 :** Sir William Grove demonstrated the first fuel cell (gas battery).
- **1920s :** Rudolf Erren converted engines to hydrogen; J.B.S. Haldane suggested the idea of renewable hydrogen.
- **1937 :** The Hindenburg disaster raised questions about H_2 safety.
- **1958 :** NASA began using liquid H_2 in rocket propulsion.
- **1959 :** Francis T. Bacon invented the first practical H_2 -air FC
- **1970 :** Interest in H_2 grew after the 1973 oil crisis. The concept of the "hydrogen economy" was born.
- **1980s-1990s:** Hydrogen vehicle, aircraft, and FC development.

- **1990s-2000s:** H_2 research gained pace with international collaborations, FC vehicle debut, and government and corporate investments.
- **2000** Ballard Power Systems presented the world's first production-ready PEMFC for automotive applications at the Detroit Auto Show.
- **2003** President George W. Bush announced in his 2003 State of the Union Address a $1.2 billion hydrogen fuel initiative to develop the technology for commercially viable hydrogen-powered fuel cells, such that "the first car driven by a child born today could be powered by FC.
- **2004** U.S. Energy Secretary Spencer Abraham announced over $350-million devoted to H_2 research and vehicle demonstration projects. This appropriation represented nearly one-third of President Bush's $1.2 billion commitment to research in H_2 and FC technologies. The funding encompasses over 30 lead organizations and more than 100 partners selected through a competitive review process. [65]
- **2004** The world's first FC-powered submarine under-goes deepwater trials (Germany navy).
- **2005** Twenty-three states in the U.S. have hydrogen initiatives in place.
- **Today-2050 Future Vision** : In the future, water will replace FF as the primary resource for hydrogen. H_2 will be distributed via national networks of H_2 transport pipelines and fueling stations. H_2 energy and FC power will be clean, abundant, reliable, affordable and an integral part of all sectors of the economy in all regions of the U.S.[65]

I.2.2 The Colors of Hydrogen :

Hydrogen can be classified by color codes, which reflect the method of its production and associated environmental impact:

- **Black or brown hydrogen :** hydrogen produced from coal gasification. Black and brown are occasionally utilized to define the coal type: bituminous (black) and lignite (brown). This production method is accompanied by high CO2 emissions (19t CO2/tH2).
- **Blue hydrogen:** Blue hydrogen is manufactured by steam reduction of natural gas. In this method, natural gas is split into hydrogen and CO2. In this steam reforming process, nevertheless, the carbon dioxide is not emitted into the atmosphere; instead, it is stored or industrially processed. Carbon Capture and Storage (CSS) technology can be employed to store CO2 underground. This means blue hydrogen also doesn't lead to any CO2 emissions. However, the long-term effects of storage are unknown and leakage can continue to damage the environment and climate. [9]
- **Green hydrogen:** First discussed in 1995, green hydrogen is produced solely from water
- renewable energy-driven electrolysis. The European green hydrogen economy
- initiative made its initial political official reference in 2020. [10]

- **Grey hydrogen :** a name for H_2 produced from FF, and mostly by steam gas reforming or coal gasification. It generates a big volume of CO2 emissions, from 10 to 19 tons of CO2 per ton of H_2 (tCO2/t H_2). Over 95% of the world's H_2 consumption is GH.
- **Orange hydrogen :** refers to novel processes for producing H_2 using plastic waste as a feedstock. It is seen as being able to address both the clean energy dilemma as well as the plastic waste problem. Orange hydrogen is in its infancy, and various technologies and processes, including pyrolysis, microwave catalysis, and photo-reforming, are being explored.
- **Pink hydrogen :** is produced by water electrolysis powered by nuclear energy, a non-fossil, clean ES with zero CO2 emissions.
- **Purple hydrogen :** is produced by water electrolysis by nuclear energy and heat.
- **Red hydrogen :** is produced by high-temperature water splitting by a catalyst with nuclear plant heat and steam. It requires significantly less electricity than conventional electrolysis.
- **Turquoise hydrogen :** this is H_2 which is produced from natural gas through methane pyrolysis, a process of breaking down the natural gas at high temperature to produce hydrogen and solid carbon. Currently, turquoise hydrogen is at the nascent stage of development.
- **Yellow hydrogen :** used as a name for GH obtained from sunpower. It is CO2 free. Yellow hydrogen is projected to become the cheapest form of renewable hydrogen in the mid-term.
- **White hydrogen :,** or natural hydrogen, is formed naturally in the Earth's crust by reactions between water molecules and iron minerals at high temperature and pressure. Hydrogen gas is released when water reacts with the minerals. There are no plans to utilize this hydrogen at present. [11]

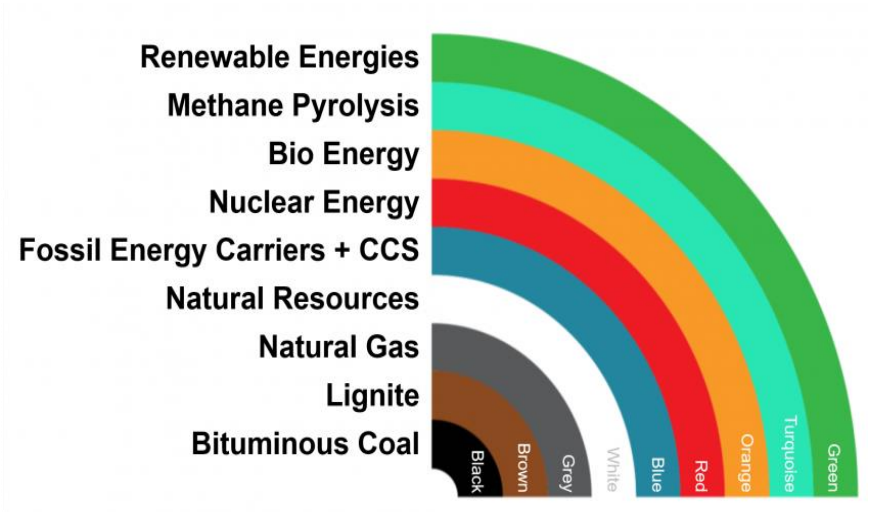

Figure I.1: The Colors of Hydrogen

I.3. Definition of Green Hydrogen :

GH is hydrogen produced via water electrolysis powered exclusively by RES such as solar, wind, or hydropower. This method contrasts with conventional hydrogen production techniques that rely on FF

and result in substantial carbon dioxide (CO_2) emissions. In green hydrogen production, the electrolysis process decomposes water (H_2O) into (H_2) and (O_2), with oxygen being the only by-product, making it a clean, sustainable, and environmentally friendly energy carrier.[12].

I.4 Hydrogen Production Techniques :

There are different ways to produce H_2, all with different carbon dioxide emissions. Currently, production H_2 is mainly made by gas reforming (62% in 2021) or by coal gasification (19%). In 2021, global hydrogen production (94 million tonnes) was responsible for 900 million tonnes of $CO2^4$. The qualifier GH refers to hydrogen that would be produced with RE, promoting production with very low CO2 emissions. Such

Hydrogen was produced in 2021 at only one million tonnes (i.e. 1% of the global production) and only 35,000 tonnes coming from electrolysis.

This chemical reaction is an oxidation-reduction reaction requiring the intervention of an anode and a cathode. In the presence of electricity, we thus obtain an oxidation reaction at the anode to recover the dioxygen and a reduction reaction at the cathode which will give GH. She accompanies herself also releases heat and has a usual efficiency of around 60% at low temperature and more of the order of 75% at high temperature.[13]

I.4.1 Steam Reforming :

The most commonly used method for producing H_2 involves an endothermic reaction between a hydrocarbon and water, catalyzed by nickel. This reaction requires an input of heat.

$$C_nH_m + nH_2O \rightarrow \left(n + \frac{m}{2}\right)\_ H_2 + nCO \qquad (I.1)$$

Synthesis gas is a mixture of hydrogen and carbon monoxide, which is produced in the first reaction. Then, to increase the hydrogen concentration, a second reaction called the "water conversion reaction" is carried out. This reaction transforms part of the carbon monoxide into carbon dioxide and H_2, which makes it possible to obtain a synthesis gas richer in H_2.

$$CO + H_2O \rightarrow H_2 + CO_2 \qquad (I.2)$$

This production step is slightly exothermic but the heat released is not sufficient to maintain the reforming reaction.

I.4.2 Partial Oxidation :

This second method of producing hydrogen involves an exothermic reaction between a hydrocarbon and oxygen.

$$C_nH_m + \frac{n}{2} O_2 \rightarrow \left(\frac{m}{2}\right)\_ H_2 + nCO \qquad (I.3)$$

As with steam reforming, conversion of the syngas is carried out. If the sulfur content of the hydrocarbon is low, the reaction can be carried out at a lower rate. temperature (850°C). This technique, however, remains much less widespread than steam reforming due to its high cost.

I.4.3 Auto-Thermal Reforming :

the combination of the two previous techniques exposed. Reforming is endothermic while oxidation is exothermic.The two processes are coupled with an adjustment of the composition of the vapor - oxygen mixture to obtain a reaction self-sustaining. The production of hydrogen from hydrocarbons is the most exploited (95% of the hydrogen production comes from hydrocarbons) [14].

I.4.4 Electrolysis :

A cleaner way to produce H_2 without using hydrocarbons involves using water as a raw material and applying an electric current. This method was discovered at the end of the 18th century and was first industrialized in 1900. Since then, improvements have been made and the first electrolyzers high-performance machines were created in 1939, with a production capacity of 10,000 Nm3 /h. THE Working principle of these electrolyzers is illustrated in Figure I.2

Several electrolyzer technologies are available. AEL uses generally concentrated potash (KOH) as electrolyte at temperatures between between 80 and 100°C and at pressures close to ambient. The PEM uses proton-conducting polymer membranes at high temperatures of around 70-80°C. Finally, the high temperature electrolyzer uses a ceramic membrane conductive to O2- ions at temperatures of around 800°C

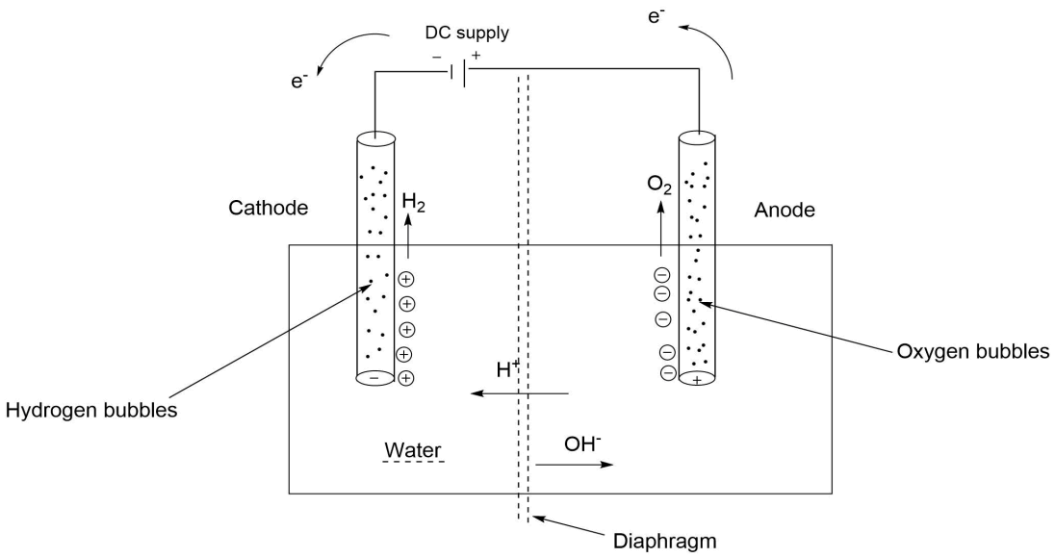

Figure I.2: Electrolysis process for hydrogen production

I.5 Potential for Green Hydrogen Production :

Supply of H_2 to industrial users is today a significant industry around the world. H_2 use, having increased over three times since 1975,- hydrogen production is essentially fuelled by fossil fuels, consuming 6% of natural gas and 2% of coal worldwide in the process- Therefore, production of hydrogen results in CO2 emissions of around 830 million tons per year. World Hydrogen production in 2019 is about 75 Mt of pure H_2 annually and 45 Mt H_2 mixed with other gases. (Show Figure I.3), nearly 55% of the hydrogen produced in the world is used in ammonia synthesis, 25% in refineries, and nearly 10% in methanol production. Approximately 10% of the world's hydrogen production is accounted for by the other applications.

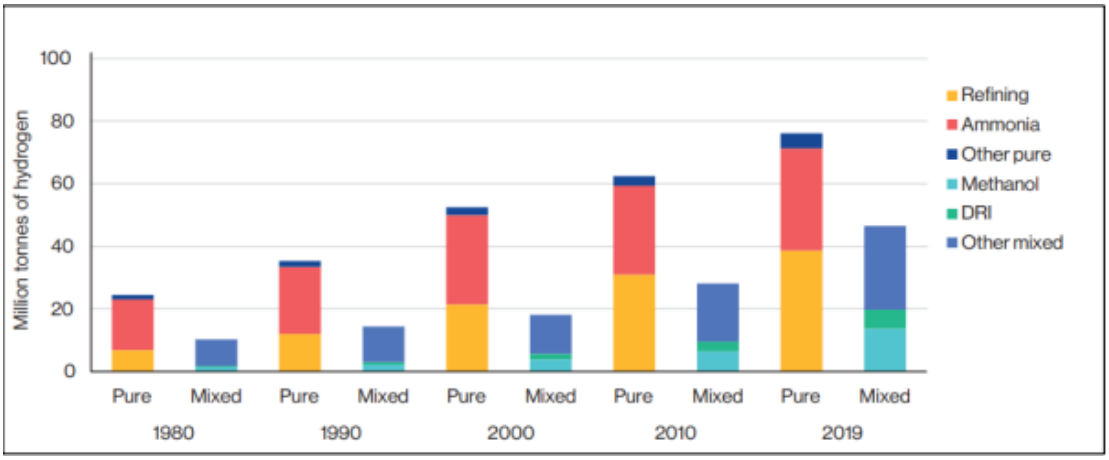

Figure I.3: Evolution of annual demand for hydrogen, 1980-2019

It is noteworthy to mention that 58% of hydrogen is manufactured on-site for captive consumption, 15% is shipped exclusively by pipeline so no shipping is needed and there is no market or disclosure on current costs. (Burchard., 2020) In the majority of nations, hydrogen is the only zero-carbon energy carrier other than electricity and ammonia that is seriously considered for low-carbon transport, industrial decarbonisation, and heat supply. Can be made from a range of renewable and non-renewable feedstock's and technical pathways , each with varying levels of greenhouse gas emissions. For H_2 to play a significant role in future low-carbon energy systems, its production must be both environmentally and economically sustainable.[26]

Table I.1 : Specifications of battery storage hydrogen production methods, their advantages, efficiency, and cost

Hydrogen production Method	Advantages	Disadvantages	Efficiency [%]	Cost [$/kg]
Steam Reforming	Developed technology & Existing infrastructure	Produced CO, CO_2 Unstable supply	74–85	2.27
Partial Oxidation	Established technology	Along with H_2 Production, produced heavy oils and petroleum coke	60–75	1.48
Auto thermal Reforming	Well established technology & Existing infrastructure	Produced CO_2 as a byproduct, use of fossil fuels.	60–75	1.48
Bio photolysis	Consumed CO_2, Produced O_2 as a byproduct, working under mild conditions.	Low yields of H_2, sunlight needed, large reactor required, O_2 sensitivity, high cost of material.	10–11	2.13
Thermolysis	Clean and sustainable, O_2-byproduct, copious feedstock	High capital costs, Elements toxicity, corrosion problems.	20–45	7.98–8.40
Electrolysis	Established technology Zero emission Existing infrastructure O_2 as byproduct	Storage and Transportation problem.	60–80	10.30

It is necessary to establish green paths of hydrogen production so that hydrogen could support clean energy transition, to generate GH around 0,04 Mt in 2010 to 0,55 Mt in 2021 It should reach the 7.92 until 2030 (Figure I.4). GH production is increasing, specifically with electrolysis, From below 1 MW in 2010 to over 25 MW in 2019 , project volume and installed electrolyzer capacity increased considerably in the last few years. Furthermore, project size rose enormously: most projects were smaller than 0.5 MW in the first half of the 2010s, whereas the largest of 2017-19 ranged from 6 MW, and others ranged between 1 to 5 MW.

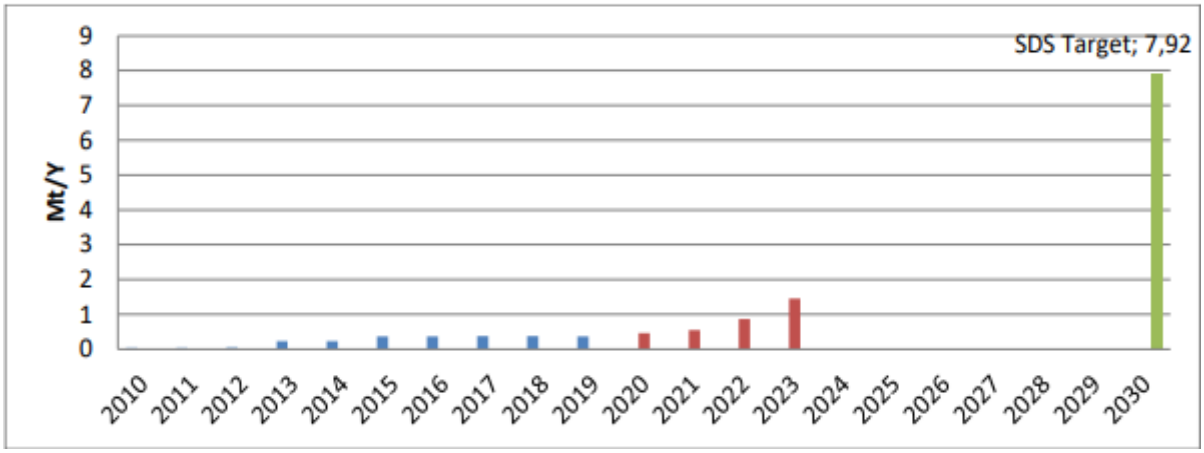

Figure I.4: Green hydrogen production, 2010-2030, historical, announced and in the Sustainable Development Scenario, 2030

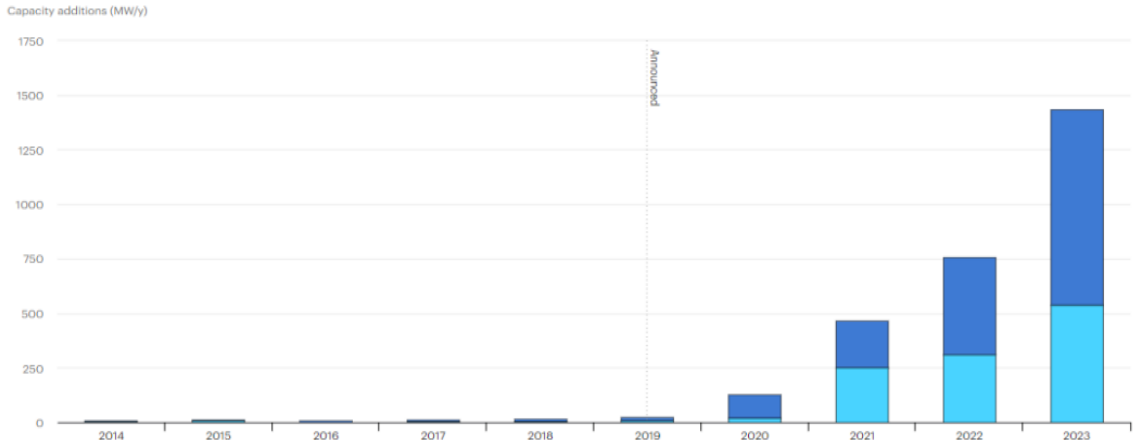

Figure I.5: Global electrolysis capacity 2014-2023, historical and announced

I.6 Hydrogen Storage Methods :

I.6.1 Storage Under Pressure :

One of the most advanced hydrogen storage techniques available today is high-pressure compression, in which H_2 is stored at pressures of up to 700 bar. The storage cylinders used in this system are primarily made from carbon fiber-reinforced composite material, which confers strength as well as lightness. As ubiquitous as it is, and as technologically advanced, this method of storage has one major drawback: the low energy density of gaseous hydrogen. This weakness is difficult to overcome when seeking to maximize the high mass energy density supplied by H_2[2]. HS by compression is an existing solution for many, but improvements have to be made to render it more efficient, less costly, and safer [15] .

I.6.2 Storage in Liquid Form :

The second widely applied hydrogen storage method is liquefaction. As evident from the H_2 phase diagram, it requires extremely low temperatures of -253°C at 1 bar pressure to convert H2 from the

gaseous state to liquid state. The primary advantage of HS in the liquid state is its significantly higher volumetric energy density. For instance, hydrogen compressed at 700 bar contains a volumetric density of approximately 42 kg/m³, whereas liquid hydrogen can deliver more mass density of approximately 70 kg/m³. Even with this advantage, however, HS in liquid form is accompanied by various challenges. The major challenge is the need for effective thermal insulation, as even minute heat transfer will cause hydrogen to evaporate. Due to the repeated phenomenon of boil-off, some amount of hydrogen is always lost as vapor and raises pressure within the storage tank. To prevent danger from explosion, excess hydrogen needs to be discharged by a safety valve, and that means losing hydrogen gradually over time. Moreover, liquefaction itself is an energy-costly process in that it extracts approximately 30% of the total energy value in the hydrogen gas. Due to these shortcomings, liquid hydrogen storage is merely utilized in specialized applications where the energy density should be extremely high and special circumstances are also required, like space exploration and space propulsion systems. [15]

I.6.3 Storage in Solid Form :

Solid state HS i.e., storage in the form of another substance, is a very promising area of research. It involves adsorption or absorption of hydrogen by materials in a manner such that it gets stored well. One excellent example is the production of solid metal hydrides through hydrogen's reaction with metal alloys. This is because of reversible chemical bonding between the atoms of the materials and hydrogen. Magnesium-based compounds and alanates are some of the most promising candidates for storage. However, among the principal weaknesses of this technology is that there is limited storage capacity for hydrogen. Currently even the best storage materials can provide a hydrogen-to-total-tank weight ratio of 2% to 3% at best. A number of issues must be resolved prior to considering mass application, however, including kinetics optimization and balancing temperature and pressure levels to provide efficient cycles for hydrogen release and absorption. [14].

I.6.4 Chemical Storage Methods:

Chemical HS methods, also known as materials-based HS, involve the interaction of hydrogen with a storage medium, unlike physical storage methods which do not rely on such interactions. These interactions can range from weak van der Waals forces to strong covalent or ionic bonds, or intermediate interactions such as those described by the Kubas mechanism. The strength and nature of these interactions determine the operational parameters of the storage system, such as the temperature and pressure required for hydrogen absorption and release. In these methods, hydrogen is stored in chemical compounds capable of undergoing reversible reactions—such as hydrolysis or dehydrogenation—to release hydrogen when needed. Notable examples include ammonia (NH_3) and hydrazine (N_2H_4). These chemical storage methods offer the advantages of high energy density and the potential for reversible

storage, making them suitable for long-term and decentralized energy storage applications. However, several challenges remain. These include the development of efficient and durable catalysts, the reprocessing of spent compounds, and safety concerns related to the handling and storage of reactive chemical substances. Addressing these issues is essential for the practical implementation and scalability of chemical hydrogen storage systems [16].

A. Hydrogenation of Organic Compounds:

Liquid Organic Hydrogen Carriers (LOHCs) offer a promising solution for safe and efficient hydrogen storage and transportation. These compounds—such as methylcyclohexane and formic acid derivatives—can reversibly bind and release hydrogen through chemical reactions [17]. This reversible behavior makes them stable and attractive alternatives to conventional hydrogen storage methods. A key advantage of LOHCs is their high energy density, comparable to that of liquid hydrogen. Additionally, they can be stored and handled under ambient pressure and temperature, simplifying the requirements for storage and distribution. Unlike gaseous hydrogen, which necessitates specialized infrastructure, LOHCs can be transported using existing logistics systems, making them economically viable for large-scale deployment. In practical applications, such as vehicular use, LOHCs are introduced in precise amounts into a reaction chamber, where hydrogen is released without the need to heat the entire storage medium. This localized reaction improves overall system efficiency and reduces energy losses. Despite these benefits, LOHC technology still faces several challenges. Key areas of improvement include the development of more effective catalysts for hydrogen release and uptake, better heat management, and efficient regeneration of spent carriers. Further research is required to optimize catalyst performance under fluctuating operational conditions and to enhance the thermal stability of LOHC systems [17]. Moreover, LOHCs are still relatively underexplored in the context of large-scale hydrogen storage. Comprehensive studies are needed to evaluate their toxicity, ensure operational safety, and develop industrial-scale production and regeneration methods. Only through such in-depth research can the full potential of LOHCs be realized, enabling their practical implementation in commercial hydrogen storage and transport systems [18].

B. Metal Hydrides:

Metal hydride storage systems offer a possible future technology for hydrogen storage effectively and safely, and exhibit some benefits over traditional gaseous or liquid-based storage methods. The systems take advantage of solid metal alloy materials that can chemically absorb hydrogen molecules at comparatively mild temperatures and pressures, with high volumetric and gravimetric hydrogen density appropriate for stationary and portable applications [36]. Hydrogen storage by metal hydrides involves an intermetallic alloy phase capable of sorbing and hold hydrogen by chemical bonding. It is formed by

reactions involving hydrogen and a metallic phase or through the formation of covalent hydrides. Following chemical theory, brought into contact with hydrogen under some pressures and temperatures, these phases absorb vast quantities of hydrogen gas to form the corresponding metal hydrides [36]. The process securely positions hydrogen in the intermetallic lattice with efficient storage retained [19]. One of the greatest advantages of metal hydride storage is its intrinsic safety compared to compressed gas or liquid hydrogen storage. Such safety is governed by rules of chemical bonding and intermolecular forces that prevent rapid release of hydrogen under circumstances. In addition, some intermetallics, including metals and alloys, can store hydrogen with a greater volume density than liquid hydrogen, as dictated by the laws of thermodynamics and gas behavior. To succeed, metal hydride alloys must possess some features, like having the ability to absorb and give off a large amount of hydrogen gas without injuring the storage material. These qualities are regulated by materials science rules and thermodynamic principles to generate the storage system stability and reliability. Additional suitable metal hydrides must be able to absorb and give off hydrogen at controlled rates, which may be realized through altering temperature and pressure conditions according to principles of reaction engineering and kinetics [19].

I.7 Qualitative comparison of storage methods :

The hydrogen storage device metal hydride DASH is remarkable with its significantly reduced environmental footprint compared to existing competing energy storage systems such as lithium batteries. The storages are entirely recyclable and energy used during the manufacturing process of the storages is far less. The features of such a form of hydrogen storage are emphasized and compared to other forms of hydrogen storage in the following table:

Table I.2 : Qualitative comparison of storage methods [20]

	Pressurized gas (low pressure)	Pressurized gas (high pressure)	Liquid	Solid state
Levelized cost of storage	Low	High	High	Low
Compressor or liquefier required	No	Yes	Yes	No
Volumetric density	Very low	Intermediate to high (700 bar(g))	High	Very high
Energy losses during charging/discharging	No	Yes (compression)	Yes (liquefaction)	No
Safety characteristics	Acceptable	Acceptable	Acceptable	Excellent

Typical pressure levels	30 bar(g)	200-700 bar(g)	Ambient	Ambient to 45 bar(g)
Other advantages	• Widely available • Low CAPEX		• Scalable	• Maintenance free
Other disadvantages	• Not the entire storage capacity can be used • Safety-related restrictions and cost	• Not the entire capacity can be used • Safety-related restrictions and cost	• Safety-related restrictions and cost • Technical complexity: boil-off, continuous cooling required, etc.	• Lower gravimetric density

I.8 Hydrogen Transport Methods :

Hydrogen can be transported in three primary ways, depending on the distance, volume, and physical state during transportation.

I.8.1 Pipelines :

Pipelines represent the most economical and efficient way to transport hydrogen over long distances for large volumes. Dedicated hydrogen pipelines are expensive to build, though, and require long-term certainty in hydrogen demand and supply in order to be economically feasible. In order to reduce cost and accelerate deployment, existing natural gas pipelines can be recycled for transporting hydrogen, if they meet the necessary technical requirements to mitigate the risks of embrittlement, which can weaken pipeline materials over time. Repurposing natural gas infrastructure to transport hydrogen also makes it easier to blend hydrogen into existing gas grids, offering a transition strategy to increase hydrogen take-up. Blended hydrogen can be used in industrial, commercial, and residential uses of numerous types, facilitating the development of demand while market and infrastructure readiness for the distribution of pure hydrogen further develops. Furthermore, dedicated hydrogen pipeline networks ought to be a key component of the future hydrogen economy, connecting production hubs with major industrial and energy-consuming zones.[21]

I.8.2 Trucks :

The transportation of liquid hydrogen by truck is the most common method for supplying hydrogen refueling stations, as is the case with demonstration stations implemented in many countries. The hydrogen is stored in cylindrical cryogenic tanks, similar to those used by tanker trucks for transporting liquids. These vehicles can carry up to 3.5 tons of liquid hydrogen, with a total weight of 40 tons. When used in large quantities as a basic chemical substance (such as in the petroleum industry or ammonia synthesis), hydrogen is generally transported via pipeline. Liquid transport by truck is typically reserved for applications requiring smaller quantities, such as in the electronics industry [22].

I.8.3 Tanker ships :

Tanker ships are becoming a significant choice for transporting bulk hydrogen over long distances, particularly for international trade. They carry liquid hydrogen (LH_2), liquid hydrogen organic carriers (LHOCs), and ammonia, which are good hydrogen carriers. However, it is still costly to ship hydrogen due to additional energy required for liquefaction or chemical conversion and the custom ship design to prevent material embrittlement. H_2 must be cooled to -253°C in order to liquefy, or converted to ammonia or LHOCs, which both have further processing costs. Despite these challenges, technology advances in hydrogen shipping, storage and infrastructure stand to make cost competitiveness improvements to permit bulk trade of H_2 and enable world energy transition. [21].

I.9 Applications of Green Hydrogen :

GH is significant in various industries and sectors, offering sustainable and clean energy solutions. The most notable applications include :

I.9.1 Transport

Green hydrogen is an option as a fuel for vehicle internal combustion engines or FC. Unlike traditional fuels, it does not give off harmful fumes when combusted. Not only restricted to personal cars, some corporations already started sending H_2 -powered lorries. Even plans for building the first commercial H_2 -powered aeroplanes were already announced to start in 2035..

I.9.2 Heating

GH is employed in the production of gas to use for household heating and cooking. The United Kingdom, for instance, intends to start supplying homes with hydrogen-based energy as early as 2050.

I.9.3 Green ammonia production :

GH also has a major role to play in the manufacturing of green ammonia, which is vital for producing fertilizer. Green ammonia is anticipated to be a low-cost replacement for gray ammonia by 2030, previously produced with the help of fossil fuels.[23]

I.10 MSila Solar potential applications :

Over the past decade, M'Sila has experienced a spectacular increase in electricity consumption, doubling, as illustrated. The increase in energy demand is largely attributed to improvements in living standards, urbanization, and increased use of electrical appliances in domestic, business, and industrial settings. Now, much of M'Sila's electricity, as in much of the world, comes from FF. with disastrous environmental consequences. Combustion of FF releases enormous amounts of carbon dioxide (CO_2) and other greenhouse gases, which cause global warming and degradation of the environment. In fact, electricity generation alone accounts for nearly 40% of total CO_2 emissions worldwide, and it is among the largest causes of global warming. These are then trailed by transportation and industrial emissions.

In the wake of such challenges, the transition to clean ES such as solar power to prevent environmental harms and facilitate sustainable development is unavoidable. M'Sila, a region with high solar radiation and adequate land resources, is a privileged location to adopt solar energy programs. Utilization of (CSP) and (PV) systems can substantially reduce fossil fuel reliance, reduce carbon footprint, and ensure energy security for the region. Solar energy infrastructure investment in M'Sila would not only enhance clean power generation but also enhance economic growth, create job opportunities, and enhance technological development in the renewable energy sector. By exploiting its solar resources, M'Sila can be at the forefront of sustainable energy development, in support of national and global efforts towards climate change mitigation. [24]

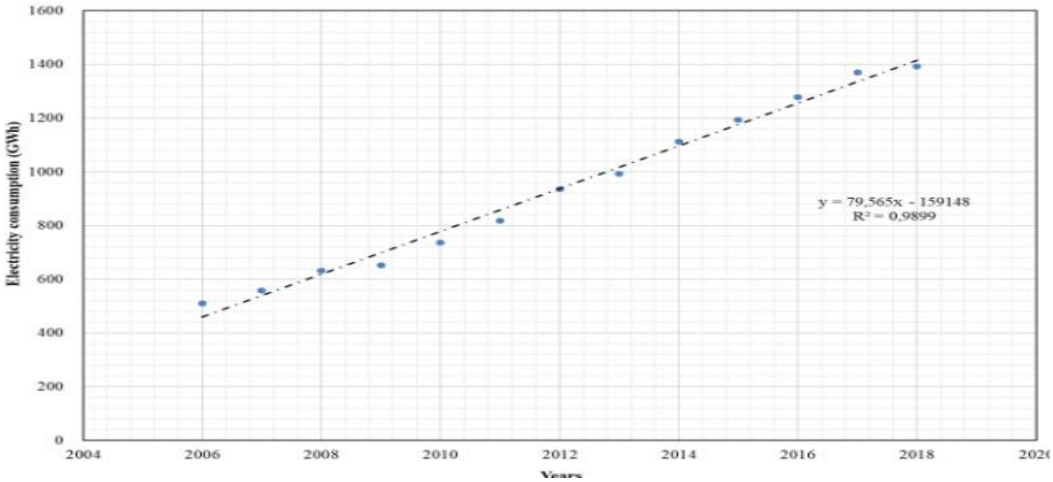

Figure I.6: Electricity consumption from 2006-2018 in M'Sila

Figure I.7 presents the highest annual average temperature and annual average temperature of M'Sila throughout the research duration. As can be seen, the maximum ambient average temperature does not surpass 40°C and even attains a value above 30°C. As such, polycrystalline PV modules are therefore advised and to be promoted as well as installed in M'Sila. [24]

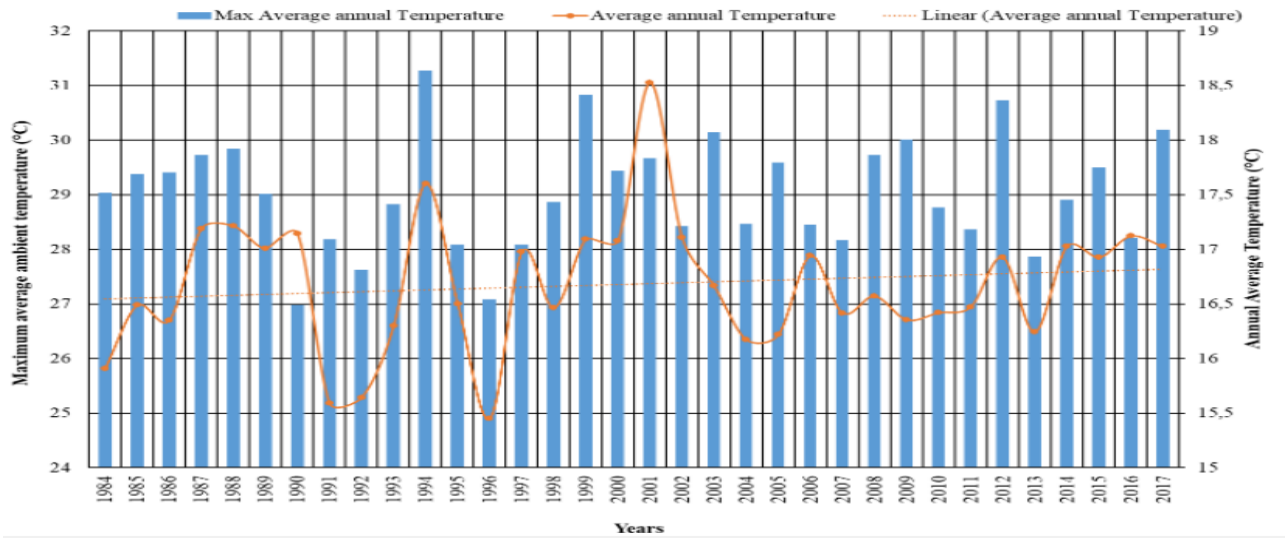

Figure I.7: Evolution of the maximum average annual temperature and annual average temperature in M'Sila over 34 years

To provide an idea, without doing any calculations, Oued Kebrit, located in the North East of Algeria, has a solar potential similar to M'Sila with a GHI of 1808 kWh/m2. A 15 MWp solar power plant has been commissioned over 32 hectares of this land. This plant has been in operation since 2015. Finally, we can also use M'Sila's solar potential to generate domestic hot water, cooking, etc. with very good efficiency because it is heat to heat conversion .[24]

I.11. Conclusion

Green hydrogen represents a vital solution for achieving a sustainable and low-carbon energy future. Produced through water electrolysis powered by renewable sources, it offers a clean alternative to fossil-fuel-based hydrogen. This chapter has highlighted the various production methods, storage and transport technologies, and key applications of hydrogen, with emphasis on the unique advantages of green hydrogen. While challenges remain in terms of cost, infrastructure, and efficiency, ongoing research and technological progress are steadily advancing its feasibility. The case of M'Sila demonstrates the regional potential for solar-powered hydrogen production, reinforcing Algeria's capacity to contribute to the global energy transition.

Chapter II

Modeling of PV system - Electrolyzer

II.1 Introduction

Hydrogen can become the best energy carrier because of its immense energy content along with ecologically friendly nature. Surely, one of the most eco-friendly methods of hydrogen production is the use of renewable energy sources such as solar photovoltaics (PVs). During this process, solar power is used to transform into electrical energy by PV cells, which is then used to fuel an electrolyzer to split water into hydrogen and oxygen using the process of electrolysis. It does not involve the use of fossil fuels and no CO_2 emissions, thus a clean and renewable way to hydrogen production (Gibson & Kelly, 2008).

To analyze the performance and efficiency of such a system, one needs to be aware of the mathematical models behind the PV system as well as the alkaline electrolyzer. The overall efficiency of the system depends on the power output of the PV array, the voltage-current characteristics of the electrolyzer, and various losses related to energy conversion..[25]

II.2. Photovoltaic Generator (PVG)

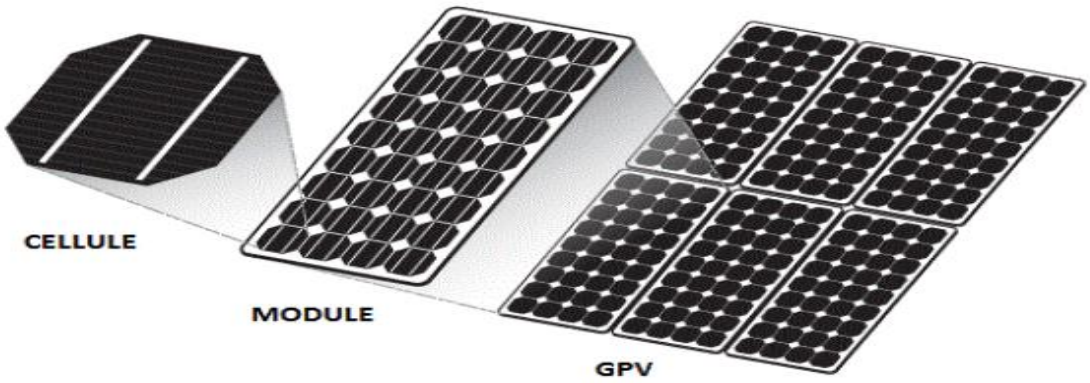

Figure II.1: Components of a PVG

Solar cells are usually connected in series and parallel configurations, and encapsulated under glass to form a photovoltaic (PV) module. A PV generator consists of various modules connected to form one unit to generate a high direct current (DC) power equivalent to standard electrical equipment (see Figure II.2). Solar modules are usually connected in series-parallel to achieve high voltage and current output of the generator. he paired modules are supported on metal supports and sloped at an optimal angle depending on the site location. Such a complete arrangement is also referred to as a module field [26].

II.2.1 Modeling of a Photovoltaic Cell

A photovoltaic (PV) cell can be modeled by an equation that characterizes the static behavior of the PN junction in a typical diode. Figure (II.3) is an equivalent circuit of a real PV cell

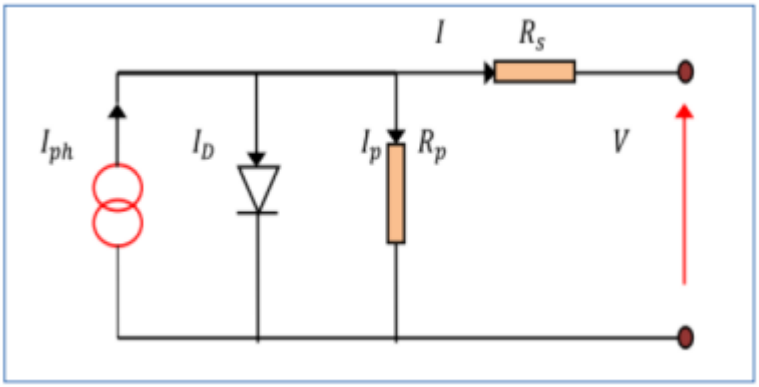

Figure II.2: Equivalent Circuit of the PV Cell

In this equation, the short-circuit current and various resistances modeling connection-related losses are taken into account. Under static conditions, the behavior of a PV cell consisting of a silicon-based PN junction can be described by the following equation [15]:

$$I = Iph - ID - IP \qquad \text{(II.1)}$$

I= current supplied by the cell

$I_{sc}=I_{scr}\ (\frac{G}{1000})$: ou I_{scr} is the reference short-circuit current

$$I_p = \frac{V+I.Rs}{Rp} \qquad \text{(II.2)}$$

I_P: current flowing through the parallel (shunt) resistance.

$$I_D=I_0\ (e^{(\frac{V+I.Rs}{nVT})} - 1) \qquad \text{(II.3)}$$

I_D: current flowing through the diode

I_0 = reverse saturation current of the diode.

n : diode ideality factor, typically ranging between 1 and 5 in practice.

$$V_T = \frac{KT}{e} \qquad \text{(II.4)}$$

V_T: thermal voltage

Ou :

e : electron charge (1.602×10−19 C).

K : Boltzmann constant (1.381×10−23J/K).

T : effective temperature of the cell in kelvin.

Using the above equations, the expression for the output current of the photovoltaic cell can be derived.

$$I=I_{ph} - I_0\ (e^{(\frac{V+I.Rs}{nVT})} - 1) - \frac{V+I.Rs}{Rp} \qquad \text{(II.5)}$$

II.2.2 Principle of operation of the cell photovoltaic :

The functioning of a photovoltaic cell is based on the photovoltaic effect, through which the sun's light energy is directly converted to electrical energy. It occurs as a result of the formation and flow of positive and negative electrical charges in a semiconductor material upon illumination.

Photovoltaic cells are primarily constructed from silicon ingots, which are treated and cut into thin wafers. The wafers are P-type or N-type, depending on whether they have been doped with materials such as boron (to create a P-type) or phosphorus (to create an N-type). Creating a PN junction—a border between two regions with mutually exclusive doping types—is the secret to creating a functional solar cell.

An electric field is established at the PN junction that allows for the ongoing separation of the positive and negative charges produced by sunlight. Metallic contacts are applied on the surface of the cell to draw out the generated electricity effectively. The contacts are typically in the form of a grid with a front contact to accept electrons and a rear contact to complete the circuit, as illustrated in Figure II.3 [27]

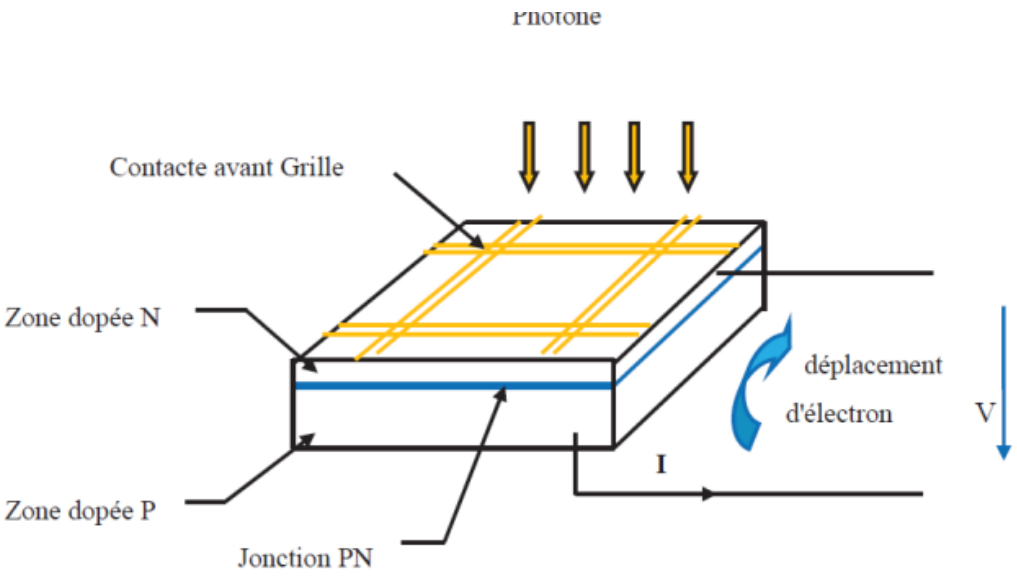

Figure II.3: schematic representation of a PV cell

II.2.3 Mathematical equivalent circuit for photovoltaic array:

The model of the PV cell circuit is shown in Figure II.3 Iph is the cell current source of photocurrent. Rsh and Rs are cell intrinsic shunt and series resistances. Rsh is generally very large and Rs is very small and can thus be neglected for simplicity in calculation (Pandiarajan and Muthu 2011). Actually, PV cells are packaged into higher units called PV modules and the modules are connected in series

or parallel to create PV arrays which are utilized to generate electricity in PV generation systems. Equivalent circuit of a PV array is shown in Figure II.4 Voltage–current characteristic equation of a solar cell is represented by [28]:

Module photo-current Iph:

$$I_{ph}=[I_{sc}+(Ki\ (T-298)]\times Ir)/100 \qquad (II.5)$$

Here,

Iph: photo-current (A);

Isc: short circuit current (A) ;

Ki : short-circuit current of cell at 25 °C and 1000 W/m2 ;

T: operating temperature (K);

Ir: solar irradiation (W/m2).

Module reverse saturation current Irs:

$$I_{rs}= I_{sc}/\exp\ (qVoc\ /Ns\ Kn\ T)-1 \qquad (II.6)$$

Here,

q: electron charge, = 1.6 × 10−19C;

Voc: open circuit voltage (V);

Ns: number of cells connected in series; n: the ideality factor of the diode;

k: Boltzmann's constant, = 1.3805 × 10−23 J/K.

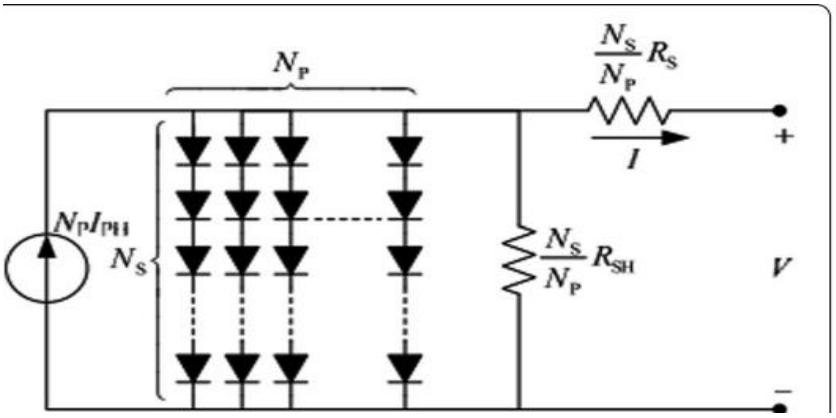

Figure II.4: Equivalent circuit of solar array

The module saturation current I_0 varies with the cell temperature, which is given by:

$$I_0 = I_{rs} + \frac{T^2}{T_r}\exp\left[\frac{q(E_{g0})x^2}{nK}\left(\frac{1}{T} - \frac{1}{T_r}\right)\right] \quad \text{(II.8)}$$

Here,

Tr: nominal temperature = 298.15 K

E_{g0}: band gap energy of the semiconductor, = 1.1 eV

The current output of PV module is:

$$I = N_P \times I_{ph} - N_P \times I_0 \times \exp\left[\left(\frac{\frac{V}{N_S} + I \times \frac{R_S}{N_P}}{n \times V_t}\right) - 1\right] \quad \text{(II.9)}$$

With

$$V_t = \frac{K \times T}{q} \quad \text{(II.10)}$$

and Here:

Np: number of PV modules connected in parallel:

Rs: series resistance (Ω)

Rsh: shunt resistance (Ω)

Vt : diode thermal voltage (V).

- **Electrical Model**

The equivalent electrical circuit of the PV cell is shown in Figure II.5 . It is a single diode model that is also known as the 5 parameter circuit. The cell can also be modeled by other equivalent circuits; such as 7 parameters but the one-diode model is the most popular circuit in literature and the solution of the circuit is not as complicated as it is in other models. The circuit parameters are; I_D, I_L, I_{SH}, R_{SH}, R_S, I and [29]

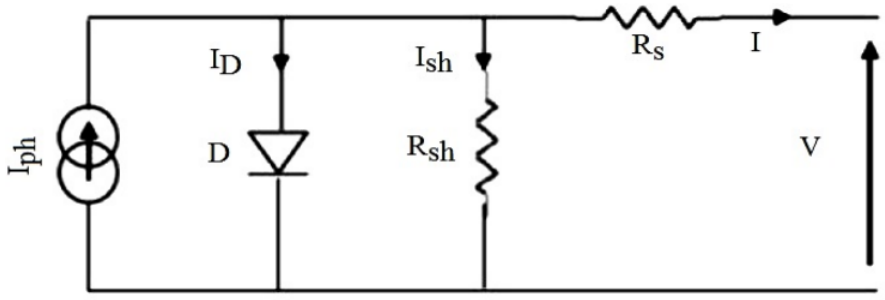

Figure II.5: Equivalent electrical diagram of the photovoltaic cell

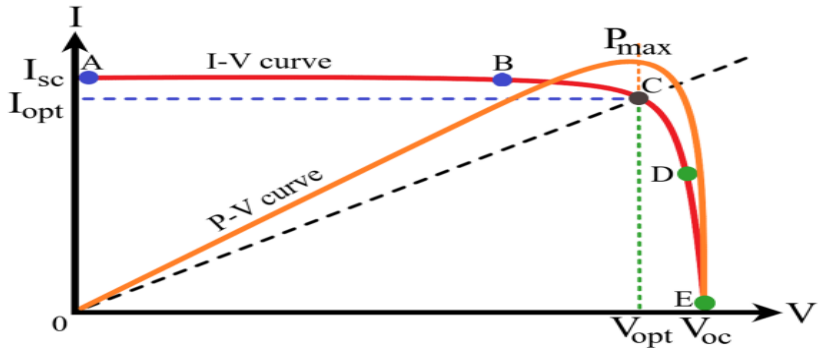

Figure II.6: Typical current-voltage characteristics of the PV cell

Single diode model

From the circuit;

$$I = I_{PH} - I_D - I_{SH} \qquad \text{(II.11)}$$

from Shockley's diode equation;

$$I_D = I_0 \left[\exp\left(\frac{(V+IRs)}{nVT}\right) - 1\right] \qquad \text{(II.12)}$$

Where;

$$V_T = \frac{KT}{q} \qquad \text{(II.13)}$$

By Ohm's Law;

$$I_{SH} = \left[\left(\frac{V+IRs}{R_{sh}}\right) - 1\right] \qquad \text{(II.14)}$$

II.2.4 Boost circuit and its control

For first-stage PV generation system, boost chopper circuit is applied at all times as the boost DC/DC converter. The DC-DC converter boosts the low solar voltage to an adequate voltage according to the ideal PV power. A capacitor is normally inserted between PV array and the boost circuit, used to reduce high frequency harmonics.

The boost converter duty cycle is determined by MPPT control system, then repeatedly perturbing between 0 and 1. Ts is a switching cycle period. During the IGBT is closed, inductance voltage and capacitor voltage obey the following relationship [30]

$$L_{pv}\frac{dI_{pv}}{d_t} = v_{pv} = v_{L(ON)} \quad \text{(II.15)}$$

$$C_{dc}\frac{dV_{dc}}{d_t} = I_{dc} = i_{C(ON)} \quad \text{(II.16)}$$

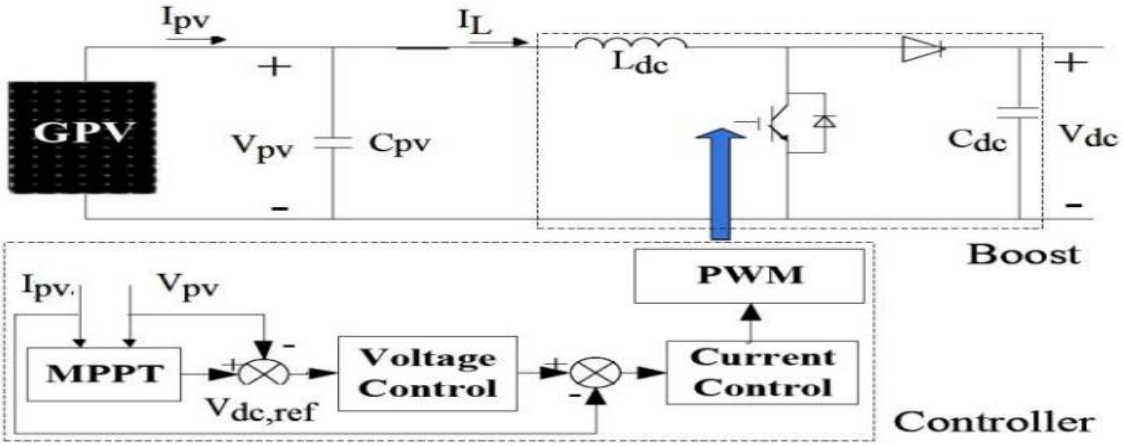

Figure II.7: Boost circuit and its control[30]

Similarly, when the IGBT is open, the equations of inductance voltage and capacitor voltage are described as:

$$L_{pv}\frac{dI_{pv}}{d_t} = v_{pv} - v_{dc} = v_{L(Off)} \quad \text{(II.17)}$$

$$C_{dc}\frac{dV_{dc}}{d_t} = I_{dc} - I_{pv} = i_{C(Off)} \quad \text{(II.18)}$$

The maximum power point by regulating the duty cycle α is used to control the boost converter as shown in Figure 9. The P&O algorithm is used to find the maximum power point of the PV system

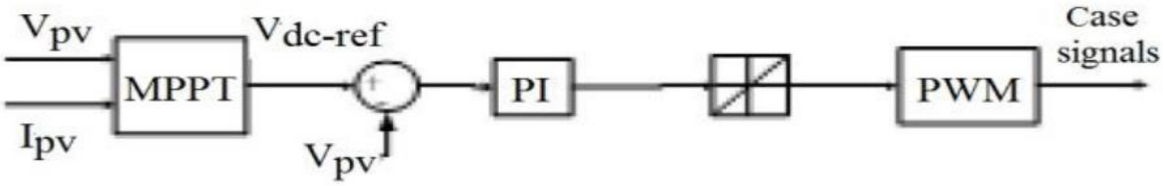

Figure II.8: Control structures of boost converter and MPPT algorithm [30]

Photovoltaic (PV) systems always have a DC-DC converter, whose role is to regulate power output. This converter is controlled by the Maximum Power Point Tracking (MPPT) algorithm such that the PV system operates at its Maximum Power Point (MPP), where it produces the maximum amount of power for given environmental conditions. Working of the MPPT system is shown in Figure II.8 ,

which shows how the system optimizes power extraction from the PV array. The MPPT continuously monitors critical electrical parameters, typically input voltage, input current, output voltage, and output current of the PV system. Depending on this real-time data, the MPPT computes the optimal operating point and supplies appropriate control signals to the DC-DC converter.

To achieve this, the sensed data is contrasted with the reference values and an error is calculated. With the error, the system then corrects the Pulse Width Modulation (PWM) signals regulating the duty cycle of the DC-DC converter. This real-time control ensures that the PV system will run at the precise point where maximum power output can be obtained, irrespective of fluctuations in environmental factors like solar irradiance and temperature.. [31]

II.3.5 Equivalent Mathematical Model

Applying Kirchhoff's laws to the two equivalent circuits corresponding to the two operating phases yields: :

$$I_{C1} = C_1 \frac{dVpv}{dt} = I_{PV} - I_L \quad \text{(II.19)}$$

$$I_{C2} = C_2 \frac{dV0}{dt} = -I_0 \quad \text{(II.20)}$$

$$V_L = L \frac{dIL}{dt} = V_{PV} - R_L I_L \quad \text{(II.21)}$$

$(1 - \alpha)\, Ts$: For the first interval

$$I_{C1} = C_1 \frac{dVpv}{dt} = I_{PV} - I_L \quad \text{(II.22)}$$

$$I_{C2} = C_2 \frac{dV0}{dt} = I_L - I_0 \quad \text{(II.23)}$$

$$V_L = L \frac{dIL}{dt} = V_{PV} - V_0 - R_L I_L \quad \text{(II.24)}$$

II.3 Maximum Power Point Tracking Algorithms

II.3.1 An overview of Maximum Power Point Tracking :

A typical solar panel can only convert 30 to 40 percent of the incident solar irradiation into electrical energy. Maximum power point tracking method is used for maximizing the efficiency of the solar panel. The power delivered by a circuit, according to Maximum Power Transfer theorem, is maximum when the Thevenin impedance of the circuit (source impedance) is equal to the load impedance. Thus our problem of maximum power point tracking is reduced to an impedance matching problem. On the source side we are using a boost convertor which is supplied through a solar panel to boost the output

voltage so that it can be used for different applications like motor load. By suitably adjusting the duty cycle of the boost converter we can match the source impedance with the load impedance.

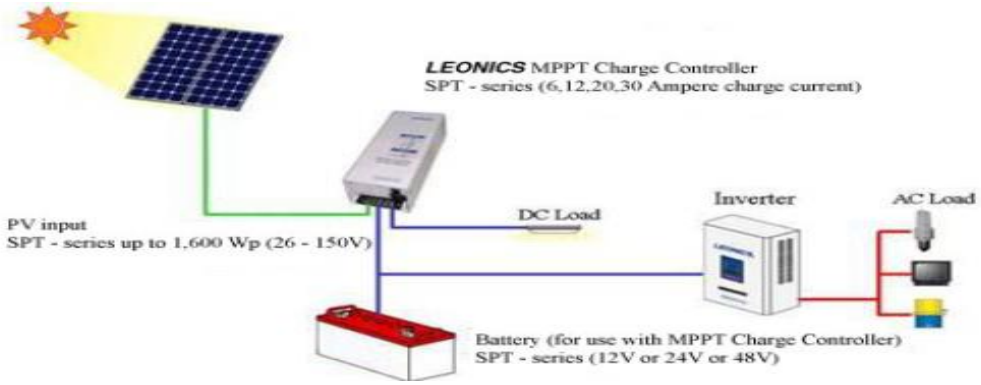

Figure II.9 : General configuration of the MPPT solar charge controller

II.3.2 MPPT Control Principle :

To improve the available power from solar panels, a (MPPT) is needed. MPPT commands continuously adjust the duty cycle associated with the static converter that charges the battery. Many researchers have reviewed and compared various MPPT techniques available in the literature [32]. In his thesis, Belkaid Abdelhakim indicates that there are about thirty MPPT techniques [33]. These MPPT commands can be compared based on their reliance on the parameters of the solar panels, their complexities, and their type of implementation, whether analog, digital, or hybrid [33]. Among these commands, the most well-known are: the Perturb and Observe (P&O) method, the Incremental Conductance (IncCond) method, the Constant Current technique, and the Constant Voltage technique [33]. In recent years, techniques based on Fuzzy Logic and Neural Networks

have also emerged. In this document, only the P&O technique will be presented.

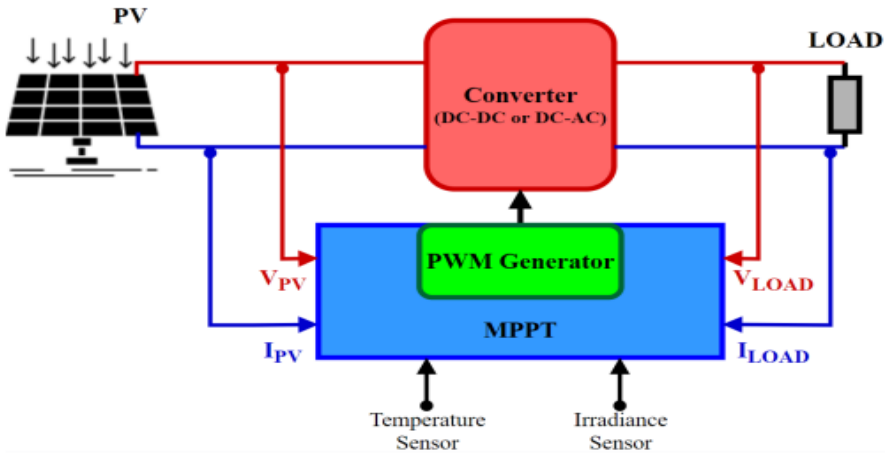

Figure II.10 Operating scheme of the MPPT system

II.3.3 Type of MPPT :

A. The Perturb and Observe (P&O) :

algorithm is the most widely used MPPT method due to its simplicity and low computational requirements. It works by continuously measuring the voltage and current of a PV array, making slight perturbations in the voltage, and measuring the resulting change in power output. As power grows, the disturbance persists in the same direction .When power falls, the direction of perturbation reverses. This cyclical process helps the system to track the (MPP) well. P&O tends to cause small oscillations around the MPP and is sluggish in responding to abrupt environmental conditions. Despite these limitations, it remains extremely popular due to its simplicity of implementation and satisfactory performance under stable conditions.[48]

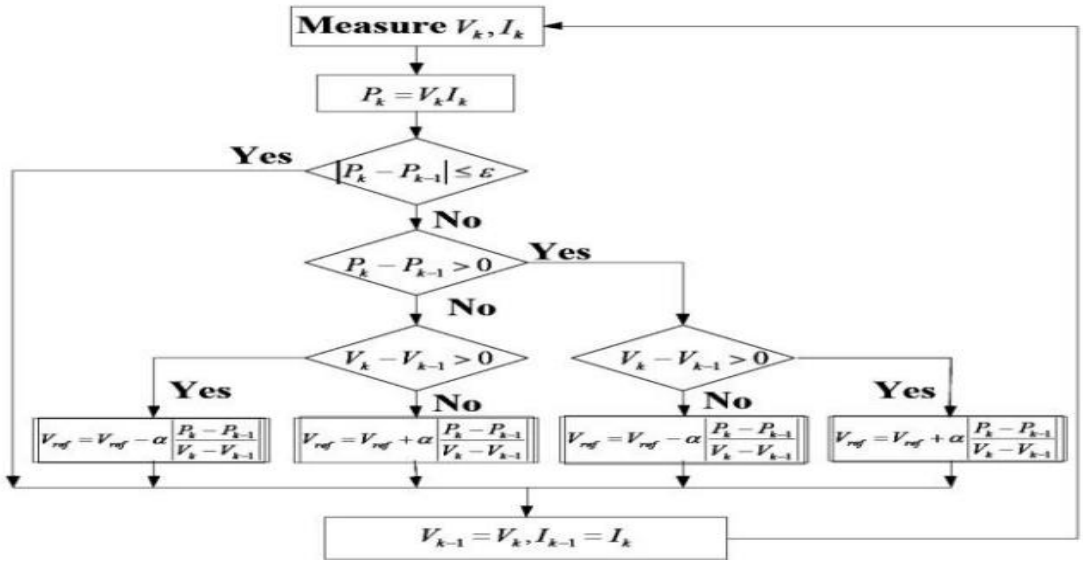

Figure II.11 The flow chart of the P&O algorithm.

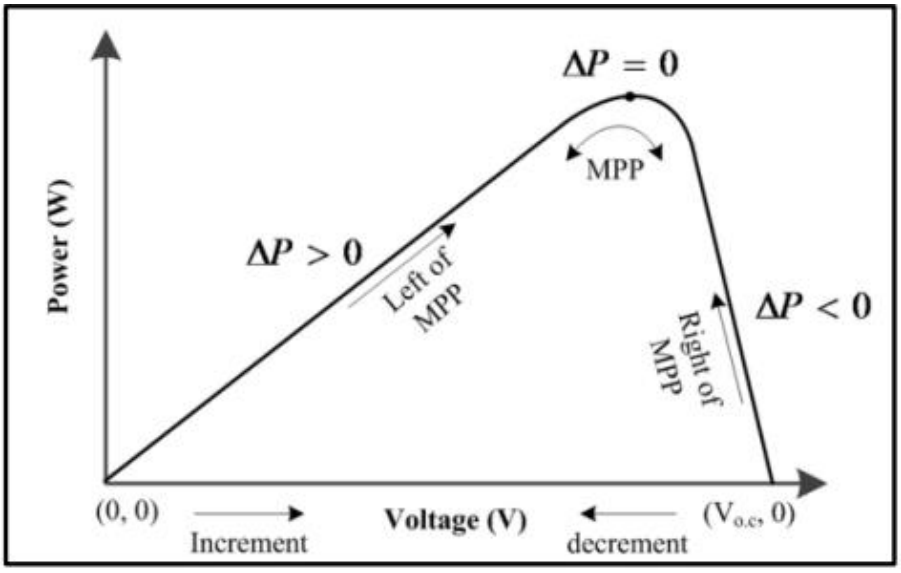

Figure II.12 Typical Power-Voltage characteristic

Where Vk, Ik are respectively the current and voltage of PV array at the instant; Vk-1, Ik-1 are respectively the voltage and current of PV array in the last sampling instant. P&O scheme works well under slowly varying environment but has some shortcomings for fast varying atmospheric conditions. Power increment d P and voltage increment dV have the following relation from the characteristics curves of PV array:

At the left of MPP- dP dV > 0

At the right of MPP- dP dV < 0

At the MPP- dP dV = 0

Besides, as the operation point is nearer to the MPP, the value of dP dV is smaller and smaller; in this manner, the perturbation can be represented as dP dV. The perturbation is big when the operation point is far from the MPP, and the perturbation is small when the PV array is operating near the MPP

B. Incremental Conductance (IncCond) :

The Incremental Conductance (IC) algorithm was developed in 1993 as an improvement on the Perturb and Observe (P&O) algorithm. It was designed specifically to prevent some of the limitations of P&O, including its oscillation near the Maximum Power Point (MPP) and its slower response to abrupt solar irradiance changes.

The IC algorithm is based on exploring the PV characteristic curve, primarily the relationship of voltage (V), current (I), and power (P). The greatest concept is how to discover the point of working versus the MPP by means of testing for the incremental volt-amp changes [35].

The fundamental principle behind this method is derived from the power equation::

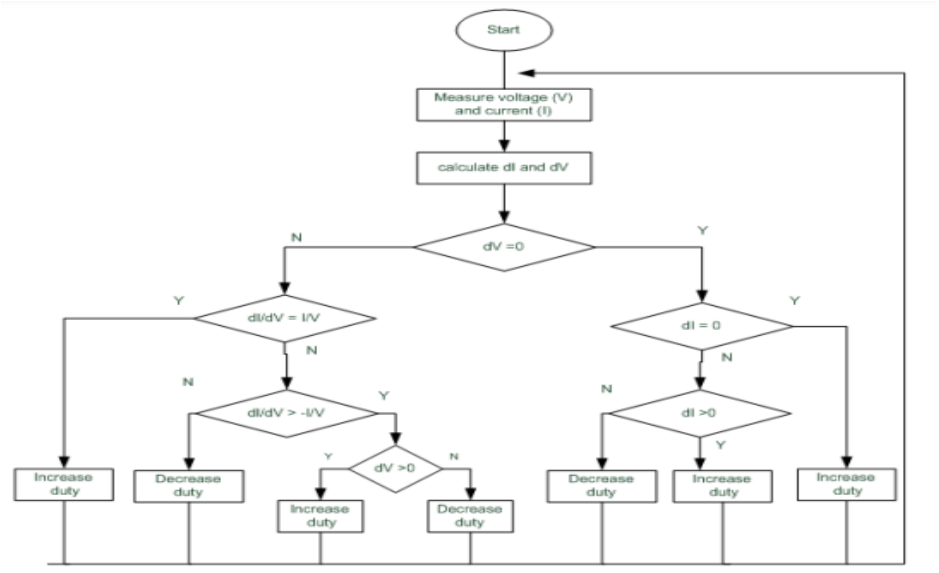

Figure II.13 .incremental conductance flow chart

If MPP is to the right, dI/dV< -I/V and now the PV voltage must be decreased to reach the MPP. IC methods can be used for MPP detection, improve the PV efficiency, reduce power loss and system cost. Application of IC on a microcontroller yielded more stable output when compared to P&O. The

vibration around MPP area also can be removed in trade off with its implementation complexity. Time tracking still not as fast as the voltage increase and decrease had been selected manually by trial and error. IC algorithm can be seen on Figure II.13

C. Fuzzy Logic Controller Based MPPT Techniques

The application of fuzzy logic control has grown in popularity in the past decade due to the fact that it is capable of handling imprecise inputs, does not require an accurate mathematical model and is capable of handling nonlinearity. Microcontrollers have also contributed to the widespread use of fuzzy logic control. The fuzzy logic has three stages: fuzzification, inference system and defuzzification. Fuzzification entails the process of converting numerical crisp inputs to linguistic variables based on the degree of membership to specific sets. Membership functions, like those in Figure 15, are used to allocate a grade to each linguistic term. The quantity of membership functions used is ascertained based on the accuracy of the controller but in most cases, between 5 and 7. Seven fuzzy levels are used in Figure 15: NB (Negative Big), NM (Negative Medium), NS (Negative Small), ZE (Zero), PS (Positive Small), PM (Positive Medium) and PB (Positive Big). The values a, b and c are calculated from the range values of the numerical variable. In certain cases the membership functions are chosen less symmetric or even optimized for the application for greater precision.[36]

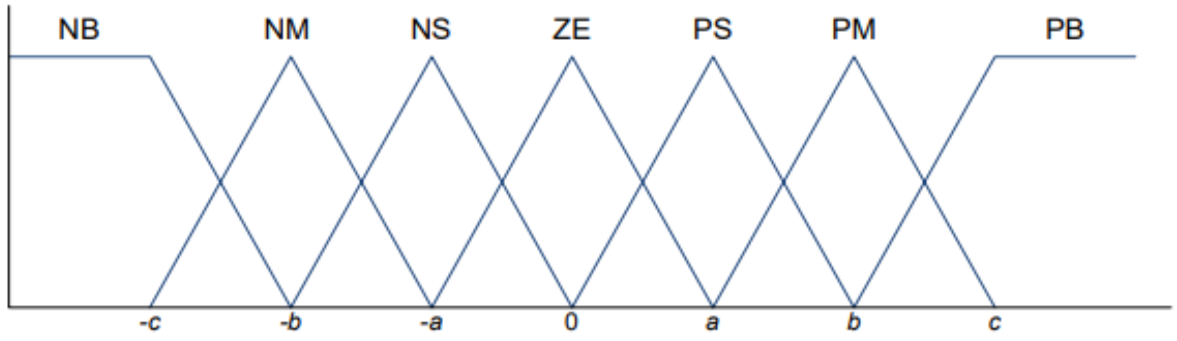

Figure II.14: Membership functions.

D. Artificial Neural Network (ANN) Based MPPT Techniques:

ANN-MPPT technique uses an artificial neural network that has multilayered feedback with a reverse propagation trained network. The 2-stage offline trained ANN-based MPPT using 2 cascaded ANNs ,evaluates the irradiance and the temperature level from the current and voltage signals shown by the PV array. The technique is better under the quickly fluctuating climatic conditions also for the constant and variable instants with normally decreasing the training set; the 3-layer RBF NN is

utilized for MPPT implementation. Home energy management system has been proposed in [28] where the neural network is utilized which is responsible for tracking the home loads, predicting the generation of PV and consumption of home, and depending on the choice of energy persuasion of the consumers. The 2-stage MPPT was utilized for enhancing the PV modules' nonuni form irradiance . The MPPT 2-stage technique based on ANN was introduced for MPP . This technique does not depend on time and trade features because of which the MPP tracking is found to be performed with no any time gap via characteristics changes of PV. The issue of PV array nonlinear characteristics with fast varying temperature and irradiation has been addressed by applying DE and ANN with the traditional MPPT for tracking the MPP . Xu et al present an innovation MPPT based on ANN. .with the incorporation of conventional INC using sensors in order to increase performance. 2-stage ANN based MPPT was presented in to estimate irradiance and temperature level from current and voltage signals to determine the best maximum operating point. In .MPPT controller based ANN in design perspective of the PV system has been explained to meet the limitations as slow and inefficient tracking and performing its operation at optimum point and minimizing oscillation while changing climatic conditions rapidly. 3-layered ANN based MPPT with a reverse propagation approachwas demonstrated .in perspective to the boost converter tuned for the PV system for the minimization of permanent system loss and for enhanced conversion efficiency. It provides maximum output voltage under different temperature conditions as well.[18]

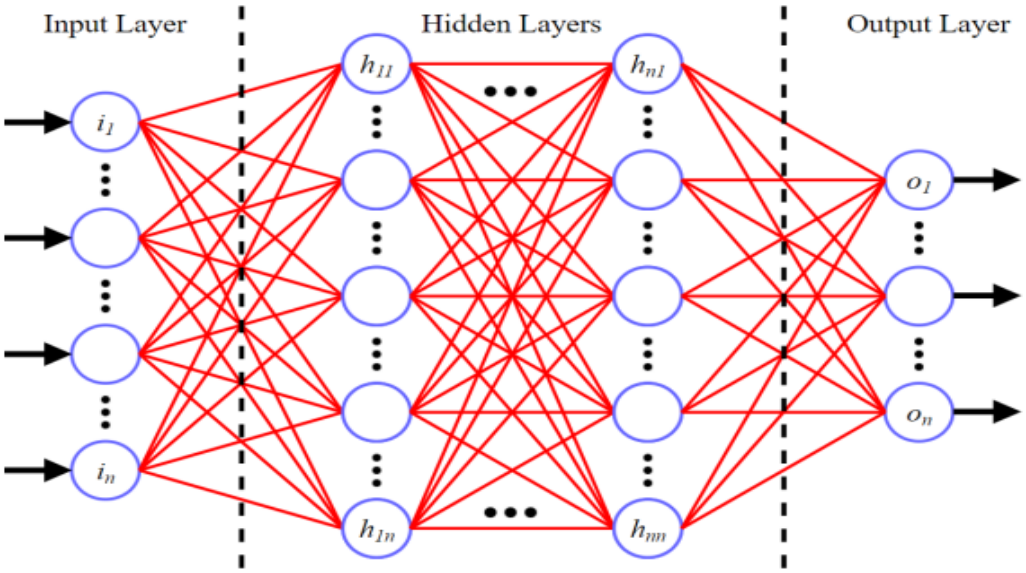

Figure II.15 Neural Network-Based MPPT Control

II.4 Overview of Electrolyzer :

II.4.1 Definition of Electrolyzer

An electrolyzer is an electric machine that breaks up water or other components into their elementary components by the process of electrolysis. Electrolysis is a process of chemistry where an electric current is employed to break up a substance into its basic components.

For the application of water electrolysis, an electrolyzer separates water molecules into oxygen and hydrogen gases by an electric current. Hydrogen gas is either stored in compressed form or as a liquid. The produced oxygen is vented back to the atmosphere or stored and then supplied to other industrial processes**. [37]**

II.4.2Electrolyzer Functionality and Fundamental Reactions

Electrolyzers are electrochemical devices that split water into hydrogen and oxygen using electricity. At the anode, water is oxidized to produce oxygen and protons, while electrons flow through an external circuit. At the cathode, hydrogen is formed by the recombination of protons and electrons. This process is summarized by the following reactions:

- **Anodic Reaction :** (Oxygen Evolution Reaction): $H_2O \rightarrow + \frac{1}{2}O_2 + H^+ + 2e^-$ (II.25)

- **Cathodic Reaction :** (Hydrogen Evolution Reaction): $2H^+ + 2e^- \rightarrow H_2$ (II.26)

- **Overall Reaction:** $H_2O \rightarrow \frac{1}{2}O_2 + H_2$ (II.27)

To initiate water splitting, the applied voltage must exceed the reversible cell potential ($E_{rev}{}^0$), which represents the thermodynamic minimum energy requirement. Under standard conditions (25°C, 1 atm), this value is calculated using the Gibbs free energy ($\Delta G_R{}^0$):

$$E_{rev} = \frac{\Delta GR}{nF} = 1.229V \qquad \text{(II.28)}$$

where:

- $\Delta G_R{}^0 = 236.483$ kJ/mol

- n is the number of electrons transferred (n = 2 for water splitting).

- F is Faraday's constant (96485 C/mo).

In practical applications, additional energy, termed thermoneutral potential (E_{th}^0), is required to account for the enthalpy of the reaction (ΔH_R^0= 285.83 kJ/mol

$$E_{th} = \frac{\Delta HR}{nF} = 1.481V \qquad (II.29)$$

II.4.3 Types of Electrolysis :

Electrolysis methods are distinguished by their operating conditions, efficiency, and suitability for integration with renewable energy. The three dominant methods Alkaline Electrolysis (AE), Proton Exchange Membrane (PEM) Electrolysis, and Solid Oxide Electrolysis (SOE) each offer unique advantages and limitations. 1. Alkaline Electrolysis (AE): Alkaline electrolysis operates at temperatures ranging from 40 to 90°C, utilizing a liquid alkaline solution such as potassium hydroxide as the electrolyte. This mature technology is cost-effective, making it widely adopted in industrial settings. However, AE systems are less efficient than other methods, with efficiencies between 55% and 70%, and exhibit slow dynamic responses to power fluctuations, limiting their compatibility with variable renewable energy sources like solar and wind. [9] Electrolysis methods are distinguished by their operating conditions, efficiency, and suitability for integration with renewable energy. The three dominant methods Alkaline Electrolysis (AE), Proton Exchange Membrane (PEM) Electrolysis, and Solid Oxide Electrolysis (SOE) each offer unique advantages and limitations. [38]

A. Alkaline Electrolysis (AE) :

Alkaline electrolysis (AE) occurs between 40°C and 90°C, employing a liquid alkalin

solution, typically potassium hydroxide (KOH), as the electrolyte. The process is water electrolysis, where electrical energy is utilized to dissociate water molecules into hydrogen and oxygen gases. The alkaline electrolyte facilitates the movement of ions between the anode and cathode, contributing to the efficiency of the process.

This technology can be graded as mature with a long history of industrial application. Its cost-saving aspect is one of its advantages, with it being applied widely in industries such as ammonia production, petroleum refining, and food industries. The simplicity of the technology and the fact that low-cost materials are employed in the construction of the electrolyzer make AE a cheap option, particularly in bulk hydrogen production.

However, AE systems have been known to be less efficient compared to other electrolysis processes. The efficiency in energy conversion of AE systems is usually between 55% to 70%. This inefficiency is primarily because AE systems achieve lower current densities, and this limits the hydrogen production potential of AE systems. As a result, much of the electrical power input to the system is dissipated in the form of heat, and thus the overall efficiency of the system is reduced.

Yet another problem AE systems create is their relatively inferior dynamic response to power supply variations. The system requires a consistent and steady supply of electricity in a position to excel. This makes AE incompatible with renewable power sources such as wind and solar energy, which constantly change output due to changing weather conditions. Because AE systems cannot react quickly to such changes, they face difficulties when trying to integrate variable renewable energy sources.

This increasing response to power fluctuation further limits the overall flexibility of AE systems, thus they are undesirable for dynamic energy markets that require quick response. Thus, even as a cost-effective technology, use of AE in uses where integration of renewable energy is critical relies on improving responsiveness and efficiency in systems. [38]

B. Proton Exchange Membrane Electrolysis (PEM)

Proton Exchange Membrane (PEM) electrolysis technology relies on the use of a solid polymer electrolyte instead of a liquid one, which helps reduce maintenance costs and the pressure required for hydrogen production. This technology also offers a dynamic response to power fluctuations and features a compact design, making it suitable for decentralized production. Despite achieving an energy efficiency ranging from 62% to 77%, its use remains limited to specialized applications such as submarines due to its reliance on noble metals like platinum, the short lifespan of membranes, and higher costs compared to alkaline technology. However, ongoing research in PEM fuel cells supports its development, particularly in enhancing stack capacity, reducing noble metal usage, and extending membrane lifespan. Currently, experiments are being conducted to operate the system at higher temperatures (130–180°C) compared to the current range (70–80°C). [39]

C. Solid Oxide Electrolysis (SOE) :

Solid Oxide Electrolysis (SOE) is one of the most efficient electrolysis technologies, operating at high temperatures between 500°C and 800°C using ceramic electrolytes, typically based on zirconia. The high operating temperatures reduce the electrical energy required to split water into hydrogen and

oxygen, achieving efficiencies between 80% and 90%. SOE is particularly suitable for large-scale industrial hydrogen production, such as in heavy industry and chemical manufacturing, with the added advantage of integrating waste heat recovery systems to further improve efficiency.

However, SOE faces significant challenges related to material durability under extreme temperatures and harsh environments, requiring advanced and often expensive materials, which increases system complexity and maintenance costs. Despite these challenges, researchers are actively working on developing stronger and more cost-effective ceramic materials to improve the reliability and reduce the costs of SOE systems, paving the way for their wider industrial adoption in the near future.[40]

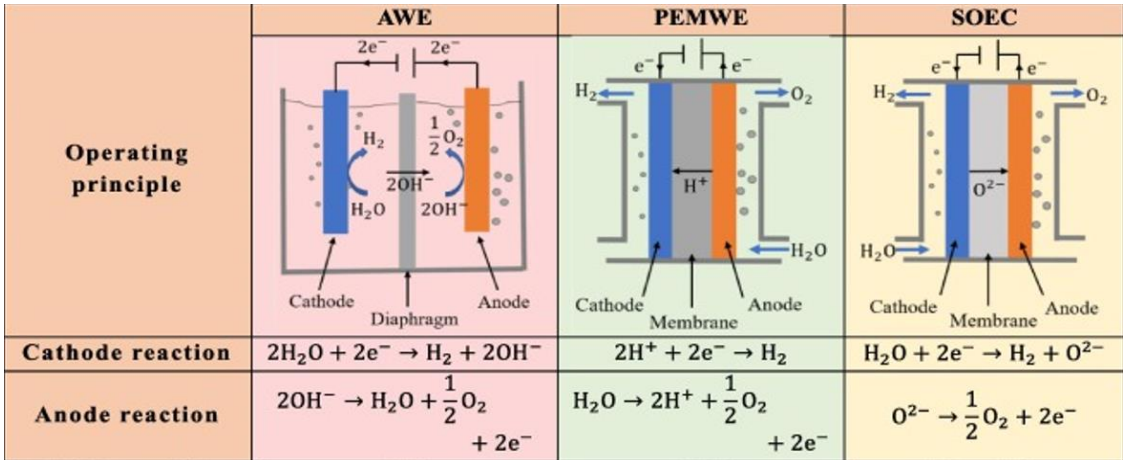

Figure II.16 Types of Electrolysers

Table II.1: Comparison of Electrolysis Methods

	Efficiency (%)	**Operating Temperature (°C)**	**Technology maturity**	**advantages**	**disadvantages**
AE	59 - 70	20 - 80	Commercial	• Low capital cost • Relatively stable and nature technology	• Long starting time • Slow dynamic response
PEM	65 - 82	20 - 200	Near commercial	• Compact design • Fast dynamic response	• Dependanse on precious metal catalysts • High cost

SOE	Up to 100	500 - 1000	Demonstration	• High electrolysis efficiency • Low energy requiements	• Short running life • High manufacturing Cost

II.4.5 Principle of operation :

Electrolysis is one of the more preferred options for hydrogen production from renewable energy. Electrolysis is the breakdown of water to hydrogen and oxygen through the use of electricity. The process is carried out in an apparatus called an electrolyser. Electrolysers can vary in size from small appliance-sized equipment appropriate for hydrogen production on a small scale to large-scale centralized production system that might be powered directly by renewable or other non-greenhouse-gas-emitting power sources. [38].

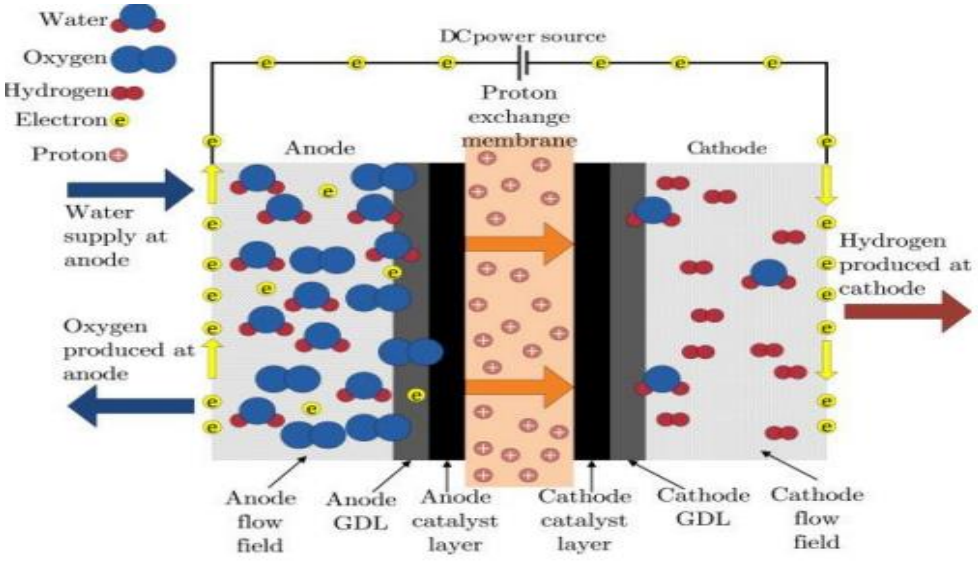

Figure II.17 Schematic diagram of an Electrolyser

- Water reacts at the anode to form oxygen and positively charged hydrogen ions (protons).
- The electrons flow through an external circuit and the hydrogen ions selectively move across the PEM to the cathode.
- At the cathode, hydrogen ions combine with electrons from the external circuit to form hydrogen gas.

Anode: H_2O 2H+ + $1/2O_2$ + 2e (II.27)

Cathode: $2H+ + 2e- \; H_2$ (II.28)

Total: $H_2O \; H2 + 1/2O_2$ (II.29)

II.4.6 Electrolyzer Modeling

Decomposition of water into hydrogen and oxygen can be achieved by passing an electric direct current between two electrodes separated by a satisfactory aqueous electrolyte having good ionic conductivity. The overall reaction for water splitting is

H2O(l) + electrical energy $\rightarrow$ H2(g) + 1/2O2 (g)

.In this reaction, there needs to be a minimum electric voltage between the two electrodes in order for the reaction to take place. This minimum voltage, or reversible voltage (Urev), depends on electrode and electrolyte properties. In an alkaline electrolyser, the electrolyte is usually aqueous potassium hydroxide (KOH) such that ionic transport is through potassium ion K+ and hydroxide ion OH−. The reactions at the anode and the cathode in this instance are The electrochemical reaction of an electrolyzer may be characterized using a semiempirical current-voltage model. One of the most utilized models is the one proposed by Ulleberg [22], which describes the voltage of an electrolyzer as a function of the parameters "s" (V) and "t" (m2 /A) corresponding to activation overpotentials and the "r" (Ω·m2) parameter for the ohmic overpotential. These parameters, in fact, have only a temperature (T) dependence. To obtain a more complete model, two additional parameters have been added: "j" (Ω·m2) and "d" (Ω·m2), which are the ohmic overpotential dependencies on the electrolyte concentration (M) and pressure (p), respectively [41]

$$U= U_{rev} +s \times \log (t.i+1)+(r+j+d) \quad \text{(II.30)}$$

$$T= t_1+t_2 / T+ t_3 /T^2 \quad \text{(II.31)}$$

$$r = r_1+ r_2 .T \quad \text{(II.32)}$$

$$j = j_1+j_2.M+j_3.M^2 \quad \text{(II.33)}$$

$$d = d_1+d_2.p \quad \text{(II.34)}$$

Regarding Faraday efficiency, it has been modelled using the equation proposed in . including a linear relation for temperature (“f1”, “f2”). The pressure and electrolyte concentration have not been included due to its slight influence

$$\eta_F = \frac{i^2}{F_1 + i^2} . F_2 \quad \text{(II.35)}$$

$$F_1 = F_{11} + F_{12} . T \quad \text{(II.36)}$$

$$F_2 = F_{21} + F_{22} . T \quad \text{(II.37)}$$

- **Voltage Submodel :**

Equation (1) shows the total cell voltage as the sum of the open-circuit voltage (Vocv), activation overvoltage (Vact), and ohmic overvoltage (Vohm).

$$v_{cell} = v_{ocv} + v_{act} + v_{ohm} \quad \text{(II.38)}$$

- The open-circuit voltage is then calculated using the Nernst equation (Equation (II.38)), where variables ppH2 , ppO2 , and ppH2O refer to the partial pressures of hydrogen at cathode, oxygen at anode, and water vapor, respectively

$$V_{ocv} = V_{ref} + \frac{R.T}{2F} . Ln(\frac{p_{H2}}{PH2O} . p^{0.5}_{O2}) \quad \text{(II.39)}$$

described in Section 2.5. The activation overvoltage comes from the energy required to start the electrochemical reaction through the electrodes,

α_{an} is determined experimentally to be 0.7353

$$V_{act} = \frac{R.T}{2.\alpha_{an}.F} . \sinh^{-1} \quad \text{(II.40)}$$

The ohmic overpotential is due to resistance of ion flow in the cell components. It can be expressed as simply as Ohm's law, using the inverse of membrane conductivity to determine the resistance of the cell, as in Equation (II.40)

- The electrical power consumed by the electrolyzer (Eq. II-10) depends on the operating point on the polarization curve, as well as on the size of the electrolyzer, namely the number of elementary cells and its active surface area [42]..

$$P_{EL} = J_{EL} . SA_{EL} . NC_{EL} . V_{EL} \quad \text{(II.41)}$$

Where:

P_{EL} : Power consumed by the electrolyzer (W)

SA_{EL} : Active surface area of a single electrolyzer cell (cm^2)

NCEL: Number of elementary cells in series in the electrolyzer (-)

- The electrolyzer has an operating threshold below which it cannot function. The value of this threshold depends on the nominal flow rate of the electrolyzer [43 , 44].

$$S_{EL} = \%_{S\_EL} . D_{N\_EL} \quad \text{(II.42)}$$

Where: **SEL:** Operating threshold of the electrolyzer (Nm^3)

$\%_{S\_EL}$: Coefficient for calculating the operating threshold of the electrolyzer (%)

D_{N_EL}: Nominal operating flow rate of the electrolyzer (Nm^3)

- The productions of hydrogen and oxygen are calculated according to Faraday's law (II.43)

The water consumption is proportional to the hydrogen production, and therefore to the current absorbed by the electrolyzer [45] Unlike the fuel cell, the Faradaic efficiency of the electrolyzer (II.44) is not constant; it depends on the absorbed current [46]. We can also define the term P_{N_EL}, which represents the nominal power of the electrolyzer.

$$Q_{PH2} = 2.Q_{PO2} = \frac{Q_{H2O}^{C}}{S_{H2O}} = \frac{3600.NC_{EL}.J_{EL}.SA_{EL}}{2.F}\eta_{F\_EL} \quad \text{(II.43)}$$

$$\eta_{F\_EL} = 96{,}5.e\ \wedge\ \left(\frac{0.09}{J_{EL}.\ SA_{EL}} - \frac{75{,}5}{(J_{EL}.SA_{EL})^2} \right) \quad \text{(II.44)}$$

Where:

Q_{h2}: Quantity of hydrogen produced ($mol \cdot h^{-1}$)

Q_{o2}: Quantity of oxygen produced ($mol \cdot h^{-1}$)

$C\_Q_{H_2O}$: Quantity of water consumed ($mol \cdot h^{-1}$)

S_H_2O: Water stoichiometry (-)

ηF_EL: Faradaic efficiency of the electrolyzer (%)

II.4.7 Link Between Electrolyzer and PV System

The electrolyzer is linked with the photovoltaic (PV) system by transforming solar radiation into electrical energy, which, in turn, is further applied in decomposing water into its basic components, hydrogen and oxygen, through the process of electrolysis. The efficacy of the above integration is

dependent upon the quality of the electrical energy that is being produced by the solar panels, which once more remains a function of solar radiation intensity as well as meteorological parameters.

Under sufficient solar radiation, the solar panels generate a direct current (DC) that can be directly supplied to the electrolyzer if the voltage and current characteristics are compatible. However, when solar power is unstable or variable, power control equipment such as DC-DC converters or energy storage devices are used to supply a continuous and stable current to the electrolyzer for better hydrogen production efficiency.

Technologies such as Maximum Power Point Tracking (MPPT) are employed to extract maximum available energy from the solar panels to improve the performance of the electrolyzer despite changing conditions. Batteries or supercapacitors can also be included to store excess electricity and use it during periods of low sunlight, allowing the electrolyzer to run continuously and generate hydrogen effectively.

Briefly, green hydrogen production directly relies on the electricity generated from the PV system, and the coupling between the two systems is tightly coupled. The performance of the electrolyzer is dependent on the quality and stability of the electricity generated from the solar system, sometimes requiring auxiliary systems for ensureng stable and sustainable operation. [47]

II.5 Conclusion

This chapter introduced the modeling of the photovoltaic (PV) system and the electrolyzer, including the theoretical background and technology used in the field. It focused on the conversion of solar energy into electric energy by solar panels and analyzed factors influencing the efficiency of such a process, such as solar radiation and temperature. The performance of the PV system at varying conditions was studied, which provided a deeper understanding of how electricity production could be optimized. Further, the working of the electrolyzer and its role in water molecule splitting to produce green hydrogen were studied, along with the technical parameters affecting the efficiency of electrolysis, i.e., electrolyte and applied voltage.

Building on the findings of Chapter II , Chapter III . I will discuss solar resources in the Wilaya of M'Sila, where the climatic data characteristics of solar radiation, temperature, and wind speed will be studied. This is a precursor to establishing the potential of solar energy production in the region and

how viable it is for the production of green hydrogen. The study will examine climate data for an extended period to establish the stability and sustainability of solar resources.

Chapter III

Analysis of solar resources and characterization of climate data

III.1.Introduction

After the successful simulation of the photovoltaic-electrolyzer system and comprehensive analysis of the process of conversion of solar energy to electrical energy for green hydrogen production, it is necessary to check whether the available solar resources can effectively and efficiently drive the system. The stability of this system is highly dependent upon the solar potential of the selected site because variations in solar radiation, air temperature, and humidity in the air can have a significant effect on the overall efficiency of the process of hydrogen production. To ensure we have a complete evaluation, we will conduct comprehensive analysis of solar radiation patterns, temperature fluctuations, and humidity content within the region of M'Sila. The research will provide us with relevant information regarding the seasonality and intensity of solar power during different seasons. Through the analysis of past and present meteorological records, we can determine whether such climatic conditions are sufficient to facilitate sustained and optimal hydrogen production. Besides, this analysis will also enable us to ascertain the best places to mount the photovoltaic-electrolyzer system strategically. By utilizing the optimum position, we will be able to maximize energy intake and efficiency and hence achieve the maximum overall hydrogen yield. Also, by ascertaining the specific climatic conditions, we will be able to accurately project the level of hydrogen yield during various environmental situations so that the system will be operating at its optimal level of efficiency while stable and dependable.

By so doing, we aim to enhance the sustainability and viability of green hydrogen production in M'Sila by harnessing the potential of the solar energy available in the area to enable the powering of the global transition to renewable energy.

III.2 Geographic location of M'Sila

M'Sila is Algeria's 28th of 58 provinces and is located in the north of the country at the gateway to the Sahara, as shown in Figure 1. Located where the East, West, North, and South meet, it has tremendous economic growth and development potential. The province is 18,175 km² large and is home to an estimated 1,210,952 inhabitants. Geographically, it occurs in Algeria's upper plateaus at a latitude of 35° 42'07", a longitude of 4° 32'43", and an altitude of 441 m above sea level.[24]

Due to global warming, M'Sila, formerly classified as semi-arid zone, is currently referred to as an arid zone.

This climatic shift has affected agriculture and domestic economic activities, which have prompted increased government intervention to stimulate investment and infrastructure growth. The

government has placed significant emphasis on the growth of the region as a key economic hub, leveraging its strategic position and natural resources.[48]

Figure III.1: Location of the Wilaya of M'Sila

III.3 Overview of PVSyst :

III.3.1 Definition:

PVsyst is a highly powerful and widely used software in the solar energy sector for designing, simulating, and analyzing photovoltaic (PV) systems. It is extremely precise and flexible and a must-use application for engineers, scientists, and developers involved in solar energy projects. The software enables one to input comprehensive data regarding their solar systems in order to conduct accurate modeling and performance analysis. This includes in-depth details about solar PV modules, inverters, and other system components in order to make the simulations as realistic as possible. One of the key benefits of PVsyst is the ability to simulate the performance of a solar energy system under a variety of conditions. The software takes into account factors such as the orientation and tilt angle of the solar panels, geographical location and climate of the installation, and electrical load and consumption profile. By incorporating these variables, PVsyst can provide a comprehensive view of how a solar installation will perform under real conditions. Additionally, it offers expert-level customization options that allow users to model different panel technologies, compensate for the impact of shading and other environmental factors, and optimize system performance based on selected criteria. Beyond technical simulations, PVsyst also plays a critical

role in financial and economic analysis. The software helps users estimate key financial metrics such as return on investment (ROI), payback period, and levelized cost of electricity (LCOE). This makes it a very handy tool for investors and decision-makers who need to evaluate the profitability and viability of solar projects. Furthermore, PVsyst offers detailed reporting and graphical representation of system performance that can be used for documentation, presentation, and further analysis. [55]

III.3.2 Benefits of Using PVsyst

- One of the critical benefits of PVsyst is its accuracy. The software uses advanced algorithms and databases to simulate solar energy systems' performance, which enables users to design optimized systems for their locations, meteorological data, and electrical load. Additionally, PVsyst is flexible and allows users to input a wide range of data and customize their simulations to their needs. This ability to input data and customize it in different ways assists users in maximizing system performance according to different situations, thus saving the user money.
- The other benefit of PVsyst is its ease of use. The software is made to be easy for solar energy professionals to enter information, run simulations, and examine results. The software also has comprehensive documentation and resources provided to help users with optimizing the program. This creates a convenient method by which even novice individuals in the solar energy industry can benefit from and learn from the program.
- The analysis phase is where PVsyst offers a variety of analysis tools to assist the user in comprehending and optimizing their system's performance. For instance, the program offers graphs and tables that reflect important performance parameters like energy produced, efficiency, and cost. PVsyst has four core project design systems: Standalone system, Grid-connected system, Hybrid system, and Solar thermal system. All the systems are designed for different solar energy systems and applications, including small independent systems not integrated into the grid or systems integrated with other technologies. This enables users to refine their strategy with multiple parameters like energy output, cost, or CO2 emissions.
- Overall, PVsyst is a flexible and robust computer system that supports solar energy system design, simulation, and analysis with high precision and flexibility. Its ease of use combined with its extremely rich support capabilities allow it to be viable for experts of varying experience levels in the solar energy industry, from beginners to experts. With PVsyst, it is

possible to achieve maximum performance of solar energy systems with various specifications, thereby saving money, increasing energy production, and preventing CO2 emissions [19]

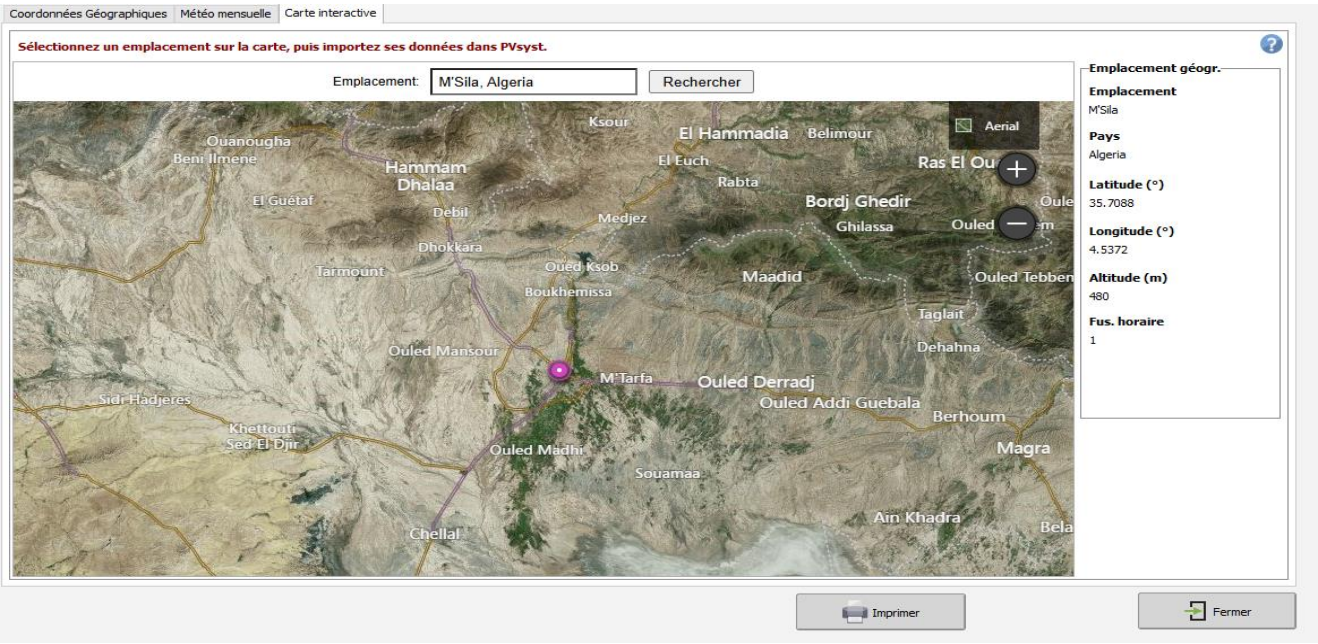

Figure III.2: Giographical Location of Msila Province , Algeria

III.4 Impact of Temperature Rise on PV System Performance :

The solar panels can convert a maximum of 25% of the solar radiation into electricity. The rest of the radiation is stored and is accountable for heating the panel . The experimental study of Cristobal and Oswaldo .conducted in Brazil under standard test conditions of radiation of 1000 W/m2, and based on their study, the temperature variation linearly reduced the efficiency. Razika et al. carried out their investigation in the Saida province, where they undertook a performance evaluation of about 30 MW polycrystalline solar panels. The investigation indicated that energy loss was recorded to rise linearly with the rise in temperature. Indra investigated the impact of temperature on polycrystalline PV modules in Nepal, he reached the conclusion that the value of the positive temperature coefficient displayed by the short-circuit current was greater than the value of the negative temperature coefficient displayed by the open-circuit voltage when the cell temperature exceeded 20 °C. These findings show that the cell performance reduces with a rise in temperature, their performance dropping by 0.05% with each added 1 °C. In yet another Nigerian study on a group of monocrystalline solar cells researched by Ike. The findings show the reverse relationship between temperature and the efficiency of a solar photovoltaic system. There is a reduction in the

energy production efficiency of solar PV systems with the rise in ambient temperature. On the other hand, ambient temperature drops led to the enhancement of the system's energy production. A Thai study by Yaowanee et al. , designed to monitor the degradation of polycrystalline solar panels for a period of one year, indicated that high temperature is ranked as one of the most significant factors in solar panel degradation and instability. Anu discovered that a rise in temperature affects solar cell efficiency differently based on material quality. Statistical analysis indicates that the rise in temperature by 1°C [48]

Study Parameters

Figure III.3 Geographical Coordinates of Msila Province

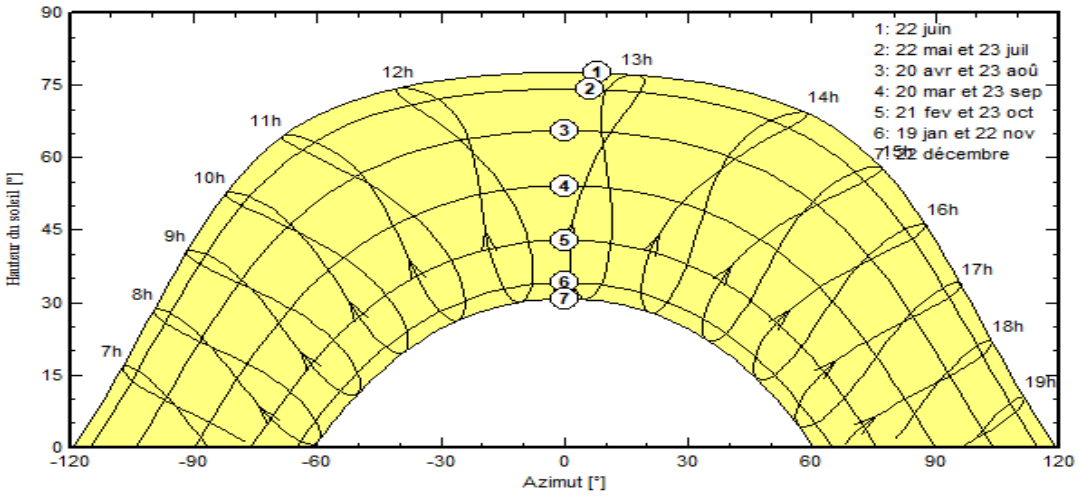

Figure III.4 Solar Path Diagram For Different Dates in Msila

III.5 Solar Irradiation

A. Global Horizontal Irradiation (GHI): is the total solar energy falling on a horizontal surface on Earth from direct sunlight and diffuse sky radiation. It is a key parameter to evaluate the solar energy resource of a site. The GHI value depends on a number of parameters such as geographic latitude, atmospheric conditions, and the time of year. Precise measurement and assessment of GHI are required for the optimization and design of photovoltaic (PV) systems and other solar technologies.[24]

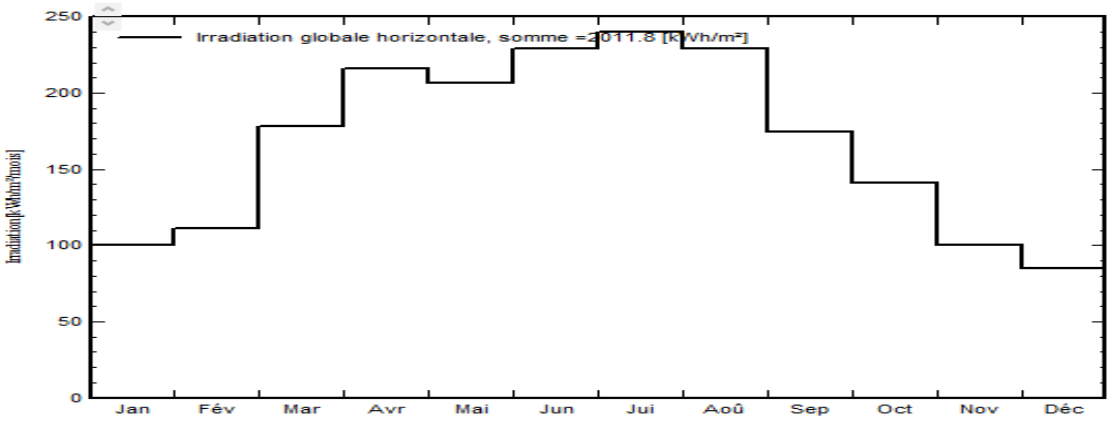

Figure III.5: Monthly Variation of Global Horizontal Irradiation (GHI) in Msila for the year 2023

B. Diffuse horizontal irradiation (DHI) : Diffuse irradiation is the directionless radiation that comes from the entire vault of the sky but has lost its direction changed by diffusion from particulates or molecules in the atmosphere .Also referred to as sky radiation, diffuse skylight, or a skylight. There are some models in the literature utilized for diffuse irradiation estimation. [24]

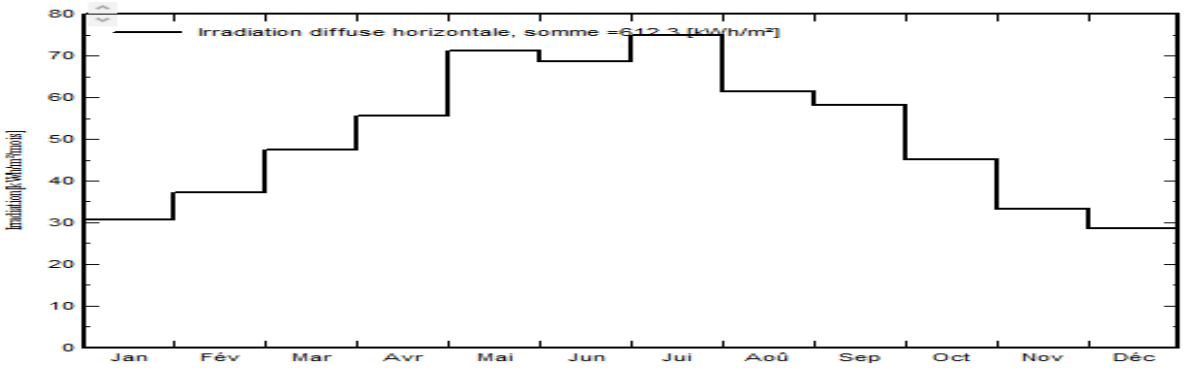

Figure III.6: Monthly Variation of Diffuse horizontal irradiation (DHI) in Msila for the year 2023

C. Direct normal irradiation (DNI): Direct normal irradiance (Gdn) is the amount of the solar radiation received per unit surface area which is maintained perpendicular to the rays that move in a straight line from the sun at its position at the moment in the sky. However, the sun possesses a time-varying position. In consideration of this, the surface must be mounted on a solar tracking system. In this, the surface follows the sun on a daily (one-axis) or daily and seasonal (two-axis) basis to maintain the beam radiation at normal incidence. [17]

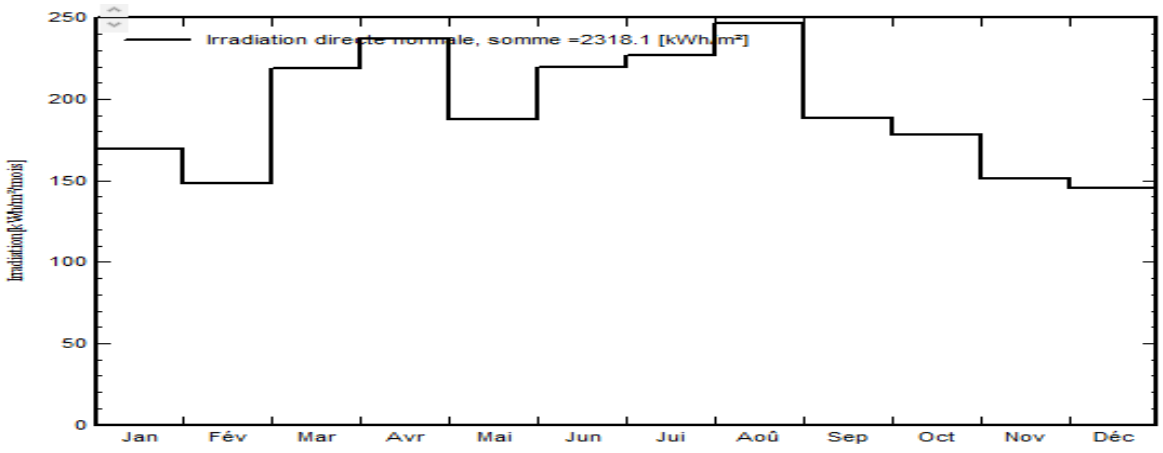

Figure III.7: Monthly Variation of Normal Direct Irradiation in Msila for the year 2023

D. Clearness Index (KT): is one of the most important parameters employed to determine atmospheric transparency and the availability of solar radiation at a location. It is the ratio of the solar radiation actually received on the Earth's surface to the extraterrestrial solar radiation incident upon the same location over a given time interval. The clearness index gives information about the influence of atmospheric constituents like clouds, aerosols, and water vapor on the transmission of solar radiation. A larger value of KT means clearer skies and more potential for solar energy, whereas a smaller value implies greater cloud cover and atmospheric interference [24]

$$K_T = \frac{H}{H0} \qquad \text{(III.1)}$$

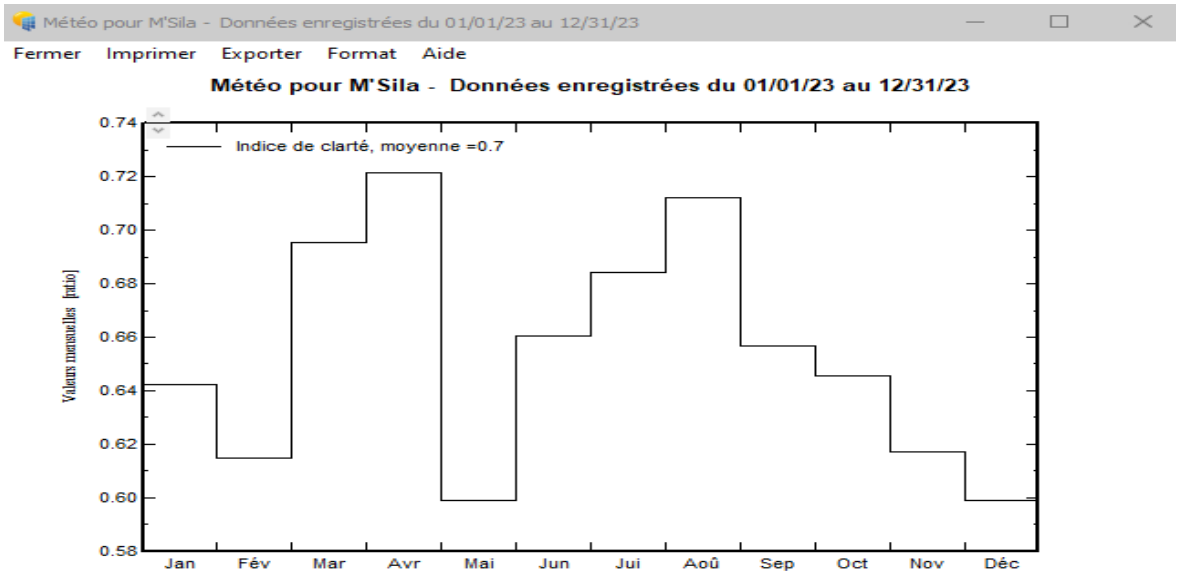

Figure III.8: Clarity index Variation in Msila for the year 2023

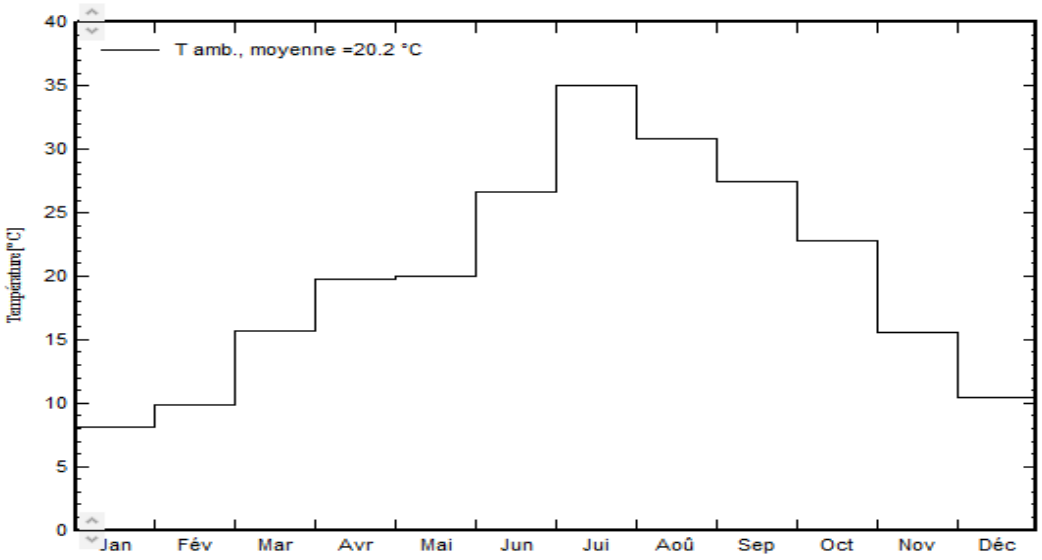

Figure III.9: Monthly Variation of Average Temperature in Msila for the year 2023

III.5 Overview of HOMER Pro :

III.5.1 Definition :

In 1993, the National Renewable Energy Laboratory (NREL) USA has developed Hybrid Optimization Model for Electric Renewables (HOMER) software [37] . HOMER Pro, or the Hybrid Optimization Model for Electric Renewables, is a powerful software HOMER is a

simplified-form optimization model, which conducts hundreds or thousands of hourly simulations on and above (to achieve optimal possible match between supply and demand to build the best system. It uses life cycle cost to rank order these systems [47]. This model enables the blending of various energy sources, from renewable equipment such as wind turbines and solar photovoltaic panels to conventional generators and storage units like batteries and hydrogen storage. HOMER Pro, by modeling actual conditions, accounts for factors like fluctuations in energy demand, meteorological information, and fuel prices to provide realistic estimates of system operation. One of the greatest things about HOMER Pro is that it is capable of conducting both technical and economic analysis. It helps identify energy system feasibility, component sizing optimization, cost assessment, and energy dispatch strategy analysis to ensure stable and efficient power supply. With its detailed cost analysis, the software helps determine initial investment, running costs, as well as the levelized cost of energy (LCOE), enabling stakeholders to make informed decisions [10]

III.5.2 Advantages of Applying HOMER Pro

HOMER Pro is a unique piece of software to design and simulate hybrid energy systems and microgrids. The software supports effective economic and technical decision-making for engineers and planners. Below are some essential advantages of using the software :

- Economic Viability Analysis : HOMER Pro performs thorough economic analysis in determining investment, operating, and maintenance costs in order to make optimal cost-saving selections.
- Technical Simulation of Performance: The software replicates the performance of the energy system over a year's period, considering climatic changes and usage of energy, in a way that efficiency is achieved and the best source of energy is identified.

- Hybrid Energy System Design : HOMER Pro integrates two or more diverse energy sources such as solar, wind, diesel, and batteries in an attempt to create efficient and renewable systems.
- Sensitivity Analysis and Future Changes : The program enables sensitivity analysis to assess the effect of environmental and economic variables (e.g., wind speed, fuel prices) on system performance in order to provide flexible and sustainable decision-making.

- Ease of Integration and Use of Data : HOMER Pro has a user-friendly graphical interface and is capable of importing weather and energy consumption data, so designing and analyzing energy systems is a straightforward process.
- Capacity to Handle Both Off-Grid and Grid-Based Systems : The software can create and analyze systems that operate independently (off-grid) or on the central power grid, and the utility program is a valuable addition to any project. [50]

III.6 Simulation and Optimization using HOMER Pro

III.6.1 Simulation Framework :

The HOMER (Hybrid Optimization Model for Electric Renewables) software utilizes extensive hourly simulations to analyze solar energy system efficiency and performance in M'Sila from detailed climatic data including solar radiation, temperature variations, and wind speed to enable complete assessment of environmental factors on solar energy production. The software compares different system configurations considering the parameters such as energy generation, consumption pattern, and storage capacity. It applies advanced methodologies to compute the most optimal solutions based on key parameters such as:

III.6.2 Solar Energy Potential of the Site :

Photovoltaic technology, which utilizes semiconductors to directly transform solar radiation into electricity with no Citation: emissions, noise, or vibration, is another scientific knowledge application. This is a significant source of power to meet electricity demands either in constructed areas or in rural and remote areas where grid connection is extremely difficult or lacking in the presence of energy infrastructure . Due to its position, Algeria has the highest solar energy prospects of North Africa and the Middle East (MENA) region and among the biggest globally. In fact, Algeria's potential energy from the sun has been quantified as 13.9 TWh per year. Additionally, the mean yearly length of sunshine hours along the Algerian coastal area is estimated to be 2650 hours. It is 3000 hours in the highlands, whereas in the Sahara, it reaches 3500. Given this important potential, The Algerian leaders have decided to utilize it to manufacture electricity for both domestic use and export via an ambitious policy. This study is part of a larger project to estimate the solar potential of each region in Algeria, a vast nation. One of the most significant states of Algeria is M'Sila high plateaus due to its distinguished geographical location, which qualifies it to be an economic and development pole, since it is regarded as a transition point of north and south, east and west. This study will evaluate for the first time the solar energy potential

of M'Sila, and to determine which technology, one that is being provided in the market now, is suited to harnessing its solar power for electricity production (PV and CSP). This is an estimate derived from data recorded at M'Sila weather station during one year and from the NASA website [26]

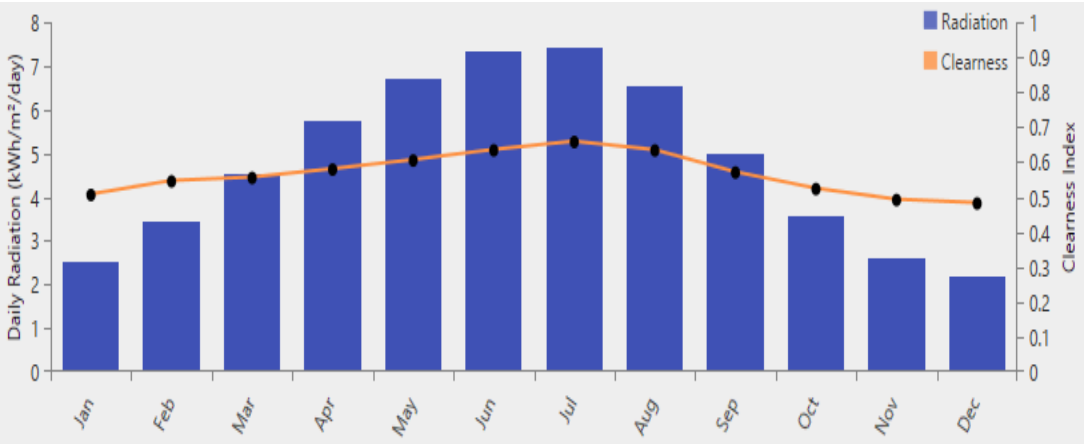

Figure III.10 Annual solar radiation profile

III.7 Conclusion :

the analysis of solar resources and the characterization of climatic data have provided essential insights into the feasibility of green hydrogen production in M'Sila. By understanding the solar potential and environmental factors, we can optimize the performance of photovoltaic-electrolyzer systems to ensure maximum efficiency and sustainability. These findings serve as a critical foundation for evaluating the economic and technical aspects of green hydrogen production. As we move forward, the next chapter will explore the techno-economic study of green hydrogen production, focusing on cost analysis, efficiency improvements, and economic viabil

Chapter IV

Analysis of solar resources and characterization of climate data

IV .1 INTRODUCTION

Green hydrogen production as a source of clean energy is gaining global attention due to its prospects in reducing carbon emissions and enabling the transition towards a cleaner energy system. However, large-scale production of green hydrogen is highly dependent on economic and technical feasibility. The aim of this chapter is to carry out a comprehensive techno-economic evaluation of green hydrogen production in M'Sila by evaluating its cost, efficiency, investment, and overall feasibility. A critical component of this analysis is to assess the capital and operational costs of hydrogen production through photovoltaic (PV) systems and electrolysis. The efficiency of the systems, as influenced by solar radiation, climatic conditions, and system design, to a large extent determines the cost-effectiveness of hydrogen production. In addition, this chapter discusses various economic models, financial incentives, and policy frameworks that could impact the large-scale deployment of green hydrogen technology.

IV.2 Hydrogrn Production from Photovoltaics (PV)

Before carrying out the economic evaluation of green hydrogen production in the Wilaya of M'Sila, it is appropriate to refer to the studies that already exist in this context. In this context, A. Mraoui and S. Menia conducted full simulations to evaluate the viability of hydrogen production from photovoltaic (PV) installations. The results were that theoretical production rates ranged from 0.10 to 0.14 Nm^3/m^2/year. The highest achievable was recorded in the arid southeastern regions and northeast lowlands, while in the northwestern region, with dense population, production was at a rate of 0.13 Nm^3/m^2/day, which showed regional variability in PV system efficiency.[16]

IV.3 Critical Gaps and Challenges :

IV.3.1 Water Resource Management Challenges

Water is highly crucial in green hydrogen production, particularly in the electrolysis process, where quality water is essential in generating hydrogen with high efficiency. However, the majority of regions with tremendous renewable energy potential arid and semi-arid regions are water-scarce. Such geographical limitations pose serious challenges to the deployment of hydrogen. For instance, in arid regions, fresh water may not be available, and desalination of seawater is necessary. Although desalination is a practical option, it increases the energy demand and operating costs of hydrogen plants, thereby decreasing overall efficiency. Moreover, the

environmental impacts of bulk desalination must be met. Therefore, combined solutions to water resource management, e.g., recycling industrial process water from local industries or employing hybrid renewable-desalination systems, are being explored to enhance sustainability. Green hydrogen project deployment success depends not only on renewable energy availability but also on efficient, localized water management strategies.[51]

IV.3.2 Hydrogen Storage Challenges

Among the most crucial technical and economic challenges of the hydrogen value chain is even today hydrogen storage. Due to its low volumetric energy density under ambient conditions, hydrogen must be stored under high pressure (typically 350–700 bar) or at cryogenic temperature (−253°C) if it is to be economically transportable or stored over the long term. Both options have huge technical, safety, and cost concerns. Compressed hydrogen gas requires robust, typically composite-structured tanks that are light but extremely pressure-resistant, increasing capital costs. Liquefied hydrogen, on the other hand, requires advanced cryogenic equipment and continuous energy input to maintain low temperatures, leading to energy loss and complexity in operation. Furthermore, hydrogen can embrittle metals, which poses additional risks to storage facilities. Therefore, tests on other forms of storage—as in the case of metal hydrides, chemical carriers, and sub-surface storage—proceed with the goal of breaking these hurdles. Effective, secure, and huge hydrogen storage necessitates such hurdles to be overcome so as to realize maximum potential as an energy carrier through clean hydrogen.[52]

IV.3.3 Hydrogen Transport Challenges :

Transportation of hydrogen from production sites to consumers is extremely difficult because it poses significant logistical, technical, and economic challenges that can greatly affect the viability and cost-effectiveness of green hydrogen implementation. Hydrogen, in contrast to fossil fuels, has a very low energy density by volume, which makes it hard to transport over long distances. Pipelines, high-pressure tube trailers, and cryogenic liquid hydrogen tankers are the most utilized modes of transportation. Each process, however, has stringent limitations. For example, hydrogen pipeline retrofitting or new construction is capital-intensive and requires the application of special materials resistant to hydrogen embrittlement—a process that weakens metals over time. Furthermore, hydrogen transport as a compressed gas is energy-intensive and offers low payloads, while liquefied hydrogen transport demands cryogenic technology that leads to boil-off losses and high operational complexity. Alternatively, hydrogen can be upgraded into carrier molecules like

ammonia or methanol for easier transportation but require conversion infrastructure and add extra energy steps. Such transportation hurdles are most glaring for countries looking to export hydrogen or supply hydrogen across large geographic areas. Therefore, optimizing hydrogen logistics is crucial to build a strong and scalable hydrogen economy.[53]

IV.4 Methodology :

The proposed system was designed to generate solar energy and hydrogen in order to meet the needs of an industrial load within a virtual power plant located in M'sila. The objective of this system is to ensure a continuous electricity supply by relying on photovoltaic panels during periods of solar radiation. The surplus energy is used to produce hydrogen through an electrolyzer and stored in hydrogen tanks, while batteries are used to store short-term energy for immediate backup. During periods of low or no solar radiation, such as nighttime or cloudy weather, a fuel cell converts the stored hydrogen into electricity to maintain load operation. The HOMER Pro software was used as the main tool for modeling and analyzing this integrated energy system, using typical climate data representing the city of M'sila

IV.4.1 Systems Design :

To ensure a constant energy supply, a fuel cell system has been employed, utilizing stored hydrogen to produce electricity during low-sunlight hours such as night-time or overcast weather. This method is quite effective in minimizing the intermittency of solar energy, providing a stable and constant power output. Figure IV.1 shows the energy system configuration, which consists of photovoltaic panels, an electrolyzer, and a fuel cell.

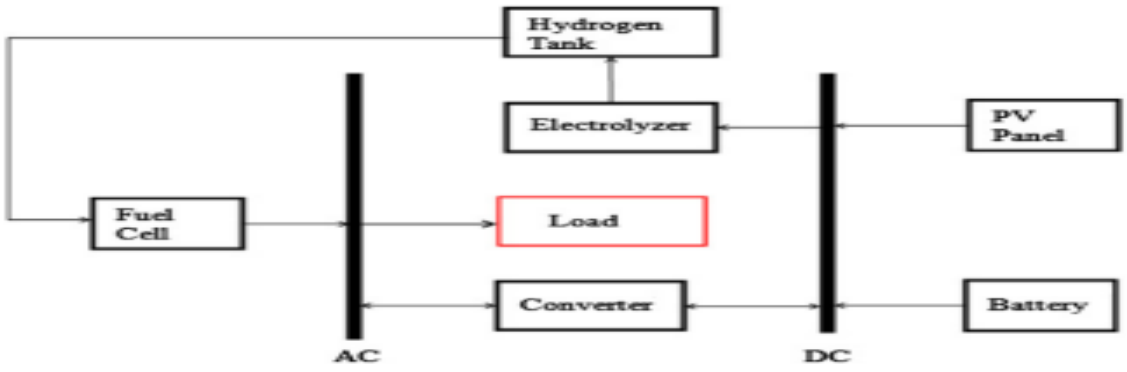

Figure IV.1: Configuration of the stand-alone PV–hydrogen power generating system.

IV.4.2 Supplementary energy solutions :

Supplementary Energy Solutions Further, as supplementary solutions, we suggest employing next-generation battery systems to store surplus energy generated during peak sun hours , which will then be utilized to compensate for energy shortfalls during low sunlight hours. This will enable us to store the generated hydrogen for future applications. Further, we suggest employing a grid-connection system, which can be used as an additional source of energy in the event of long durations of poor sunlight, thereby ensuring that energy needs are always met without dependency on a particular method.

IV.4.3 Geographic and Climatic Application :

The proposed system for the generation of solar energy and hydrogen is specifically designed for a virtual solar power plant located near the university campus in M'Sila province. This study focuses exclusively on assessing the performance of the suggested system at this site. The primary objective is to compare the different system components, particularly the battery storage and the fuel cell, in order to identify the most cost-effective and efficient configuration for hydrogen production under the climatic conditions of M'Sila .

IV.4.4 Data Acquisition and Analysis

In terms of solar energy resources, our study utilized NASA's forecast and data in order to extract meaningful information regarding solar energy potential. Our study, based on NASA data, aims to devise effective solar energy alternatives tailored to Algerian climatic conditions. What was achieved after performing these analyses was carefully computed, considering interest in performance rates, cost effectiveness, and environmental impacts of systems suggested.

IV.5 Inputs data

IV.5.1 Meteorological data :

The meteorological input data are solar radiation and temperature for PV array, and wind speed for wind turbine and stream flow for hydropower. HOMER uses these inputs data to calculate the output energy from such sources. Two possibilities exist by utilizing HOMER software to input the meteorological data either manually or gathered from the NASA POWER (NASA Prediction of Worldwide Energy Resource) database, such that one can obtain this information for any

particular month simply by using geographical coordinates (latitude and longitude), for the specified load location.

IV.5.2 Load profile

HOMER Pro software provides two types of loads electric or thermal. The profile load or also known as energy demand is the most significant input data within HOMER's operation for evaluating properly the sources and optimization. This average load consumption data are entered into HOMER Pro as daily profile and HOMER Pro uses them for determining the average electricity consumption in kWh/day with the peak demand in kW as it is also used in power balance constraint. For loads that have real load consumption data, it is easy to know the load consumption profile, but it is better to conduct a study to detail the load profile.

IV.5.3 Energy sources :

Homer Pro software simulates a variety of renewable and non-renewable energy sources. They include photovoltaic (PV) arrays, wind turbines, hydropower systems, and diesel generators. In addition to stand-alone system modeling, Homer Pro offers the option of grid connection of the (HRES). This interface allows the system to draw power from the grid or sell excess electricity to it, thereby rendering the model more realistic and adaptable to different energy scenarios

IV.5.4 Equipment characteristics :

In Homer Pro, equipment in an HRES setup is any component that generates, delivers, converts, or stores energy. Some examples of equipment include solar panels, wind turbines, diesel generators, batteries, inverters, and other essential devices. These equipment components are defined in the software with specific parameters such as size, capital and operating costs, fuel type and cost, efficiency, and power rating. Homer Pro uses these variables to simulate and evaluate the performance of each component in the HRES. The program evaluates these parameters and determines the most efficient and least expensive operating strategy for the overall system so that users can make effective decisions about system configuration and energy management

IV.5.5 Economic data :

During simulation and optimization phases, Homer Pro requires detailed cost data on all the elements involved in the design of the HRES. This is so that the software can find the most economical system design with the lowest TNPC. Thus, various types of economic data must be defined, including: initial construction cost, capital cost, operating and maintenance cost, component replacement cost, fuel cost, electricity purchase cost from the grid, emissions penalty, system fixed capital cost, and project lifetime in total. Homer Pro takes all these factors into consideration to effectively determine the financial feasibility and performance of the energy system.

IV.6 Case study: Feasibility of expanding solar power for green hydrogen in MSila

IV.6.1 Description of location :

M'Sila Province is considered one of the most promising regions in the field of RE , benefiting annually from over 2,000 to 3,900 hours of sunshine, with global horizontal solar irradiation ranging from 1,860 to 2,410 kWh/m², according to data from the Algerian Renewable Energy Development Center. Based on these excellent natural resources, we propose the establishment of a virtual GH production plant near the university campus of M'Sila, relying on solar PV energy as the primary source to power electrolyzers for water splitting. The goal of this project is to convert solar energy into clean hydrogen, which can be used as a sustainable energy carrier or to feed FC systems, supporting national efforts toward a green energy transition and enhancing scientific research in this vital sector

Figure IV.2: The Geographic Location Under Study

IV.6.2 Model Component Description :

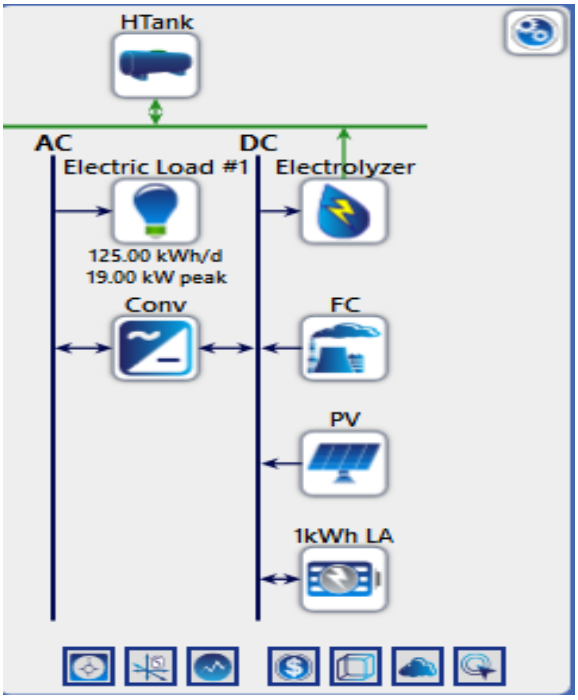

Figure IV.3: Illustration of the designed system

According to available sources, the exchange rate of the US dollar against the Algerian dinar is 132.9

$$1\$ \rightarrow 132.9 \text{ DA}$$

A. Photovoltaic Panels :

In this study, 8 Kw flat plate PV panel is used. HOMER Pro software calculates the power output of the PV array according to Equation 1 [54].

$$P_{PV} = A_{PV} k_{pv} \left(\frac{HL}{HL,STC}\right) [1+ \beta_P(L_c - L_{c,STC})] \qquad \text{(IV.1)}$$

Table IV.1 : Modelling parameters for PV panel

PV Panel		
Efficiency	20 %	
Capital	300 $ / KW	39,870 DA / KW
Replacement	300 $ / KW	39,870 DA / KW
O&M	10 $ / year	1,329 DA / year
Lifetime	25 years	

A. Electrolyser:

The most common method of hydrogen production is. Alkaline electrolysis is a common process whereby an alkaline electrolyte of sodium hydroxide or potassium hydroxide solution is used . Electricity passing through electrodes yields H_2 at the cathode and oxygen gas at the anode than a minimum decomposition voltage defined by [15]

This chemical process can be expressed by

$$H_2O + \text{electricity} \rightarrow H_2 + \frac{1}{2}O \qquad \text{(IV.2)}$$

(IV.2) For starting up the electrolyzer to produce H_2 , the working voltage between its two electrodes must be higher [55]

$$V_H = \frac{-\Delta h}{2F} \qquad \text{(IV.3)}$$

Table IV.2: Modelling parameters for Electrolyser

Electrolyser		
Efficiency	85 %	
Capital	500 $ / KW	66,450 DA / KW
Replacement	500 $ / KW	66,450 DA / KW
O&M	20 $ / year	2,658 DA / year
Lifetime	15 years	

B. Converter System

The converter in this research has a crucial role to play in effectively linking the AC and DC sides of the system. It is required for the inversion of the energy generated from renewable sources into consumable electricity for AC loads. In standalone systems, the converter also regulates power quality compliance by maintaining output voltage levels, frequency setpoints, and minimizing current harmonics. For this case study, the HOMER generic converter has been selected, with regard to power conversion loss. The converter also facilitates continuous energy flow between the DC components and the AC electrical load of the hybrid system. The cost provided for the converter is only indicative in nature, since real costs are subject to a variety of market factors. In addition, the operational and maintenance cost is approximated to be about US$100 per year.[56] As highlighted by Sinha and Chandel (2015), converters are an integral component in hybrid renewable energy systems, specifically when simulation tools like HOMER are used to ascertain energy balance and system performance between AC and DC subsystems [57]

Table IV.3: Modelling parameters for Converter

Converter		
Efficiency	95%	
Capital	160 $ / KW	21,264 DA / KW
Replacement	160 $ / KW	21,264 DA / KW
O&M	10 $ / year	1,329 DA / year
Lifetime	25 years	

C. H2 Tank :

Once the hydrogen has been produced by the electrolyser, it is stored in hydrogen tanks to be used later. The most common means of storage is that of high-pressure gas cylinders. In recent years, technology has developed to a level where lightweight composite cylinders can be utilized. which has a resistance of 800 bar pressure and can allow hydrogen to become 36 kg/m³ dense [54]. Hydrogen energy produced by the electrolyzer provides solar energy storage in excess of demand. Equation (IV.4) gives the method of transforming the capacity unit mol of H_2 tanks to the unit kWh is given in following equation

$$E_{Tank}\,(KWh) = M_{Tank}\,(mol) \times 2\times 10^{-3}\,(\frac{kg}{mol}) \times LHV\,(\frac{KWh}{Kg}) \qquad (IV.4)$$

Where Etank and Mtank are the size of hydrogen tanks in units of kWh and mol respectively and LHV is the low heat value of the H_2 . [58]

Table IV.4: Modelling parameters for H2 tank

H2 storage tank		
Initial capital cost	1000 $ / Kg	132,900 DA / Kg
Replacement cost	1000 $ / Kg	132,900 DA / Kg
O&M cost	10 $ / year	1,329 DA / year
Lifetime	30 years	

D. Fuel Cell :

The hybrid energy system also has the provision to have a FC for power generation and allows us to specify the type of FC. Since a fuel cell is essentially a DC generator, we can utilize the generator component in HOMER Pro to model it. By specifying the parameters above, HOMER Pro can accurately model the performance of the FC in the hybrid system. This allows the system design to be optimized such that FC power generation is maximized subject to hydrogen consumption and overall system economic feasibility. FC efficiency, as measured by the ratio of electrical power output to energy content of hydrogen consumed, is an important input. FC power output, in kilowatts (kW), determines its electricity generation capacity. In addition, the hydrogen consumption rate, in normal cubic metres per hour (Nm^3/hour), defines the amount of hydrogen the FC requires to generate electricity. If the system is using surplus electricity to generate hydrogen through an electrolyzer, and it is being stored in a hydrogen tank and consumed by the fuel cell, select "Stored Hydrogen" as the fuel source. This approach entails the cost of both the components and defining a fuel curve that represents the electrical output of the FC based on the fuel input to the reformer.[59] . The overall chemical reaction is as follows:

$$H_2 + \frac{1}{2}O_2 \rightarrow H_2O \qquad (IV.5)$$

The Hydrogen consumption at rated power Ppc k W of FC in 1 h can be calculated by [60]

$$HY_{Fc} = \frac{Prc\ x3600}{2 \times VFC \times F}\ (mol/h^{-1}) \qquad (IV.6)$$

The fuel curve input for Homer was generated with a slope 0.07kg/hr/kW. This was taken from literature review (Himadry Shekhar Das, 2017).

The fuel curve on Homer is as shown in Figure IV.4,5

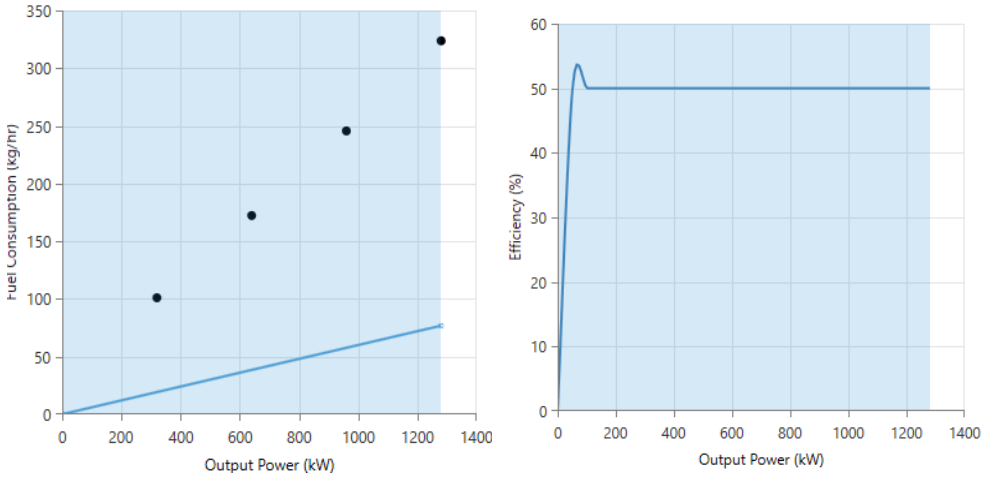

. **Figure IV.4 :** FC power curves and FC efficiency curves

Table IV.5: Modelling parameters for FC

Fuel Cell		
Minimum Load Ratio	10$ / KW	1,329 DA/ KW
Capital	7,000$ / KW	930,300 DA / KW
Replacement	800$ / year	106,320 DA/ year
O&M	0.03$ / Hour	3.987 DA / Hour
Lifetime	50,000 Hours	

E. Battery :

we mean is Batteries are required in the stand-alone scenario, where power generation and usage are isolated. The battery type for this project used is the 1kWh Lead Acid [ASM] battery The storage capacity (CWh) is calculated by

$C_{Wh} = (E_L \times AD)\ \eta_{inv} \times \eta_b \times DOD$ (IV.7)

where:

E_L = Total energy demand; AD = Daily autonomy; DOD = Battery's depth of discharge

η_{inv} = Inverter efficiency ; η_b = Battery efficiency.

Table IV.6: Specifications of battery storage

Battery storage		
Name	Lead acid	
Efficiency	80%	
Capital	140 $/KW	18,606 DA / KW
Replacement	140 $/KW	18,606 DA / KW
O&M	10 $/KW	1,329 DA / KW
Lifetime	3 years	

IV.6.3 Homer simulation :

HOMER is an acronym for Hybrid Optimization Model for Electrical Renewable [61]. The micropower optimization model approximates the performance of a system by carrying out energy balance calculations for each of the 8,760 hours in a year. For each hour, HOMER equates the electric demand during the hour with the energy that can be supplied during the hour by the system, and calculates the flows of energy to and from each piece of the system. HOMER performs these energy balance calculations and system cost calculations for each of the system configurations being evaluated. Simulation returns a list of all of the possible system sizes, sorted by NPC.

A. Load Profiles:

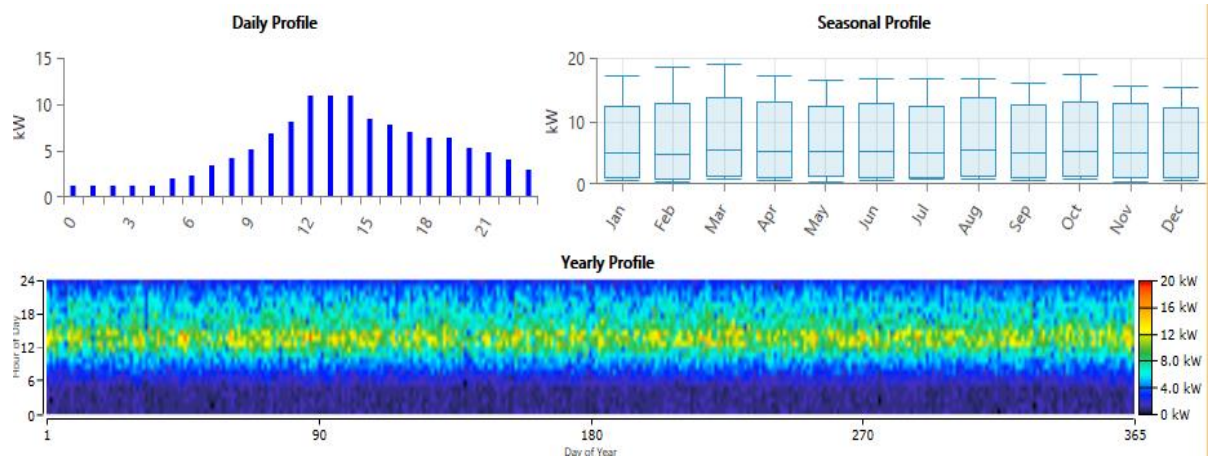

Figure IV.5: Electricity demand profile Daily , Monthly and Yearly variation.

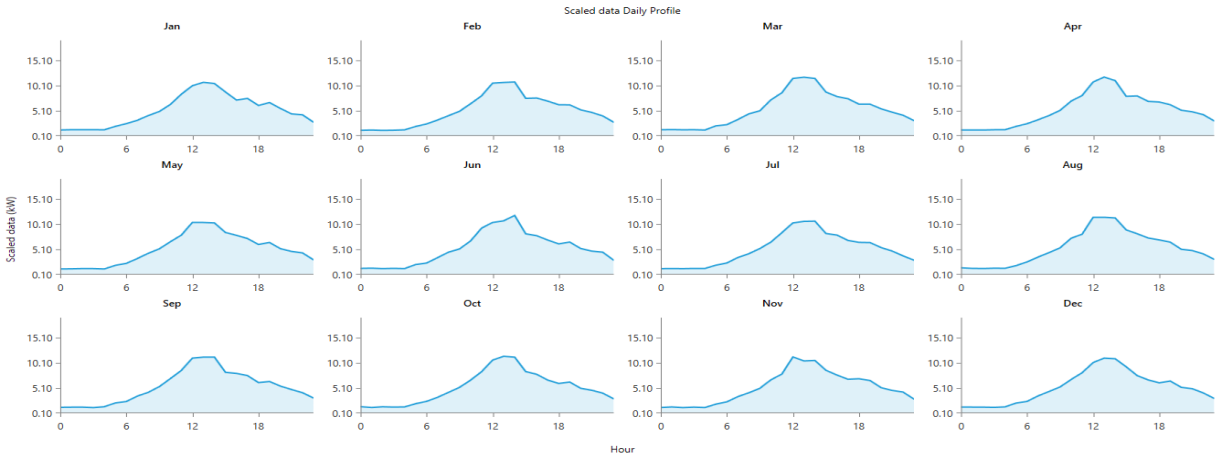

Figure IV.6: Profile of the average power demand per month

B. Resource and Load Data :

Power generation from solar panels depends on climatic conditions, which vary according to the location and season. Therefore, an important requirement for solar energy harvesting is information on the amount of solar radiation and temperature received at the study site. Figure VI.7 shows the both solar radiation and temperature data for the studied site.

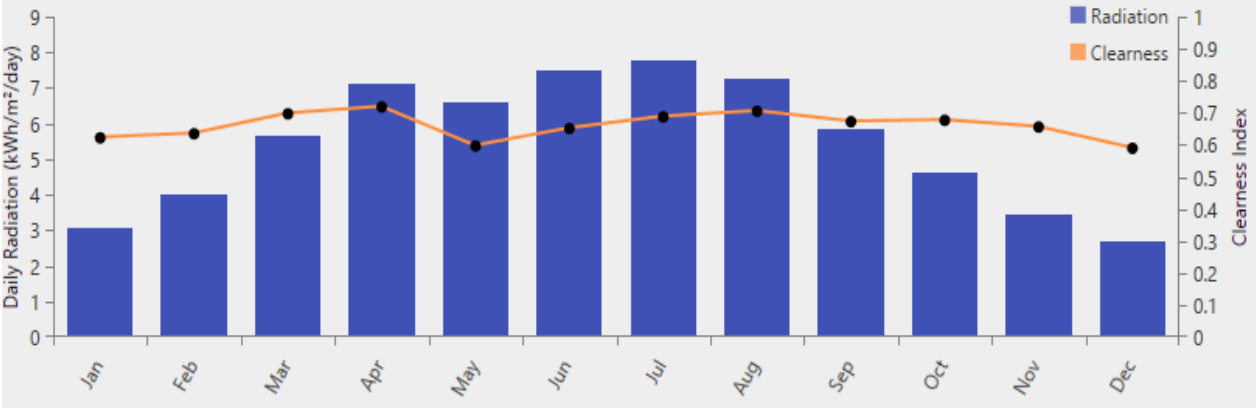

Figure IV.7: Annual solar radiation profile

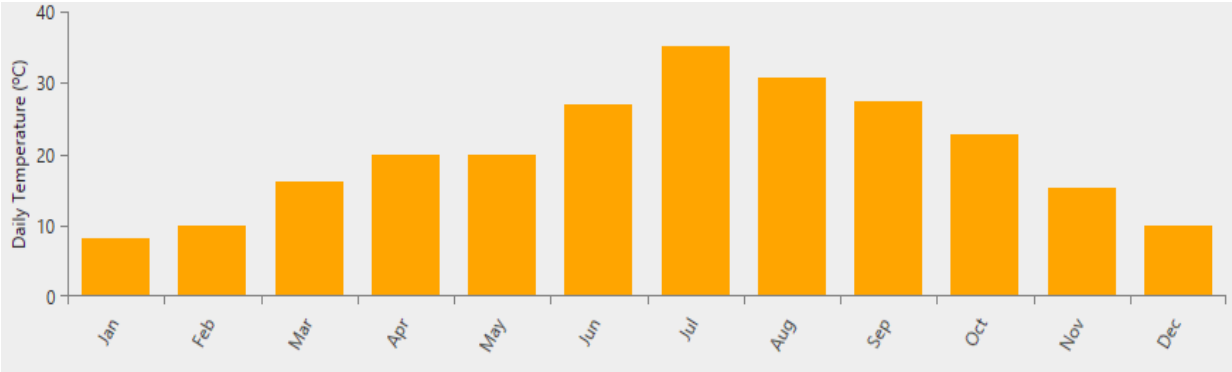

Figure IV.8: Annual ambient temperature

From Figure VI.6 ranges between 2.378 kWh/m2/day as minimum value registered in December and 7.760 kWh/m2/day as maximum value registered in June, in which it is high during the summer period and decreases during the winter period. The same applies to temperature values where the monthly average minimum is 8.20 °C and the maximum is 35°C.

C. Economic parameter :

In order to examine the economic efficiency of the system are formulated, there are four economic parameters which have to are identifiable in the analysis. They are LCOE, TNPC, LCC, and salvage cost. These costs are used by HOMER to determine the optimum system. The value of each parameter can be obtained from Eqs. (IV.8) /(IV.9) [62].

1. Total net present cost (TNPC) :

In HOMER software, the net present cost of a system is the present value of all the costs it incurs over its lifetime, minus thepresent value of all the revenue it generates over its lifetime period.

The costs are calculated as initial capital, replacement costs, operation and maintenance (O&M) costs, fuel costs, emission penalties, and the cost of buying power from the grid. Thus, TNPC is HOMER's key economic parameter and all the simulated systems are ranked according to it [63]. Mathematically, the TNPC expression is as follows:

$$C_{TNPC} = C_{ann,tot} / CRF(I,R_{Proj}) \quad \text{(IV.8)}$$

$$CRF_{(i,N)} = \frac{i(1+i)\hat{}n}{(1+i)\hat{}n-1} \quad \text{(IV.9)}$$

Where Cann;tot : total annual cost ($/yr) , CRF : capital recovery factor , i : interest rate (%)

Rproj : Project lifetime (N)

2. Levelized cost of energy (LCOE):

The levelized cost of energy (LCOE) in HOMER software is as the average price per kWh of useful electric energy produced by the system. While estimating the LCOE, HOMER divides the annualized cost of electricity produced (the total Annualized cost minus thermal load serving cost, divided by aggregate use ful electric energy output. [63],

The equation for the LCOE is as follows :

$$LCOE = C_{ann;tot} / E_{prim,AC} E_{prim;DC} E_{grid;sales} \quad \text{(IV.10)}$$

Where, $C_{ann;tot}$: total annualized cost ($/yr) , $E_{prim;AC}$:AC primary load served (kWh/yr),

$E_{prim;DC}$: DC primary load served (kWh/yr) , $E_{grid,sales}$: total grid sales (kWh/yr)

3. Life cycle cost :

According to life cycle cost (LCC) is defined as cumulative design, manufacturing, sales, servicing and recycling of discards expenses. It is usually the approach to analysis that evaluates benefits of projects to select the most optimal substitute of general power resources. [4],

$$LCC = IC + \sum \frac{TEU\ XEP}{(1+r)\hat{}i} + \sum \frac{ML}{(1+r)\hat{}i} \qquad (IV.11)$$

4. Salvage cost :

The salvage value is the amount left in a part of system at the end of the project duration. It is assumed linear depreciation of the components. This means that the salvage value of component is proportional to its life left. Apart from, the cost of salvage is assumed to be derived from the cost that replaces rather than the initial capital outlay .

To calculate the salvage value of each component at the end of the project lifetime, Homer uses the following equation [64]:

$$\text{Salvage cost , } S = C_{rep}\, R_{rem} \,/\, R_{com} \qquad (IV.12)$$

Where :

Crep = replacement cost of the component , Rcomp = lifetime of the component ,

Rrem = Rproj = Project Lifetime

5. Impacts on the system of capacity shortage fraction :

Givler and Lilienthal established that allowing some of the load to go unserved the entire year would suggest that the system components did not need to be made to worst-case conditions; and as a result, economic performance of the system would be improved [64]

IV.7 Simulation Results :

IV.7.1 Optimization results :

HOMER software simulates all the possible designs and gives the result in the form of a list of the possible ones, that meet the load requirements at minimal cost, listed by their NPC from lowest to highest. HOMER also provides results in tabular as well as graphical formats . Figure V.14 shows the overall optimization results of HRES generated by HOMER software.

Architecture															
							PV (kW)	FC (kW)	1kWh LA	Electrolyzer (kW)	HTank (kg)	Conv (kW)	Dispatch	NPC ($)	COE ($)
							69.6	1,280		45.0	60.0	19.0	CC	$157,515	$0.267
⚠							68.5	1,280	1	45.0	60.0	19.9	LF	$158,132	$0.268
							138		119	45.0	60.0	21.1	CC	$272,119	$0.462

Figure IV.9: Optimization results of PV/Fuel cell hybrid configuration.

The table in Figure IV.9 provides the detailed economic analysis of the HRES components. There is one row assigned to every system component such as fuel cell, battery storage, electrolyzer, solar photovoltaic panel, converter, and hydrogen tank. Various columns provide several financial metrics relevant to these components such as capital cost, replacement cost, operation and maintenance (O&M) cost, fuel cost, salvage value, and total cost over the project life. The bottom row determines the overall economic parameters for the entire system, which includes the total capital investment, cost of operation, and NPC of the HRES arrangement.

Table IV.7: Cost detail of the HRES components

Component	Capital ($)	Replacement ($)	O&M ($)	Fuel ($)	Salvage ($)	Total ($)
Fuel cell	$8,000.00	$618.99	$2,978.50	$0.00	-$166.09	$11,431.39
Generic 1kWh Lead Acid	$140.00	$558.60	$129.28	$0.00	-$22.36	$805.52
Generic Electrolyzer	$22,500.00	$9,546.16	$11,634.76	$0.00	-$1,796.68	$41,884.24
Generic flat plate PV	$20,546.90	$0.00	$8,854.01	$0.00	$0.00	$29,400.91
Generic large, free converter	$3,184.25	$1,351.00	$2,572.78	$0.00	-$254.27	$6,853.76
Hydrogen Tank	$60,000.00	$0.00	$7,756.51	$0.00	$0.00	$67,756.51
System	$114,371.15	$12,074.75	$33,925.84	$0.00	-$2,239.41	$158,132.33

IV.7.2 Economic analysis :

The cash flow detail of the system over the project lifetime is shown in Figure IV.11. It is observed that the replacement and O&M costs, belonging to FC and ELC equipments, raised the SC over the project lifetime. In order to decrease these costs, the initiation values for the FC/ELC must be limited to a number that lengthens the life of membranes. This means the selection of less backup power or more allowable CS fraction for the system designers.

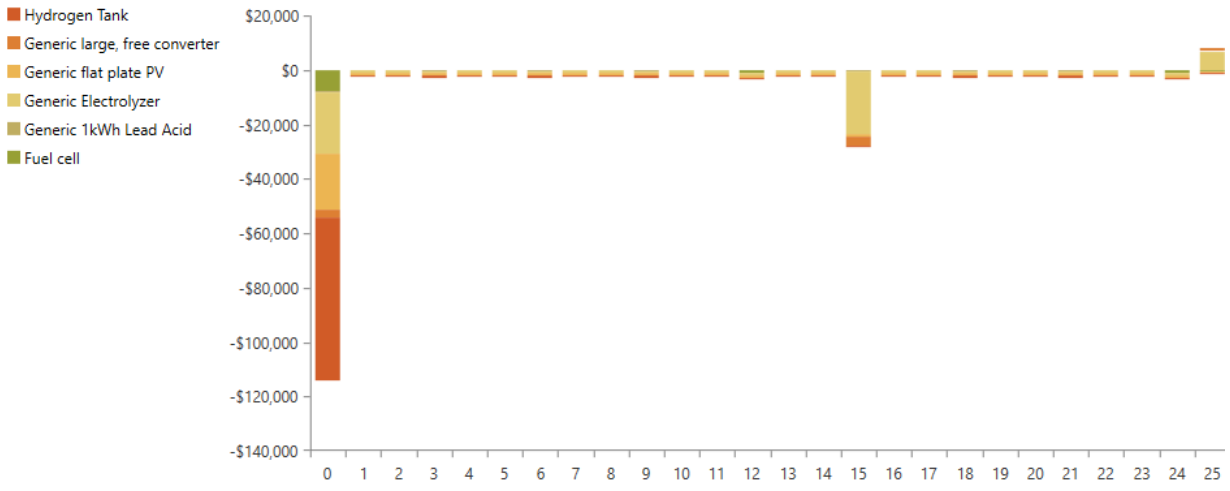

Figure IV.10: Cash flow details for the SA system.

IV.7.3 Technical analysis

In this part, details of electrical production and consumption rates generated by HOMER Pro software for all sources and loads are presented in Table VI.2. An Analysis of this data shows that the total energy production that was generated from the HRES was about 126,752 kWh/yr with the PV array dominates the power generation by providing 87.2 % of the total generated power or about 110.575 kWh/yr, followed by then PEMFC by providing power at 12.8 % or about 16,177 kWh/yr. The reason for this is due to the largest load consumption is during the day, while PEMFC is used at night for the operating strategy and the high energy cost of energy of hydrogen based system. From HOMER Pro software, the maximum output power from the solar PV array is 60.9 kW with monthly average energy production of just about 12.6 kW, as well as for PEMFC the maximum output power is 11.5 kW with monthly average energy production of just about 2.04 kW.

Figure VI.14 shows the monthly average electric production from PV and PEMFC.

As for the energy consumption results, the analyzing consumption of electrical power is Load and the electrolyzer, in which reaches at 92,496 kWh/yr. load consumes 45,552 kWh/yr, which represents 49.2 % of total consumption, while the electrolyzer consumes 46,944 kWh/yr, with percentage is 50.8 %. On the other hand, the whole system in terms of energy production shows an excess of energy of 25.1 % i.e. about 31,858 kWh/yr. Also, the unmet electric load is only 0.16 % which represent 73.1 kWh/yr, with electricity shortage is 0.298 % which represent 136 kWh/yr. Therefore, the HRES can supply almost the whole load demand.

Production	kWh/yr	%
Generic flat plate PV	110,575	87.2
Fuel cell	16,177	12.8
Total	126,752	100

Consumption	kWh/yr	%
AC Primary Load	45,552	49.2
DC Primary Load	0	0
Deferrable Load	0	0
Total	92,496	100

Quantity	kWh/yr	%
Excess Electricity	31,858	25.1
Unmet Electric Load	73.1	0.160
Capacity Shortage	136	0.298

Figure IV.11: Production and Consuption electrical

Quantity	Value	Units
Rated capacity	45.0	kW
Mean input	5.36	kW
Minimum input	0	kW
Maximum input	45.0	kW
Total input energy	46,944	kWh/yr
Capacity Factor	11.9	%

Quantity	Value	Units
Electrical Production	16,177	kWh/yr
Mean Electrical Output	2.04	kW
Minimum Electrical Output	0.0172	kW
Maximum Electrical Output	11.5	kW

Figure IV.12: Input elecrolyzer and Output fuel cell

Quantity	Value	Units
Rated Capacity	60.0	kW
Mean Output	12.6	kW
Mean Output	303	kWh/d
Capacity Factor	21.0	%
Total Production	110,575	kWh/yr

Quantity	Value	Units
Minimum Output	0	kW
Maximum Output	60.9	kW
PV Penetration	242	%
Hours of Operation	4,356	hrs/yr
Levelized Cost	0.0180	$/kWh

Figure IV.13: Output pv

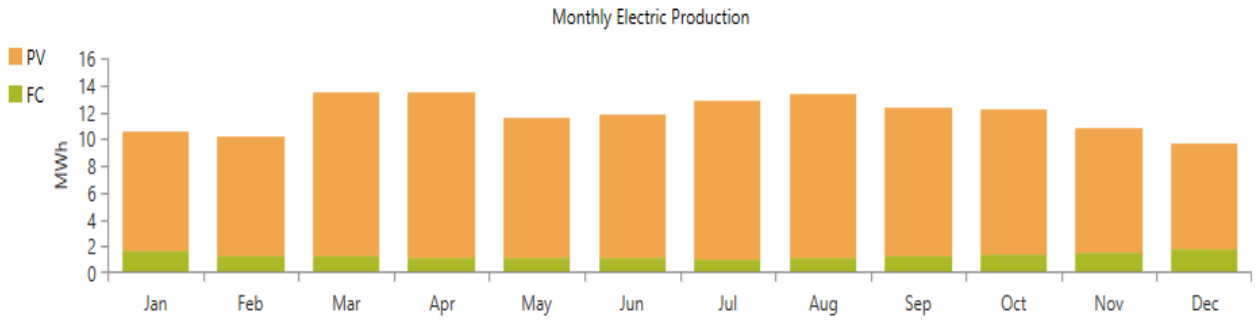

Figure IV.14: Monthly average electrical production results.

IV.7.3 Hydrogen Production

The surplus energy powers the electrolyzer, which produces green hydrogen by splitting water into hydrogen and oxygen without any carbon emissions. The produced hydrogen is stored for use during the night or on cloudy days when solar energy is unavailable, where it is consumed in a fuel cell to generate electricity and meet energy demand. The figure VI.20 shows the hydrogen produced over a year. Total hydrogen production is 1,012 kg/year where the monthly average hydrogen production fluctuates between 2.2 kg/day to 4.3 kg/day. This fluctuation of production is due to the availability of electricity to the electrolyzer through PV system.

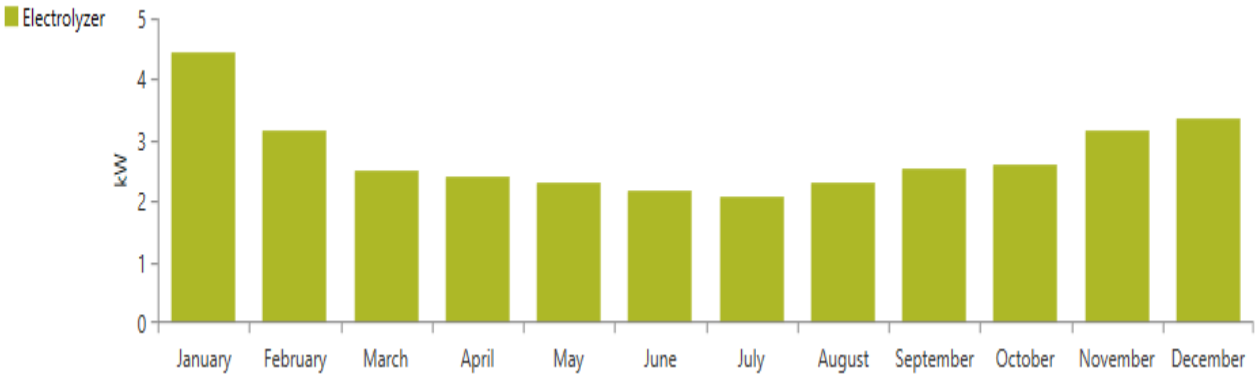

Figure IV.15: The amount of yearly hydrogen production

The optimization sizing of PV array obtained has a rated capacity of 125KW. Mostly, the PV array of the HRES can produce the energy needed for every day of the year with some exceptions due to various weather conditions. From figure VI.18, which shows the output of the PV array during the days of the year, the operation of the PV array generally starts generating power from 7 to 8 in

the morning and stopped producing energy around 6 PM. The PV array was operated for about 4,356 hours per year, and the LCOE produced was 0.0180 $/kWh. On the other hand, the color key on the right-hand side of figure VI.18 shows the output power produced from PV array is most during the middle of the days of the winter months. Further the production of PV array is affected during the summer months as a result of the angle slope and the high temperatures, which may reach 48°C, as the excess temperature acts as a parasitic load on the photovoltaic system, reducing its production. Therefore, HOMER software resort to increase the size of both the solar PV array and the PEMFC system to compensate for the loss of energy due to high temperatures

For the PEMFC, electrolyzer and hydrogen tank, the optimization sizing architecture included a 1,280 kW PEMFC system along with a 45 kW electrolyzer and a 60 kg storage tank. PEMFC generate Load during year for about 7929 hours, as it can be seen that it has more operating hours than PV due to the weather changes or other unknown factors. The PEMFC is primarily operated during the nighttime hours and optimized or forced off during day according to operating strategy chosen, and the highest demand for energy comes in the evening hours of the

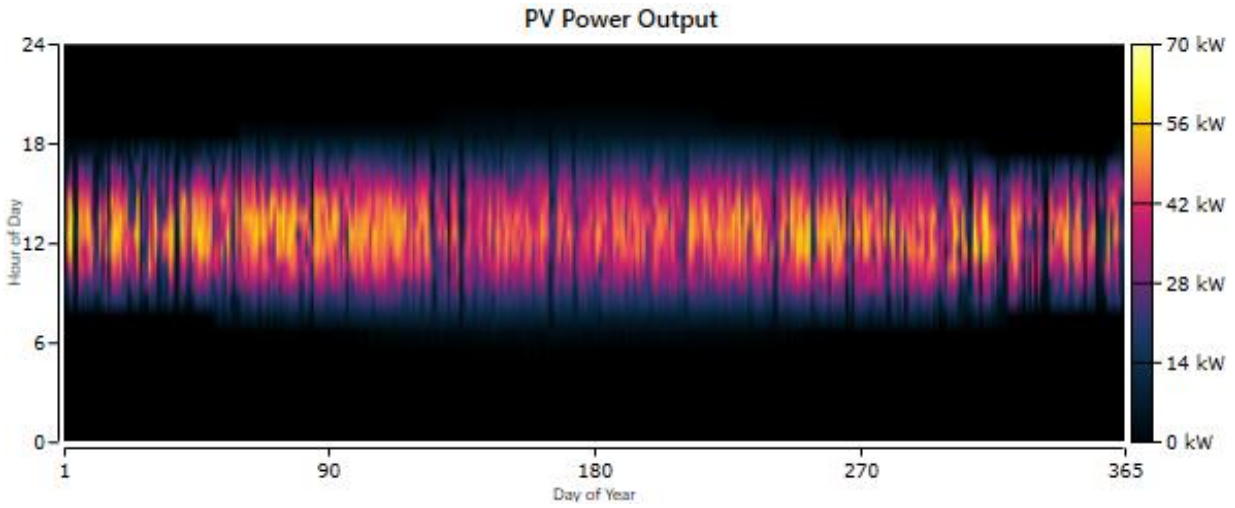

Figure IV.16: PV array output power results

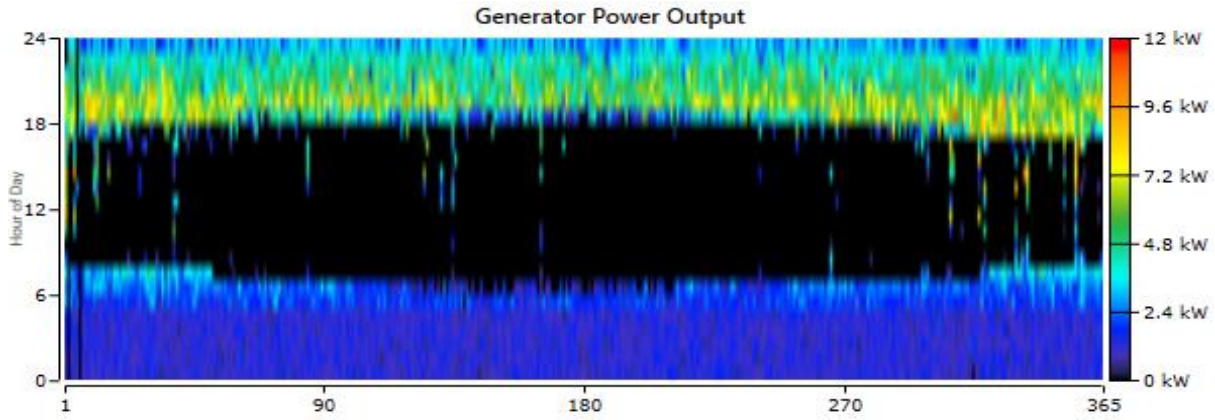

Figure IV.17: FC array output power results

IV.7.4 Power output hourly data

In this study, the performance of the hybrid energy system was simulated and analyzed with HOMER Pro by simulating the system's behavior on four provided days that represent the four seasons of the year, i.e., January 15 (winter), April 15 (spring), July 15 (summer), and October 15 (autumn). The objective of this research is to investigate the performance of the system components, PV array, FC, the electrolyzer, and the hydrogen storage tank , under varying climatic conditions of solar irradiation and temperature. For each day selected, energy production, number of operating hours, and contribution to meeting the energy requirement were examined. This approach provides insight into how the system functions and its component interactions over a whole year and therefore improves the decisions to reduce the system design and operating parameters in order to achieve a secure and efficient power supply.

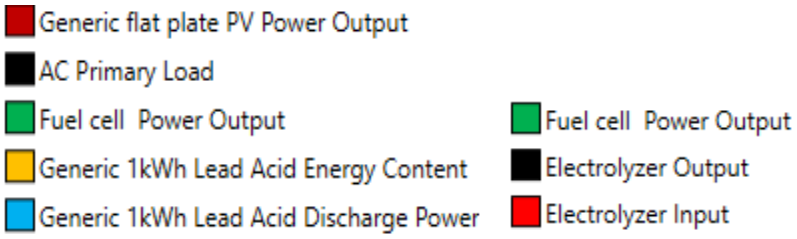

Figure IV.18: Legend of Energy System Components

A. January 15 (winter) :

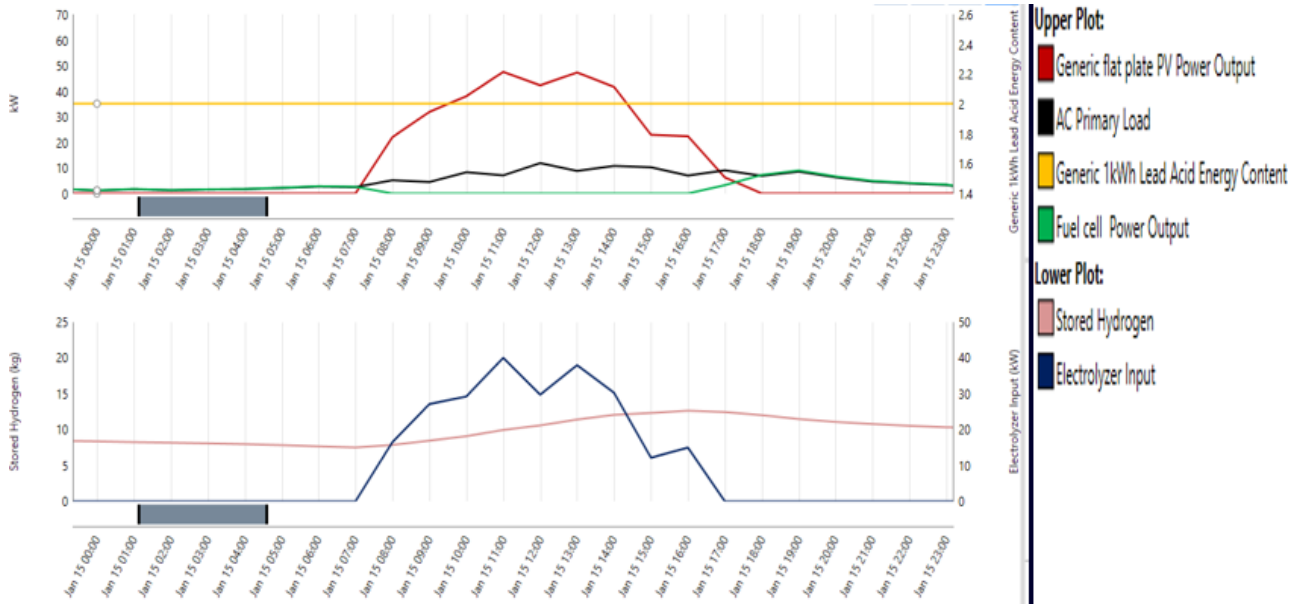

Figure IV.19: Performance Metrics of the Energy System on January 15

B. April 15 (spring) :

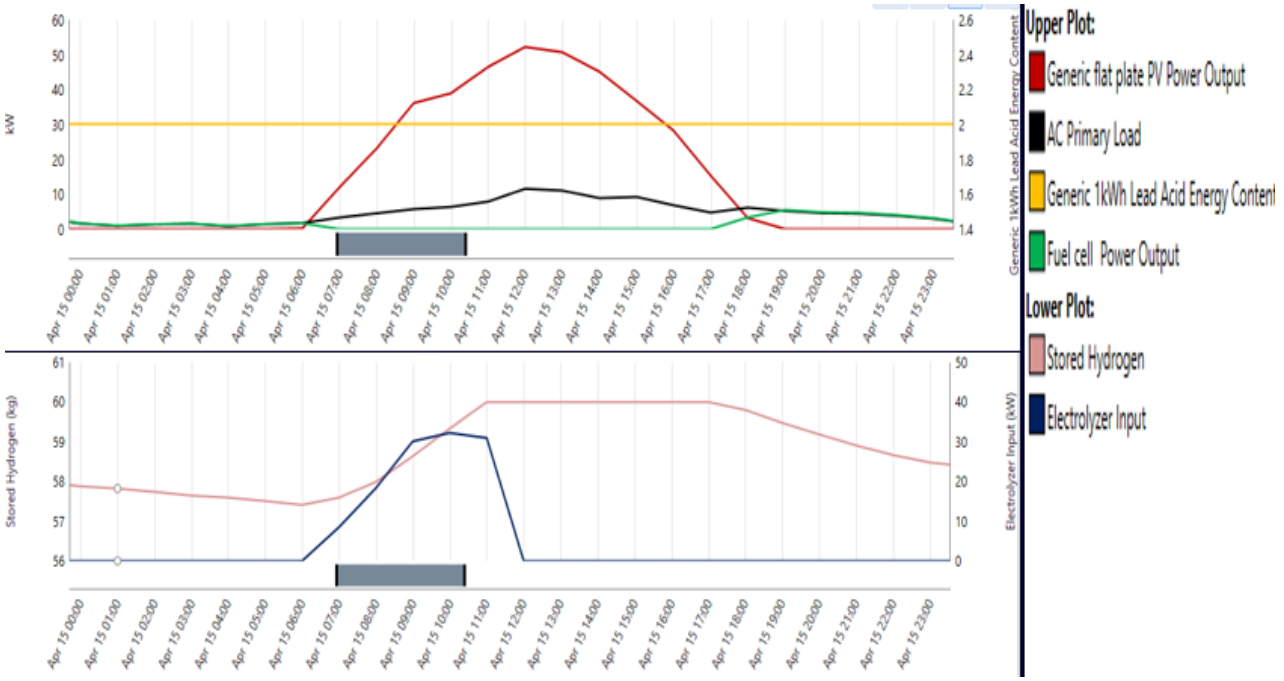

Figure IV.20: Performance Metrics of the Energy System on April 15

C. July 15 (summer) :

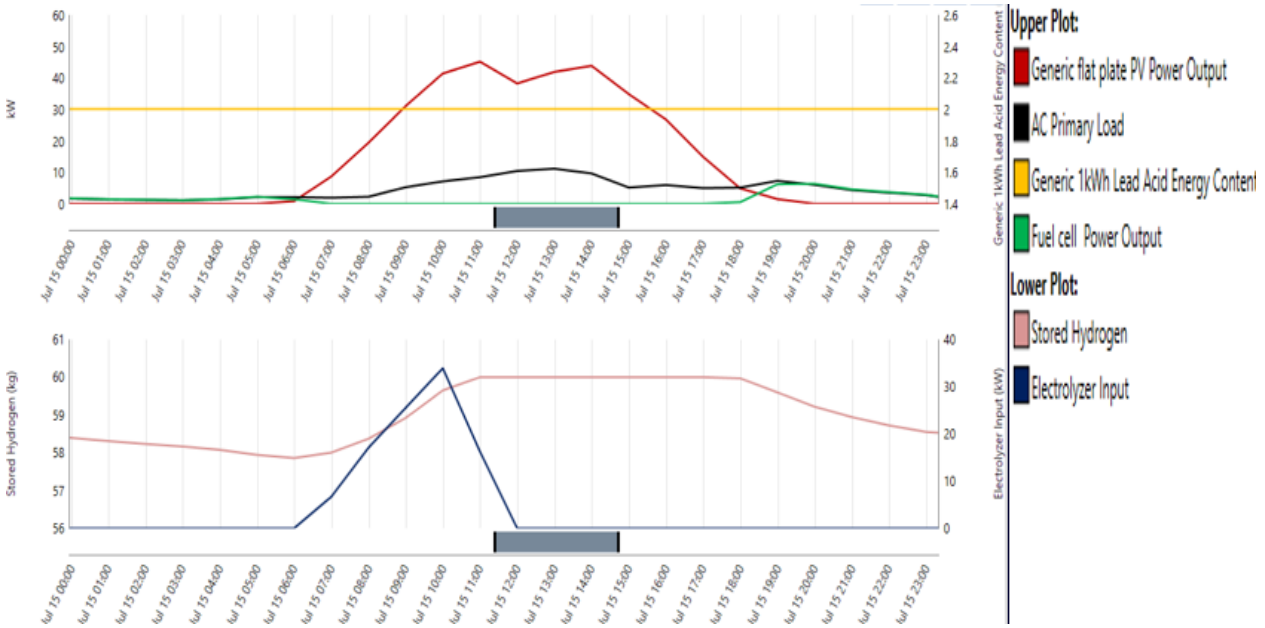

Figure IV.21: Performance Metrics of the Energy System on July 15

D. October 15 (autumn) :

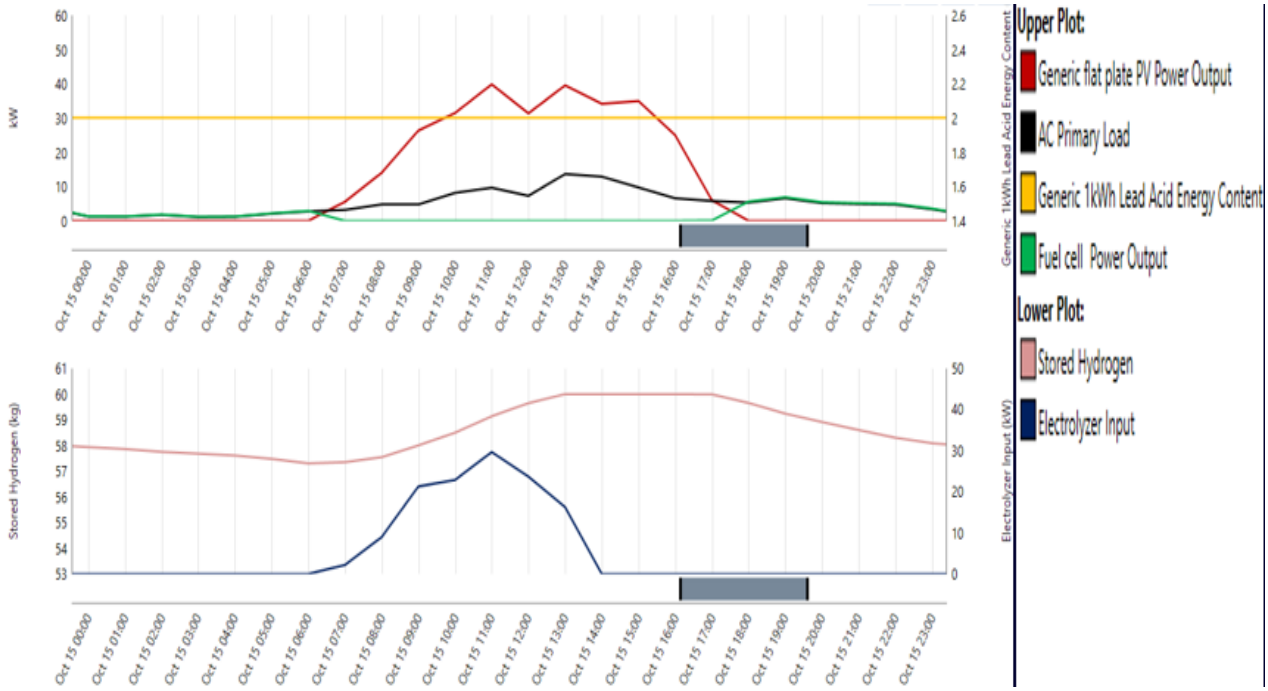

Figure IV.22: Performance Metrics of the Energy System on October 15

HOMER software hourly data analysis allows the detailed simulation results to be examined in many ways for a deeper understanding of the system operation strategy. So, the demand load profile, power flow from each source PV/FC, electrolyzer input, battery input/output power and battery state of charge are shown in Figure VI.21, for 24 hours

- **Performance Analysis in Winter (15 January):**

During the night periods, between midnight and 7:00 and 18:00 to midnight, there is zero solar irradiance. Hence, the electrical load is being provided by the fuel cell with the support of the battery. As sunrise advances, photovoltaic power generation begins to increase from around 7:30 a.m., reaching its peak at noon and exceeding 50 kW. As for the electrolyzer, it is operated from 7:00 to 17:00 by the excess solar energy from the photovoltaic array. Hydrogen production is at its maximum rate of 0.8 kilograms during this short period

- **Performance Analysis in Spring (15 April):**

The solar energy system begins supplying power between 6:00 and 7:00 , peaking at noon with a total of around 50 kW. The electrical load varies during the day, with a maximum value of 11 kW at midday. When there is low irradiation, particularly in the evenings, the fuel cell is switched on to supply the shortfall, whereas the battery remains steady at 2 kWh without being discharged during the day. The electrolyzer operates between 6:00 and 12:00 based on surplus solar power and generates a maximum of approximately 0.7 kilograms of hydrogen per hour

- **Performance Analysis in Summer (15 July):**

It begins operation at sunrise in the summer season. PV array generates electricity from 6:00 AM to 7:00 PM, with its peak generation of approximately 50 kW at midday. The electrical load also varies during the day, with its maximum at around 11 kW at midday. The battery neither discharges at all throughout this period, and the discharge power remaining at 0 kW. Whereas the energy content of the battery is constant at 2 kWh throughout the day to indicate no charging or discharging process. The fuel cell operates for a brief duration during times of low solar irradiance, such as early morning and evening after sunset, to help meet the energy demand. It then switches off during the peak solar production hours. The electrolyzer operates between 6:00 AM and 12:00

PM with surplus solar power. Hydrogen production has a maximum rate of 0.8 kg/h at 10:00 AM. After noon, the electrolyzer does not operate since excess solar power decreases**.**

- **Performance Analysis in Autumn (15 October):**

In the autumn months, the PV system operates from 6:00 AM to 6:00 PM and maximizes at 40 kW. The load starts at a low level and maximizes at 11 kW in the middle of the day. The battery energy content remains constant at 2 kW with no apparent discharge. The FC operates at low level at sunrise, but it is utilized more after sunset to meet the demand. The electrolyzer works from 7:00 AM to 2:00 PM with a yearly maximum hydrogen production of 0.6 kg

IV.8 Sensitivity analysis :

As part of this work, a comparative analysis was done between four different geographical locations so that the most suitable location for the setup of a virtual power station, taking into account climatic, topographical, and economic factors, could be determined. These locations were selected because they have considerable geographical and climatic differences, and therefore a balanced and comprehensive comparison could be done. The selected sites are: Aïn El Melh, located in southern M'Sila province, having a semi-arid climate with hot temperatures; and El Maadid, located in Hodna Mountains of northern M'Sila, with a relatively higher altitude and cooler climate. Besides, Bouchagroun, a commune of Tolga in Biskra province, was chosen because it has a clear desert climate, and Hassi Bahbah in Djelfa province, which represents the typical climate of the High Plateaus. This heterogeneity of environmental settings between the selected sites offers a scientific basis for comparison on the basis of expected solar energy output, economic feasibility, infrastructure cost, and grid connectibility, ultimately guiding the selection of the most appropriate site for the desired power station.

Table IV.8: Identification of Geographical Locations

Locations	Identification of Geographical	Annual average (GHI)	Annual average a T
Bouchagroun – Biskra Province :	An area located in the south of Biskra, characterized by a hot, arid desert climate with strong year-round solar resources.	5.73	23.11
Hassi Bahbah – Djelfa Province	A town in the High Plateaus, north of Djelfa, with a semi-arid climate — cold in winter and mild in summer.	5.52	17.32
El-Maadhid – M'Sila Province	A mountainous area in eastern M'Sila, with a relatively cold winter and mild summer climate, and medium-altitude terrain.	5.41	19.05
Ain El Melh – M'Sila Province	A municipality in southern M'Sila, featuring a hot, semi-arid climate in summer and cold winters, with open spaces suitable for solar projects.	5.69	18.78
University compus of M'sila	An urban location west of M'Sila city, with a mild semi-arid climate and close proximity to infrastructure and urban services.	5.47	20.17

IV.8.2 Indicators Used for Comparison :

- **Technical Indicators :**

The installed PV capacity bar graph gives clear differences between the five selected sites. Hassi Bahbah recorded the highest PV capacity at 64.2 kW, followed by Maadid at 61.8 kW, and M'sila University at 60 kW. Ain Melh recorded at the lowest level at 48 kW, and Bouchagroun at 45.9 kW. These differences are an indication of the varying energy needs and maybe different climatic conditions at each site. Based on overall hydrogen production per annum through the use of the electrolyzer, Maadhid led with 1,013 kg/year, closely followed by University compus of Msila at 1,012 kg/year, then Bouchagroun at 1,003 kg/year, Ain Melah at 999 kg/year, and finally Hassi Bahbah at 991 kg/year. From the observations, it is clear that the sites with higher PV capacity do not necessarily generate more hydrogen. That helps to highlight the importance of other factors influencing such quantities, such as the technical efficiency, levels of solar radiation, and local temperature.

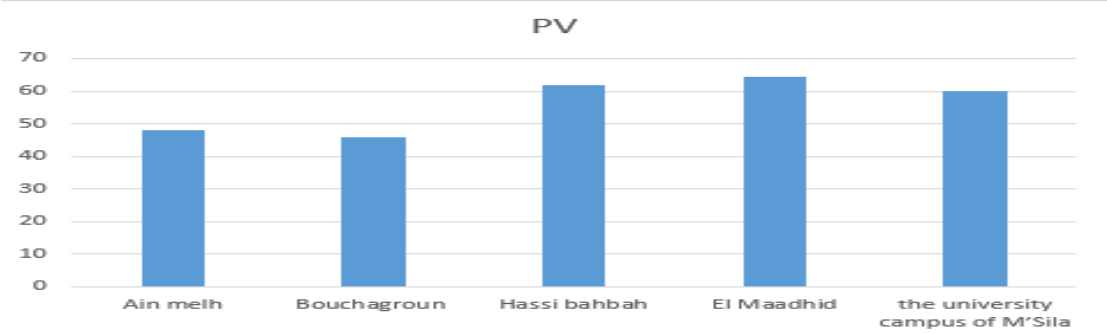

Figure IV.23: Installed PV Capacity at the Five Geographic Sites

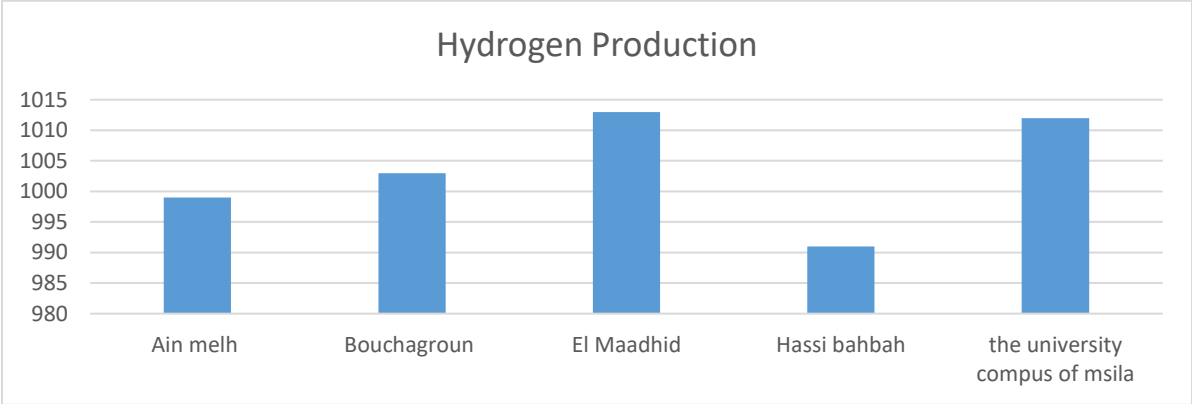

Figure IV.24: Annual Hydrogen Production via Electrolyzer in the Five Locations

- **Economic Indicators :**

The NPC bar chart shows that of the five locations, Ain Melh has the highest NPC of $149,234 followed very closely by El Maadhid at $155,427 and Hassi Bahbah at $155,179. University compus of M'sila comes in at $154,190 and Bouchagroun with the lowest NPC at $148,239. These reflect the varying cost of investment and operating expenses at every site. For the COE , the most costly is Ain Melha at $0.253 per kWh, followed by Bouchaqroun at $0.252, the University of M'sila at $0.262, while El Maâdid and Hassi Behbah both stand at $0.264. The values above indicate the sites' differences in economic efficiency. In plain words, there is a linear relationship between PV capacity and NPC greater PV capacity sites bear greater NPC, while smaller PV capacity sites have smaller NPC. This illustrates the enormous impact of PV system size on the overall investment as well as cost structure.

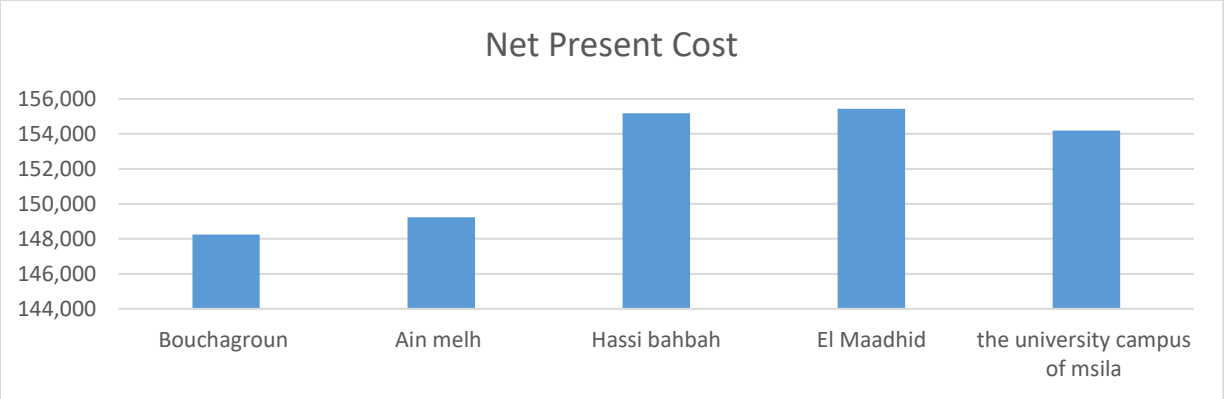

Figure IV.25: NPC Comparison Across the Five Selected Locations

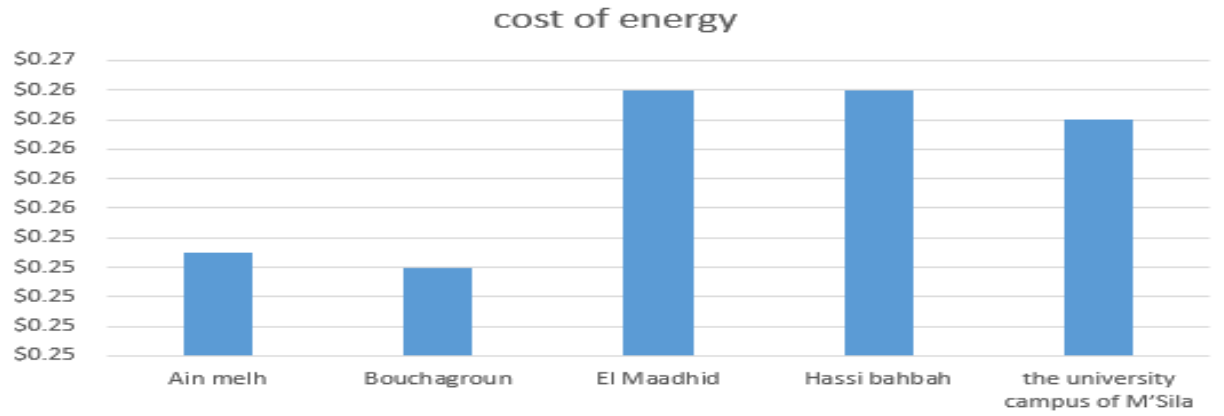

Figure IV.26: COE for Each of the Five Locations

IV.9 Conclusion :

This study explored the potential of harnessing solar energy in the province of M'Sila to produce GH through the HRES design. Proposed is a system with PV panels, batteries, an electrolyzer, hydrogen storage tank, and a PEM fuel cell that works together to provide a 125 kWh daily load. The HOMER computer program was used to model, simulate, and optimize the technical and economic performance of the system using detailed solar radiation information, load profiles, and cost values. Results have shown that the selected site near the university campus in M'Sila receives sufficient solar irradiance to power the energy needs of a small community. During periods of surplus solar generation, electricity is used to power the electrolyzer and save hydrogen for later use, rendering the system reliable despite the absence of sunlight. Sensitivity analysis was also conducted by comparing the system's performance at five different geographical locations: Djelfa,

Biskra, Ain Melah, El-Maadhid, and the main study area surrounding the university at M'Sila. This was done to evaluate the influence of site selection on techno-economic performance of the system, mainly with regards to COE, TNPC, hydrogen production, and PV capacity requirements. The results validated that the location selected has a considerable effect on the system's cost-effectiveness and energy yield Although the COE of the optimized system remains higher than the national electricity tariff, the shift towards renewable energy represents a strategic solution to address the growing energy demand, especially in rural and remote areas. It also aligns with Algeria's goals for energy diversification and local economic development. Overall, this study highlights the effectiveness of HOMER software as a powerful tool for designing and analyzing hybrid energy systems, provided that accurate meteorological and economic data are available. Furthermore, it emphasizes the importance of carefully selecting the installation site to achieve a balance between energy performance and economic feasibility.

General Conclusion

General Conclusion

Lastly, this dissertation has shown the importance of utilizing renewable resources of energy, particularly solar energy, for the production of GH as a strategic option towards achieving sustainable development and reducing FF dependence. Through the analytical study and technical processing of the climatic data specific to the Wilaya of M'Sila, it was confirmed that the region possesses significant solar potential, making it a suitable environment for green hydrogen production projects. The simulation results using HOMER Pro software demonstrated the technical and economic feasibility of the proposed system .

This study also proved that employment of a FC in the hybrid power system provides better performance compared to batteries, especially during low or zero solar irradiation hours. The FC keeps providing power to the load continuously from stored hydrogen and thus renders the system more stable and reliable compared to battery-based systems.

In contrast, the simulation showed that the site with highest irradiation levels of solar irradiation is not always optimal for H_2 production since the high temperatures that come with high solar radiation compromise the performance of solar PV panels and lower their electrical output. This calls for considering temperature factors, along with solar irradiation rates, in selecting the most suitable locations for GH projects.

Accordingly, this dissertation recommends further research in this field through practical and experimental projects at the local level, while encouraging investments in the RE and GH sector in Algeria. It also advocates for the development of integrated hybrid systems incorporating FC to ensure greater flexibility and continuity in energy supply, while taking into account various climatic and environmental factors when determining the optimal locations for such projects.

Bibliographic References

[1] BP, Statistical Review of World Energy 2023.

[2] International Renewable Energy Agency (IRENA), Future of Solar Photovoltaic: Deployment, investment, technology, grid integration and socio-economic aspects, 2019.

[3] REN21, Renewables 2023 Global Status Report.

[4] Ministère de la Transition Énergétique et des Énergies Renouvelables – Algérie, Programme national des énergies renouvelables et de l'efficacité énergétique.

[5] International Renewable Energy Agency (IRENA), Algeria Country Profile 2022

[6] International Renewable Energy Agency (IRENA), Green Hydrogen: A Guide to Policy Making, 2020.

[7] Modeling and Simulation of Direct Coupling of an Electrolyzer to PV System for Hydrogen Production

[8] Hydrogen Association .(n.d) , history of hydrogen fact sheet

[9] EWE Group.(n.d) the colour of hydrogen retrieved from

https://www.ewe.com/en/shaping-the-future/hydrogen/the-colours-of-hydrogen

[10] Douha MOKADEM , Title : Study of the production of green hydrogen from wind energy in isolated sites in Algeria , Memory ACADEMIC MASTER ,UNIVERSITY Kasdi Merbah-OUARGLA 06 /2024

[11] Dee Blasio N,(2024,july8)the colors of hydrogen . harvard kennedy school , belfer centre for sxience and international affairs

https://www.belfercenter.org/research-analysis/colors-hydrogen

[12] IEA (International Energy Agency). (2022). Global Hydrogen Review 2022. International Energy Agency.

[13] M. Chakib BOUALLOU, IRES , La filière « hydrogène vert » : Etat de l'art technologique et comparatif économique international

[14] Mansouri Abdelbasset , Guemmoula Abdeldjalil , MASTER , Production et exploitation de l'hydrogen vert en algerie , Université Kasdi Merbah –Ouargla 2023

[15] CHAOUCHE Noumane, DJOUHRI Abdelkader, FROUHAT Hamza , Faculté des Hydrocarbures, Energies Renouvelables et Science de la Terre et de l'Univers , Master , Université Kasdi Merbah- Ouargla 2022

[16] A. Mraoui, "Renewable electrolytic hydrogen potential in Algeria," International Journal of Hydrogen Energy, 2019

[17] Miranda, P.E.V. (2019). "Hydrogen Production and Practical Applications in Energy Generation.

[18] Teichmann, D., Arlt, W., Wasserscheid, P., Freymann, R. (2011). "A future energy supply based on liquid organic hydrogen carriers (LOHC)." Energy Environ.

[19] CRE-Expert.com , https://www.cre-expert.com/what-is-pvsyst-beginners-guide-2023/

[20] grz TECHNOLEGIES

[21] Bassou Walid , Djouahi Fares Theme Suitable sites for solar hydrogen production: a case study. MASTER , KASDI MERBAH - OUARGLA 2023

[22] KHERIDLA Youcef , KHINECHE Kaddour , Modélisation Et Simulation D'un Système De Production D'hydrogène Par Voie Photovoltaïque , MASTER ACADEMIQUE , UNIVERSITE KASDI MERBAH OUARGLA , Le: 08/06/2014

[23] kenani douaa (n, d**).**uses of green hydrogen .Mawdoo3 .Retrieved from https://mawdoo3.com

[24] Younes Kherbiche1,2, Nabila Ihaddadene1,4, Razika Ihaddadene1,4, Feres Hadji1 , Jed Mohamed3 , Abedel Hadi Beghidja , IIETA , Solar Energy Potential Evaluation. Case of Study: M'Sila, an Algerian Province , International Journal of Sustainable Development and Planning , December, 2021,

[25] max moore .A. (2015) Feasibility Study Of A Solar Photovoltaic to hydrogen electrolyzer system the Richmond field station . US Berkeley

[26] BOUCHAREB Khaled , THEME Exploitation de l'Energie Solaire à M'Sila , DOCTORAT LMD , Université Mohamed Boudiaf - M'Sila 2024

[27] ZEHRI Nassim , Master , Modélisation et Simulation d'un Système Photovoltaïque. , Ecole Nationale Polytechnique, rue des frères Oudek, Hacen Badi, El Harrach, - Alger 2015

[28] Xuan Hieu Nguyen and Minh Phuong Nguyen , Mathematical modeling of photovoltaic cell/module/arrays with tags in Matlab/Simulink , 2015

[29] Arman Uluoğlu , SOLAR-HYDROGEN STAND-ALONE PO , WER SYSTEM DESIGN AND SIMULATIONS , MASTER , MIDDLE EAST TECHNICAL - UNIVERSITY 2010

[30] E. Benkhelil and A. Gherbi , Modeling and simulation of grid-connected photovoltaic generation system , Revue des Energies Renouvelables SIENR'12 Ghardaïa (2012) 295 – 306 , Ferhat Abbas University, Setif, Algeria

[31] Ömer Faruk Tozlu, A Review and Classification of Most Used MPPT Algorithms for Photovoltaic Systems , Article in Hittite Journal of Science & Engineering · September 2021

[32] Reza Reisi A, Hassan Moradi M, Jamasb S. Classification and comparison of maximum

power point tracking techniques for photovoltaic system: A review. Renewable and

Sustainable Energy Reviews.

[33] ABDELHAKIM B. Design and implementation of an MPPT control of high performance for a conversion chain autonomous photovoltaic system. Université Ferhat Abbas setif1; 2015

[34] Ajaamoum, M. Comparison of the takagi-sugeno fuzzy controller and "P&O"command for extracting the maximum power from a photovoltaic system. International Journal of Innovation and Applied Studies. 2015

[35] Ratna Ika Putria,*, Sapto Wibowob , Muhamad Rifa'ia **,** Maximum power point tracking for photovoltaic using incremental conductance method , 2nd International Conference on Sustainable Energy Engineering and Application, ICSEEA 2014

[36] David Sanz Morales **,** Maximum Power Point Tracking Algorithms for Photovoltaic Applications , Maximum Power Point Tracking Algorithms for Photovoltaic Applications , Aalto University School of Science and Technolog , Espoo 14.12.2010

[37] https://www.accelerazero.com/news/what-is-an-electrolyzer-and-what-is-it-used-for

[37] K. Y. Lau, M. F. M. Yousof, S. N. M. Arshad, M. Anwari, A. H. M. **Yatim ‘**'Performance analysis of hybrid photovoltaic/diesel energy system under Malaysian conditions'' Energy, 2010,

[38] K. Hu, "Comparative study of alkaline water electrolysis, proton exchange membrane water electrolysis and solid oxide electrolysis through multiphysics modeling," Applied Energy, vol. 313, 2022.

[39] LE BOULZEC Hugo , La production d'hydrogène «vert » , Nouvelles technologies , Article : 108 , juin-16

[40] Baurens, P., & Brisse, A. (2019). High Temperature Electrolysis for Hydrogen Production: Solid Oxide Electrolyzer Cell (SOEC) Technology and Applications. In Hydrogen Supply Chains

[41] M. Sánchez a, E. Amores a , L. Rodríguez b, C. Clemente-Jul c , MATHEMATICAL MODEL AND EXPERIMENTAL VALIDATION OF A 15-kW ALKALINE ELECTROLYZER ,ICE 2017

[42] Chun-Hua Li, Xin-Jian Zhu, Guang-Yi Cao, Sheng Sui, et Ming-Ruo Hu, « Dynamic modeling and sizing optimization of stand-alone photovoltaic power systems using hybrid energy storage technology », Renewable Energy 34 (2009) 815–826

[43] HELION Hydrogen Power Company, documentation technique 2010 (confidentielle), Aix-en-Provence, France.

[44] C. Darras, S. Sailler, C. Thibault, M. Muselli, P. Poggi, J.C. Hoguet, S. Melscoet, E. Pinton, S. Grehant, F. Gailly, C. Turpin, S. Astier, et G. Fontès, « Sizing of photovoltaic system coupled

with hydrogen/oxygen storage based on the ORIENTE model », International Journal of Hydrogen Energy, Volume 35, April 2010

[45] J. Labbe, « L'hydrogène électrolytique comme moyen de stockage d'électricité pour systèmes photovoltaïque isolés », thèse de l'Ecole des Mines de Paris, CEP, Sophia Antipolis, soutenue en décembre 2006

[46] M. Uzunoglu, O.C. Onar, et M.S. Alam, « Modeling, control and simulation of a PV/FC/UC based hybrid power generation system for stand-alone applications », Renewable Energy 34 (2009)

[47] http://www.nrel.gov/international/tools/HOMER/homer.html

[47] Barbir, F. (2005). PEM electrolysis for production of hydrogen from renewable energy sources. Solar Energy.

[48] Guelbi Abdelouadoud , Kadri Ahmed Abdesslam , Thème Etude Expérimentale d'un Système de Refroidissement Éco-Intelligent pour I'Optimisation en Temps Réel les Performances des Systèmes Photovoltaïques en Région Saharienne , UNIVERSITE KASDI MERBAH OUARGLA 06/2024

[49] Gage Kellogg , What is PVsyst Solar Design Software ,

https://www.partneresi.com/resources/articles/what-is-pvsyst-comprehensive-guide-2023/

[50] Lambert, T. ?Gilman ,P ? &Lilienthal, P .(2006) ."Micropower System Modling With HOMER " . Nationel Renewable Energy Laboratory (NREL)

[51] International Renewable Energy Agency (IRENA). (2022). Green Hydrogen Supply: A Guide to Policy Making. Abu Dhabi: IRENA

[52] Sherif, S. A., Zeytinoglu, N., & Barbir, F. (2005). Hydrogen storage for fuel cell vehicles. Energy Conversion and Management, 46(7–8), 1169–1177.

[53] Melaina, M. W., Antonia, O., & Penev, M. (2013). Blending Hydrogen into Natural Gas Pipeline Networks: A Review of Key Issues. National Renewable Energy Laboratory (NREL), U.S. Department of Energy

[54] Luta, D. N., & Raji, A. K. (2018, May). Decisionmaking between a grid extension and a rural renewable off-grid system with hydrogen generation. International Journal of Hydrogen Energy,

[55] M. J. Khan and M. T. Iqbal, "Dynamic modeling and simulation of small wind-fuel cell hybrid energy system," Renewable Energy , 2005

[56] Mohammed OH, Amirat Y, Benbouzid M, Feld G, Tang T, Elbast A**.** Optimal design

of a stand-alone hybrid PV/fuel cell power system for the city of Brest in France. Int J Energy Convers 2014

[57] Sinha, S., & Chandel, S. S. (2015). Review of software tools for hybrid renewable energy systems. Renewable and Sustainable Energy Reviews .

[58] Prabodh Bajpai , Sowjan Kumar, and N. K. Kishore , Sizing Optimization and Analysis of a Stand-alone WTG System Using Hybrid Energy Storage Technologies, Department of Electrical Engineering , Indian Institute of Technology Kharagpur

[59] DAHMANI Mohamed Abdel Ghafour. , ARFA Mohamed Amine., The Analysis of the Integration of Green Hydrogen Into Energy Networks Using HOMER PRO , Masters of Renewable Energy in Mechanics, University of Sciences and Technology Houari Boumediene 2023 / 2024

[60] Khan, M. J., and Iqbal, M. T. 2005. Dynamic modeling and simulation of a small wind-fuel cell hybrid energy system, Renewable Energy

[61] Home page of HOMER, Available: http://www.nrel.gov/homer/.

[62] Touhami, N. Assessment of Solar Energy Potential in Algeria. Renewable Energy Journal , (2017).

[63] Normazlina Mat Isa a, b , Himadry Shekhar Das b , Chee Wei Tan b, A.H.M. Yatim b,Kwan Yiew Lau , A techno-economic assessment of a combined heat and power photovoltaic/fuel cell/battery energy system in Malaysia hospital , Universiti Teknologi Malaysia, 81310 Skudai, Johor, Malaysia 2016

[64] Lilienthal P, Givler T. Using HOMER Software, NREL's micropower optimization model, to explore the role of gen-sets in small solar power systems. NREL; 2006. Technical Report, Case Study: Sri Lanka, Power-Gen Conf

[65] James Jonas , THE HISTORY OF HYDROGEN ,

https://www.altenergymag.com/article/2009/04/the-history-of-hydrogen/555/

Abstract :

Solar energy is one of the most abundant and sustainable energy sources, playing a crucial role in green hydrogen production. M'Sila, with its geographical location and high solar potential, represents a promising site for solar hydrogen production. This study analyzes solar resources in M'Sila Province to assess their suitability for hydrogen generation. Using HOMER Pro software, we simulate a system integrating a photovoltaic generator and an electrolyzer to evaluate energy performance and economic feasibility. The results provide insights into the seasonal variability of solar resources and highlight the potential of M'Sila as a strategic location for green hydrogen production in Algeria.

Keywords : solar energy, hydrogen production, photovoltaic generator, water electrolyzer, HOMER Pro, M'Sila.

Résumé :

L'énergie solaire est l'une des sources d'énergie les plus abondantes et durables, jouant un rôle essentiel dans la production d'hydrogène vert. La wilaya de M'Sila, avec sa position géographique et son fort potentiel solaire, représente un site prometteur pour la production d'hydrogène solaire. Cette étude vise à analyser les ressources solaires de la région afin d'évaluer leur aptitude à la production d'hydrogène. En utilisant le logiciel HOMER Pro, nous avons simulé un système intégrant un générateur photovoltaïque et un électrolyseur pour évaluer la performance énergétique et la faisabilité économique. Les résultats mettent en évidence la variabilité saisonnière des ressources solaires et soulignent le potentiel de M'Sila en tant que site stratégique pour la production d'hydrogène vert en Algérie.

Mots-clés : énergie solaire, production d'hydrogène, générateur photovoltaïque, électrolyseur, HOMER Pro, M'Sila.

الملخص:

تُعتبر الطاقة الشمسية من أكثر مصادر الطاقة وفرةً واستدامة، وهي تلعب دورًا رئيسيًا في إنتاج الهيدروجين الأخضر. تتميز ولاية المسيلة بموقعها الجغرافي وإمكاناتها الشمسية العالية، مما يجعلها موقعًا واعدًا لإنتاج الهيدروجين الشمسي. تهدف هذه الدراسة إلى تحليل الموارد الشمسية في ولاية المسيلة لتقييم مدى ملاءمتها لإنتاج الهيدروجين. باستخدام برنامج HOMER Pro ، قمنا بمحاكاة نظام يجمع بين مولد كهروضوئي ومحلل كهربائي لتقييم الأداء الطاقوي والجدوى الاقتصادية. تسلط النتائج الضوء على التغيرات الموسمية في الموارد الشمسية وتبرز إمكانيات المسيلة كموقع استراتيجي لإنتاج الهيدروجين الأخضر في الجزائر.

الكلمات المفتاحية: الطاقة الشمسية، إنتاج الهيدروجين، مولد كهروضوئي، محلل كهربائي، هوموار برو

The First National Conference on Renewable Energies

The First National Conference on Renewable Energies and Advanced Electrical Engineering (NC REAEE'25)

May 06-07th, 2025

University of M'Sila

Faculty of Technology

Electrical Engineering Laboratory (LGE)

NC-REAEE'25

CERTIFICATE Of PARTICIPATION

This Certificate is Awarded to:

BenNaadja Oussama

for presenting a paper entitled: **Analysis of solar resources in the wilaya of Msila For the production of green hydrogen**

Authors: ***Nadji Ayman , Zemmit abderrahim , Loukriz abdeloudoud***

at the First National Conference on Renewable Energies and Advanced Electrical Engineering (NC-REAEE'25), held at M'Sila University- Algeria, on May 6–7th 2025.

Paper ID: **180**

Conference Chair

Dr. Abderrahim ZEMMIT